



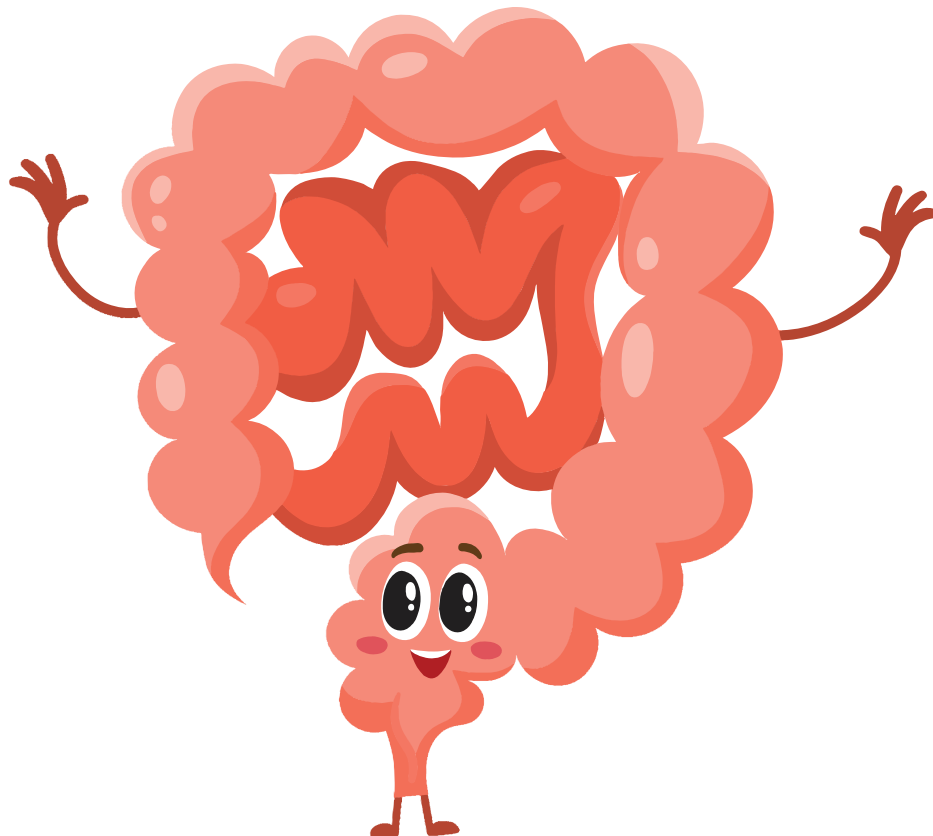
UiT The Arctic University of Norway

Faculty of Health Sciences
Department of Pharmacy

The Metabolome and Lipidome of Ulcerative Colitis

Joseph Diab

A dissertation for the degree of Philosophiae Doctor - June 2020



A dissertation for the degree of Philosophiae Doctor

The Metabolome and Lipidome of Ulcerative Colitis

Joseph Diab



Tromsø, June 2020

Natural Product and Medicinal Chemistry Research Group
Department of Pharmacy
Faculty of Health Science
UiT The Arctic University of Norway
Norway

“The best workers, like the happiest livers, look upon their work as a kind of game: the harder they play the more enjoyable it becomes”

Robert Baden-Powell

“If you want to go fast, go alone. If you want to go far, go together”

African Proverb

Acknowledgments

This work is funded by UiT – The Arctic University of Norway and Helse Nord. It was carried out at the Natural Products and Medicinal Chemistry Research Group, Department of Pharmacy, UiT The Arctic University of Norway. I would like to express my gratitude to everyone that has helped me along the way.

First, I want to express my deep gratitude to my supervisors; To Guro Forsdahl for being the most understanding, patient, and motivating person ever. Thanks for guiding my PhD journey, and for providing all the scientific and the personal support. To Terkel Hansen for being there every time I needed a guidance, and for the numerous conversations on Mass spectrometry, data analysis, beers, and dogs. To Einar Jensen for establishing the collaboration with the Swedish Metabolomics centre (SMC). To Jon Florholmen for being the father of ASIB, for providing his extent knowledge, and for his amazing passion for science. For Rasmus Goll, for dedicating his time to share his valuable opinion and experience, for letting me experiencing his cooking skills, and for being the best ECCO traveling companion. I really hope to continue being part of your cool (poop) projects.

I could never complete my PhD work without the help of many collaborators. Thanks to all personals at SMC, especially Thomas Moritz. Thanks a lot for hosting me in your lab. I feel privileged to be able to perform metabolomic analysis in SMC under the supervision of the best in the field! Thanks to Sandra Gouveia for her significant contribution in my project, and to Maria Ahnlund for providing me with hands-on training on data processing. Many thanks to Hans Stenlund for babysitting me, and for providing me with the toolbox that I needed to complete my PhD. I am honoured to get to know (and to have access) to such a great mind like yours. Thanks for my co-author, Rania al Mahdi. Thanks for Ines Heiland and Roland Sauter for helping me putting our finding into a wider biological context.

I want to thank former and current colleagues at the Department of Pharmacy. I will never forget our legendary Christmas parties, ‘summer’ BBQs, wine tasting, seminars, and cakes. I want to thank all formers and current members of my research group, especially Martina Havelkova and Trude Andersen for being my trust circle, and for Terje Vasskog for sharing his wisdom and experience with me. I am still looking forward for our first fishing trip ☺

Over the last 4 years, I was blessed to have an amazing family of friends in Tromsø. Thanks for Beate for taking me on amazing adventures. Thanks for Julia and Theresa for their great friendship. Thanks for Fabrizio for his advices, his authentic ice cream and pizza. Thanks for Vidar and Joao for all the bromance. Thanks for Christina and Jan Håkon for making me be part of their family. Thanks for Merete for being there in every great moment of my PhD. Thanks for Dominik for helping me since the very first moment I started at UiT. I will miss our ritual of B&B. Thanks for my PhD colleagues, my brother and sister in arms, especially Nina, Margherita, Jennifer, Julie, Anup, Lorenz, and Chris. I wish you all the best in your future.

Last, I am overwhelmed by the love and the unconditional support of my family. My amazing wife Katrine whom filled my life with happiness, and provided me with the purpose. My father and mother, Marwane and Rima, who made me the person I am. I will always try to make you proud of me. To my beloved brother Rami and his wife Marie, who stood by me through my worst episode. To my in laws, Mette and Kim, who took me as son and provided me with care and beers ☺.

Seven years ago, I left Syria for a journey that took me to Lebanon, Spain, Germany, and Norway. I was lucky to survive one of the deadliest war in the last 50 years, while many could not... I am grateful for Norway for hosting me, for allowing me to chase my dreams, and for giving me a safe home. However, I will always be proud of my mother country Syria and of all the sacrifices of its daughters and sons.

Table of Contents

List of Papers.....	I
Summary	III
Abbreviations	IV
1.Introduction	1
1.1 Inflammatory Bowel Disease	1
1.1.1 Epidemiology	1
1.1.2 Pathogenesis of Ulcerative Colitis	1
1.1.3 Management of Ulcerative Colitis	6
1.1.4 Biomarkers for UC	9
1.1.5 Clinical outcome.....	10
1.1.6 ASIB study	12
1.2 Metabolomics and Lipidomics	13
1.2.1 Definition	13
1.2.2 Analytical approaches for metabolomics	15
1.2.3 Analytical platforms for metabolomics	15
1.2.4 Sample preparation.....	16
1.2.5 Metabolite separation	18
1.2.6 Metabolites detection and quantification by MS.....	19
1.2.7 Data processing	21
1.2.8 Data normalization and scaling.....	22
1.2.9 Data analysis	22
1.2.10 Biomedical interpretation.....	23
1.2.11 Metabolomics in IBD	23
2. Aims of the study	26
3. Methods	27
3.1. Biopsies collection	27
3.2. Global metabolomics by CG-MS	27
3.3. Global metabolomics by LC-MS	27
3.3. Global lipidomics by LC-MS	28
3.4. Targeted metabolomics by LC-MS	28
3.5. Data analysis	29
4. Summary of results.....	30

4.1 Paper I	30
4.2 Paper II	33
4.3 Paper III.....	35
5. Discussion	37
5.1 Methodological considerations.....	37
5.1.1 Study design	37
5.1.2 Mucosal biopsies	38
5.1.3 Metabolomics and lipidomics analysis.....	38
5.2 The mucosal metabolic landscape in treatment-naïve UC	39
5.2.1 Mucosal lipid profiles in treatment-naïve UC	39
5.2.2 Mucosal metabolic signature in treatment-naïve UC reflects the state of dysbiosis	40
5.3 Discriminative lipids and metabolites for the UC state	40
5.4 Mucosal bioactive lipid mediators in UC	42
5.4.1 The imbalance between pro- and anti-inflammatory molecules during UC.....	42
5.4.2 The association between oxylipins and eCBs profile and cytokines gene expression	42
5.5 Metabolic signatures with potential clinical utility	43
5.5.1 Fatty acid metabolism	43
5.5.2 Phosphatidylethanolamine and sphingomyelin composition	44
5.5.3 Tryptophan metabolism.....	44
6. Conclusion.....	45
References	45
Appendix	61

List of Papers

Paper I ‘*A Quantitative Analysis of Colonic Mucosal Oxylipins and Endocannabinoids in Treatment-Naïve and Deep Remission Ulcerative Colitis Patients and the Potential Link with Cytokine Gene Expression*’

Joseph Diab, Rania Al-Mahdi, Sandra Gouveia-Figueira, Terkel Hansen, Einar Jensen, Rasmus Goll Thomas Moritz, Jon Florholmen, and Guro Forsdahl. *Inflammatory bowel diseases*, 2019. **25**(3): p. 490-497.

Paper II ‘*Lipidomics in Ulcerative Colitis Reveal Alteration in Mucosal Lipid Composition Associated With the Disease State*’

Joseph Diab, Terkel Hansen, Rasmus Goll, Hans Stenlund, Maria Ahnlund, Einar Jensen, Thomas Moritz, Jon Florholmen, and Guro Forsdahl. *Inflammatory bowel diseases*, 2019, **25**(11), p.1780-1787.

Paper III ‘*Mucosal Metabolomic Profiling and Pathway Analysis Reveal the Metabolic Signature of Ulcerative Colitis*’

Joseph Diab, Terkel Hansen, Rasmus Goll, Hans Stenlund, Einar Jensen, Thomas Moritz, Jon Florholmen, and Guro Forsdahl. *Metabolites*, 2019. **9**(12): p. 291.

Summary

Inflammatory bowel disease (IBD) is a chronic, relapsing inflammatory disorder in the gastrointestinal tract that affects up to 0.5% of the population of the Western world. The two major forms of IBD, Ulcerative Colitis (UC) and Crohn's Disease (CD), are characterized by a dysregulated mucosal immune response triggered by several genetic and environmental factors in the context of host-microbe interaction. This overwhelming complexity makes IBD ideal for metabolomic and lipidomic studies to unravel the disease pathobiology and to improve the patient stratification strategies toward personalized medicine.

In this work, we explored the mucosal metabolomic profile in UC patients, and identified the metabolic signatures of IBD. Colon mucosa biopsies were collected from treatment-naïve UC patients at the debut of the disease (inflamed mucosa), UC patients in deep remission, and healthy subjects. Metabolomic analysis was performed by combining GC-TOF-MS and UPLC-QTOF-MS, while lipidomic analysis was performed by means of UPLC-QTOF-MS. In total, 177 metabolites from 50 metabolic pathways, and 220 lipids from 11 lipid classes were quantified. Additionally, we mapped the omega-3 and omega-6 polyunsaturated fatty acids related bioactive metabolites, which are known as oxylipins and endocannabinoids (eCBs). Accordingly, the levels of 35 oxylipins and 11 eCBs were quantified by means of UPLC-TQ-MS/MS.

Multivariate analysis revealed a distinct lipidome and metabolome profile for each of the study groups. Altered phospholipid and sphingolipid metabolism is the hallmark of the active UC metabolome. Several mucosal metabolic signatures might reflect the interaction between the mucosal inflammation and the state of dysbiosis in the gut, such as the disruption in the acyl carnitine profile, amino acids metabolism, galactosylceramide profile, and short chain fatty acids metabolism. In addition, the results show increased levels of ω -6-related oxylipins and decreased levels of ω -3-related eCBs in UC patients compared to healthy controls. This highlights the altered balance between pro- and anti-inflammatory lipids in UC.

We report several metabolic fingerprints of potential clinical value as markers for monitoring the UC activity, and for predicting the response to treatment. For instance, the alteration in lipid mediators correlates with the severity of inflammation, and may be considered as potential targets for intervention. Moreover, lipidomic analysis unravel several potential prognostic and diagnostic markers for UC, such as PE38:3 and very long chain ceramids. Likewise, The tryptophan metabolism seems to be a key aspect of the impaired metabolism in the onset of UC. Thus, its clinical utility need to be assessed using a targeted analytical approach.

This work demonstrates the importance of metabolomics in IBD to identify key drivers of pathogenesis which prerequisite personalized treatment.

Abbreviations

15-HETrE	15-hydroxy-eicosatrienoic acid
2-AG	2-arachidonoylglycerol
5-ASA	5-aminosalicylic acid
AA	Arachidonic acid
AEA	Arachidonoyl ethanolamine
AHR	Aryl hydrocarbon receptor
AIF	All ion fragmentation
ANCA	anti-neutrophil cytoplasmic antibodies
APCI	Atmospheric pressure chemical ionization
APPI	Atmospheric pressure photoionization
ASCA	Anti- <i>Saccharomyces cerevisiae</i> antigen
ASIB	The Advanced Study in Inflammatory Bowel Disease
AZA	Azathioprine
BCoAT	Butyryl-CoA acetate CoA-transferase
CD	Crohn's disease
CDH1	Cadherin-1
CE	Capillary electrophoresis
Cer	Ceramide
CFI	Complement factor I
CI	Chemical ionization
CID	Collision-induced dissociation
COX	Cyclooxygenase
CRP	C-reactive protein
CSH	Charged surface hybrid
CYP450	Cytochrome P450
DA	Discriminant analysis
DDA	Data dependent acquisition
DGLA	Dihomo-gamma-linolenic acid
DHA	Docosahexaenoic acid
DHEA	Docosahexaenoyl ethanolamine
DIA	Data independent acquisition
eCBs	Endocannabinoids
ECCO	European crohn's and colitis organization
ECS	Endocannabinoid system
EDA	Eicosadienoic acid
EI	Electron impact
EPA	Eicosapentaenoic acid
EPEA	Eicosapentaenoyl ethanolamine
ESI	Electrospray ionization
EWAS	Epigenome-wide association study
FA	Fatty acid
FAB	Fast-atom bombardment
FADS1	Fatty acid desaturase

FC	Fold Change
FCal	Faecal calprotectin
FDR	False discovery rate
FMT	Faecal microbiota transplant
FTICR	Fourier transform ion cyclotron resonance
GalCer	Galactosyl ceramide
GC	Gas chromatography
GWAS	Genome wide association studies
HETE-12	12-Hydroxy-eicosatetraenoic acid
HILIC	Hydrophilic interaction liquid chromatography
HLA	Human leukocyte antigen
HMDB	Human metabolome data base
HNF4A	Hepatocyte nuclear factor 4 alpha
HRMS	High-resolution mass spectrometry
IBD	Inflammatory bowel disease
IBS	Irritable bowel syndrome
IBSEN	Inflammatory Bowel South-Eastern Norway
IS	Internal standards
JAK 2	Janus kinase 2
KEGG	Kyoto encyclopedia of genes and genomes
Kyn	Kynurenine
LA	Linoleic acid
LC	liquid chromatography
LCFA	Long chain fatty acid
LIT	Linear ion trap
LLE	Liquid liquid extraction
LOX	Lipoxygenase
LPC	Lysophosphosphatidyl choline
LPE	Lysophosphosphatidyl ethanolamine (LPE)
LTB4	Leukotriene B4
LXA4	Lipoxine
MALDI	Matrix-assisted laser desorption ionization
MDR1	Human multidrug resistance 1
MRM	Multiple reaction monitoring
MS	Mass spectrometry
MSTFA	Methyl-N-(trimethylsilyl) trifluoroacetamide
MTBE	Methyl tert-butyl ether
MVA	Multivariate data analysis
NetCDF	Network common data form
NMR	Nuclear Magnetic resonance
OPLS	Orthogonal projections to latent structures (O-PLS)
PC	Phosphatidylcholine
PCA	Principle component analysis
PCR	Polymerase chain reaction
PE	Phosphatidyl ethanolamine

PGE₂	Prostaglandins E ₂
PGI₂	Prostacycline
PLA₁	Phospholipase 1
PLA₂	Phospholipase 2
PLS	Partial least square
PPT	Protein precipitation technique
PREDiCCt	PRognostic Effect of Environmental Factors in Crohn's and Colitis
PREDICTS	PRoteomic Evaluation and Discovery in an IBD Cohort of Tri-service Subjects
PS	Posphatidyl serine
PUFA	Polyunsaturated fatty acid
Q	Quadrupole
QC	Quality control
QIT	Quadrupole ion trap
RP	Reversed Phase
S1P	Sphingomyelin 1 phosphate
SCCAI	Simple Clinical Colitis Activity Index
SCFA	Short chain fatty acids
SL	Sphingolipids
SL	Sphingolipid
SM	Sphingomyelin
SNP	Single nucleotide polymorphism
SPE	Solid phase extraction
SPINK4	Serine protease inhibitor
sST2	Soluble suppression of tumourigenicity-2
SWATH	Sequential window acquisition of all theoretical fragment-ion spectra
TFF3	Trefoil factor 3
T_H	Helper T cells
TMS	Trimethylsilylation
TNF- α	Tumour necrosis factor- α
TOF	Time of flight
T_{reg}	Regulatory T cells
Trp	Tryptophan
TXB	Tromboxane
UC	Ulcerative colitis
UNN	University hospital of North Norway
UPLC	Ultra-high-performance LC
VIP	Variable influence on projection
VLCFA	very long chain fatty acid
WSD	Western style diet

1. Introduction

1.1 Inflammatory Bowel Disease

Inflammatory bowel disease (IBD) is a chronic relapsing intestinal disorder, which consists of two major forms, Crohn's disease (CD) and ulcerative colitis (UC) [1]. CD is defined by transmural discontinuous inflammation of the intestine, and could affect any part of the gastrointestinal tract from mouth to perianal area [2]. UC, on the other hand, is a superficial continuous mucosal inflammation extending from the rectum to more proximal colon [3]. The hallmark symptoms of IBD are abdominal pain, bloody diarrhea, and fever [4]. The clinical course of IBD is characterized by periods of remission and exacerbation. Those periods may occur spontaneously or may be induced in response to treatment [5].

1.1.1 Epidemiology

The first descriptions of UC was published in 1859 [6]. CD, on the other hand, was first described later in 1932. Nowadays, IBD has become a global disease affecting 6.8 million individuals worldwide with increasing prevalence [7]. For instance, between 1990 and 2017, the age-standardised prevalence rate increased from 79.5 per 100 000 population to 84.3 per 100 000 population [8]. The highest prevalence rate is in North America with nearly a quarter of global IBD patients living in the USA [9]. By countries, the highest age-standardised prevalence rate is found in the USA (464.5 per 100 000 population), followed by the UK (449.6 per 100 000) [8]. In the Nordic region, the highest prevalence is found in Norway, followed by Sweden (274.4 and 98.7 per 100 000 population, respectively). Interestingly, the incidence is rising in newly industrialised countries in Africa, Asia, and South America [9]. This demonstrates the influences of urban life style, industrial development, and Westernization on the risk of IBD [10]. Notably, UC is seen more commonly than CD [11]. Furthermore, IBD is more common among females than males (57% of prevalent cases occurred among females in 2017) [8]. Although IBD can occur at any age, nearly 25% of IBD patients are diagnosed before the age of 20 [12].

1.1.2 Pathogenesis of Ulcerative Colitis

The pathogenesis of IBD, including CD and UC, involves an interaction between several pathogenic factors such as abnormal gut microbiota, dysregulated immune response, environmental factors, and genomic variation [13]. This interaction triggers immune-mediated intestinal inflammation that leads to the onset of IBD [14]. However, the full etiology and pathophysiology of IBD remains far from being understood [15]. Therefore, the concept of the 'IBD interactome' (Figure 1) has been introduced to define the network of interaction between pathogenic components in IBD [16]. Each of these components will be further discussed in detail. In the current work, only UC patients were included, thus, the pathogenesis of UC will be highlighted.

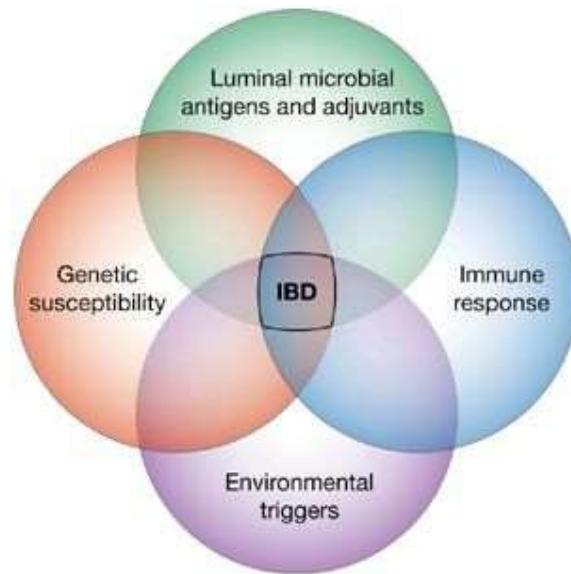


Figure 1. The interactions between genetic, environmental, microbial, and immunological components lead to IBD. This network of interactions is defined as ‘IBD interactome’. Used with permission from [17]

1.1.2.1 Genetic component

Genome wide association studies (GWAS) and meta-analyses have identified variants in 163 loci associated with IBD [18]. Interestingly, 67.5% of the reported loci were risk factors for both CD and UC. However, 23 of the identified loci were UC specific. As expected, >50% of the reported IBD loci overlap with those of other immune-mediated diseases, such as ankylosing spondylitis, psoriasis, and primary sclerosing cholangitis [19]. The largest genetic effects in IBD were found in pathways regulating the adaptive immunity [18]. For instance, single nucleotide polymorphisms (SNPs) in the interleukin-23 receptor (IL23R) [18, 20], the Interleukine-12 subunit beta (IL12B) [21], Janus kinase 2 (JAK 2) [22], and macrophage stimulating protein (MSP) [23] were found to be susceptible for IBD. Among the 23 UC specific loci, the largest effect was found in human leukocyte antigen (HLA), specifically the SNP rs6927022 near the class I gene HLA-DQA1 [24]. Moreover, several SNPs in genes involved in mucosal barrier function have been found to be UC specific, such as Cadherin-1 (CDH1), hepatocyte nuclear factor 4 alpha (HNF4A) [25], organic cation transporter 2 (OCTN2) [26], and human multidrug resistance 1 (MDR1) genes [27].

The study of DNA methylation by epigenome-wide association study (EWAS) revealed 61 UC-associated loci in genes related to inflammatory processes, such as complement factor CFI, the serine protease inhibitor (SPINK4), and the adhesion molecule THY1 [28]. Genetic pathogenesis were supported by a systematic review which included 86,824 UC patients and found the prevalence of a family history of IBD to be 12% [29]. Additionally, in a recent study in UK, which has included 864

Ashkenazi Jewish IBD patients, 40% had a positive family history, and 25% had at least one affected first-degree relative [30]. Despite of those evidences, genetic variances, solely, explained only 14% and 8% for CD and UC cases, respectively [18]. For instance, many of the identified variants are found in healthy individuals as well as IBD patients [31], and most of the reported variants have minor effect [32]. Therefore, other components need to be considered to better understand the role of genetic variation in IBD.

1.1.2.2 Environmental component

It is well established that IBD is a modern society related disease, and several environmental factors are associated with IBD [33]. Accordingly, increased hygiene in developed countries has been linked to the rising prevalence of IBD [34]. In addition, stress and anxiety are associated with the early onset of IBD in both adults and children [14]. Furthermore, socioeconomic, educational and occupational status could affect the IBD pathogenesis [35]. Recently, the term ‘exposome’ has been introduced to summarize the environmental factors a human is exposed to during lifetime. These factors can be categorized in diet, drugs, stress, lifestyle, and previous surgery [36].

Western style diet (WSD) plays a vital role in the onset and progression of IBD [37]. For instance, the high intake of refined carbohydrate, from soft drinks and cakes, leads to alterations in gut microbiota and a higher risk of IBD [38]. Moreover, high animal protein diet, mainly red, white and processed meat consumption, is considered as a risk factor for IBD [39]. Conversely, dietary fibres have a protective effect against IBD [40]. This effect is through improving the microbial composition in the gut, protecting of intestinal barrier permeability, increasing bowel transit time, and increasing the production of short chain fatty acids (SCFA) [40]. Recently, the role of dietary omega 3 and omega 6 polyunsaturated fatty acids (ω -3 and ω -6 PUFAs) in IBD prevention and therapy has been highlighted [40]. PUFA derived bio-active lipids, known as oxylipins, are heavily involved in regulating the immune response during inflammation [41]. For instance, prostaglandins E_2 (PGE_2) and leukotriene B_4 (LTB_4), derived from omega 6 (ω -6) arachidonic acid (AA), contribute to the infiltration of inflammatory cells and tissue injury that characterizes IBD [42]. On the other hand, inflammation-resolving oxylipin termed resolvins, lipoxins, protectins and maresins are produced from ω -3 eicosapentaenoic acid (EPA) and ω -3 docosahexaenoic acid (DHA) [43]. It is hypothesized that the onset of IBD is triggered by an imbalance between pro- and anti-inflammatory molecules, and a deficiency in inflammation resolution mechanism [44]. Indeed, a protective role was found for ω -3 PUFAs in UC [45]. However, the effectiveness of dietary ω -3 PUFAs in the prevention and management of IBD need to be explored further [46]. Notably, studies addressing the direct effect of the exposome on the pathogenesis of IBD have generated more questions than answers [16].

1.1.2.3 Immunological component

Innate immunity mediated by immune, endothelial, and epithelial cells, is a key driver in IBD pathogenesis [47]. For instance, neutrophils play a role in IBD by impairing epithelial barrier function, and realising multiple inflammatory mediators [48]. Moreover, pro-inflammatory macrophages release pro-inflammatory cytokines such as IL-1, IL-6, TNF α , and IL-23 in the IBD- affected mucosa [49]. Furthermore, evidences suggest that intestinal as well as extra-intestinal pathology of IBD is characterized by antibody-mediated immune response [47]. Accordingly, serological levels of anti-neutrophil cytoplasmic antibodies (ANCA) are elevated in 50-90% of UC patients [50].

The differentiation of naïve T cells to the regulatory T cells (T_{reg}) or to the helper T cells (T_{H1}, T_{H2}, T_{H17}) is a crucial step in modulating the immune response IBD [51]. Indeed, inflamed mucosa from UC and CD patients showed an increase in T_{H17} and a decrease in T_{reg} [52]. T_{H17}, under the effect of IL-23, sustains the inflammatory state by attracting neutrophils, releasing several cytokines (TNF, IL-17, IL-22), and suppressing the anti-inflammatory effect of T_{reg} [53]. Interestingly, the treatment with anti-TNF prevent the apoptosis of T_{reg} in UC inflamed mucosa [54]. Despite all these findings, the exact mechanism of the immune response in IBD is not clear. This is mainly due to the complexity in immune cell subpopulations and its function [55]. Indeed, until the last years, Crohn's disease and ulcerative colitis were classified based on type T_{H1}, T_{H2}, and T_{H17} profiles, as well as cytokine profiles. However, this assumption was found inaccurate by experimental and clinical trials [16]. Currently, the differential diagnosis between CD and UC is established based on symptoms, clinical features, endoscopic, and microscopic characteristics [56]. However, the discrimination between CD and UC remains unsolved in up to 10-15% of IBD cases [57]. Therefore, the role of the immune system in IBD should be carefully explored in the light of other compartments.

1.1.2.4 Microbial component

It was hypothesized that the impaired immune response in IBD is driven by 'lack of tolerance' toward the gut microbiota [58]. Accordingly, the higher serological level of antibodies against intestinal flora, e.g. anti-*Saccharomyces cerevisiae* antigen (ASCA) in IBD patients provided the first evidence [58]. This hypothesis led to an increase in studies exploring the role of microbiota in the pathogenesis of IBD [16]. For instance, *Mycobacterium avium paratuberculosis* was the first bacterium to be considered as an IBD pathogen [59]. Studies on faecal microbiota in IBD patients have revealed significant decrease in the total number of species, known as α diversity [60]. In addition, data from intestinal tissues indicated a structural imbalances, or dysbioses, between bacterial species in IBD [61]. Moreover, a study on a large cohort of treatment-naïve CD patients found that the increased abundance in *Enterobacteriaceae*, *Pasteurellaceae*, *Veillonellaceae*, and *Fusobacteriaceae*, and the decreased abundance in *Erysipelotrichales*, *Bacteroidales*, and *Clostridiales*, correlates strongly with disease status [62]. Other studies on both CD and UC patients found a decrease in several taxa within

the *Firmicutes* phylum, and an increase in the *Gammaproteobacteria* [63]. Likewise, *Fusobacterium* species were found to be at higher abundance in the colonic mucosa in UC, and were linked to a higher risk of developing colorectal cancer in UC patients [64]. Conversely, several bacteria can have protective effect against IBD [65]. For instance, *Bifidobacterium*, *Lactobacillus*, and *Faecalibacterium* genera reduce the intestinal inflammation, mainly by improving the balance between anti- and pro-inflammatory cytokines [35]. Similarly, increased levels of *F. prausnitzii* is associated with remission maintenance in UC [66]. The role of microbiota dysbiosis and symbioses in inflamed and normal mucosa is illustrated in figure 2.

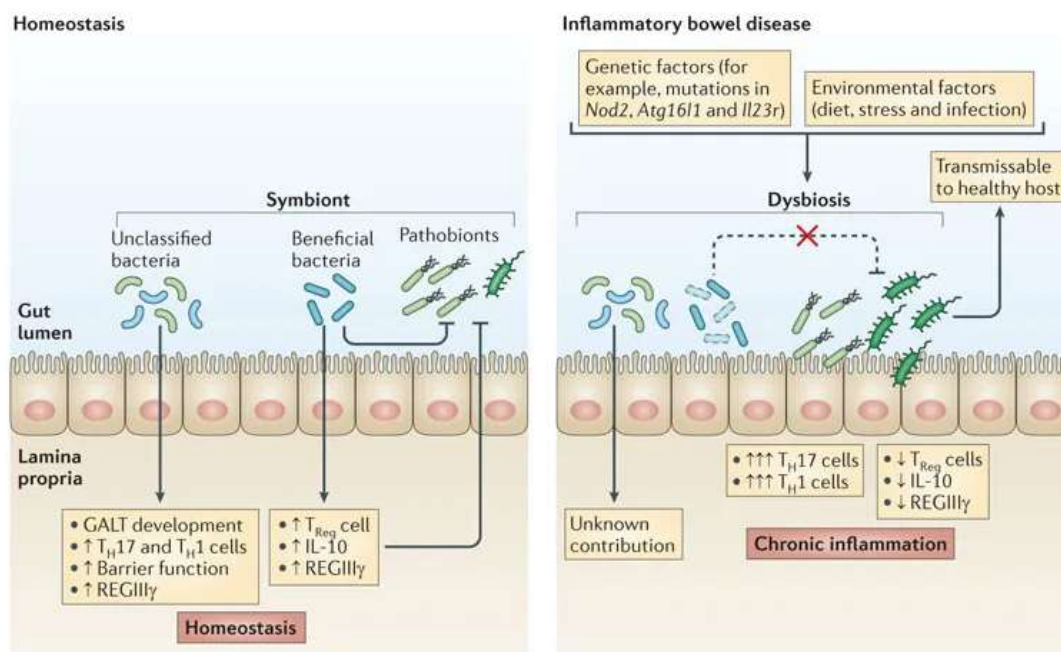


Figure 2. Protective and pathogenic role of the gut microbiota in IBD. Used with permission from [65]

IBD is also associated with functional change (gene metagenome) in the gut microbiota composition [67]. Accordingly, microbiome metagenomics data revealed that 12% of the metabolic pathways are altered in IBD patients compared to healthy subjects [68]. For instance, data show a reduction in the abundance of short chain fatty acid (SCFA) producing bacteria, namely *Ruminococcaceae*, *Odoribacter* and *Leuconostocaceae* [68]. Additionally, the IBD metagenome showed an increase in amino transporter genes [68], sulphate reduction genes [69], and oxidative stress managing genes [68]. Despite all evidence on the disruption of microbiota composition during IBD, results from clinical trials aiming to restore the ‘normal’ composition are inconclusive [63]. As an example, randomized clinical trials of faecal microbiota transplant (FMT) in UC achieved clinical response in only 52% of treated patients [70]. Meanwhile, results from clinical trials with probiotics and antibiotics were inconsistent

[71]. Thus, it is still unclear whether the impaired microbiota is primary or secondary to IBD [16]. Several dietary components have been linked to alterations in the microbiome that have been associated with IBD [72]. For instance, WSD seem to promote the intestinal colonization with IBD-associated pathobionts, such as adherent invasive *Escherichia coli* [73]. Additionally, animal protein-based diets increase the abundance of sulfide reductases and sulfide-reducing bacteria [74].

1.1.3 Management of Ulcerative Colitis

The initial presentations of new UC are symptoms of an acute inflamed rectum, such as, bleeding, urgency, and tenesmus [75]. The main goal of treatment in these patients is to induce clinical remission (quiescence) of symptoms while improving quality of life, and preventing morbidity. However, some UC patients have persistent disease activity even with medical therapy, and 20% of UC patients suffer from a rapid-onset progressive type of UC known as acute severe colitis [76]. Generally, the efficacy of all treatment options is assessed based on their ability to achieve mucosal healing [77]. UC is classified based on the disease severity. Accordingly, the major disease activity scores rank the UC as mild, moderate and severe. The most common scores, such as Mayo score [75], Simple Clinical Colitis Activity Index (SCCAI) [78], and Ulcerative Colitis Disease Activity Index [79], are based on endoscopic findings and the severity of symptoms. Other scores, such as Geboes Score [80], Nancy index [81], and Robarts Histopathology Index [82] are based on histological features. Despite all available scoring systems, there is a lack of an agreement of the definition of endpoint remission [83]. The term ‘deep remission’ was introduced to describe symptomatic and endoscopic remission [84]. Therefore, in the current work, deep remission was defined by both histological and immunological remission. Thus, enrolled subjects in the UC deep remission group met two criteria; Firstly, endoscopic healed mucosa (Mayo score = 0) according to the European Crohn’s and Colitis Organization (ECCO) 2017 consensus [85] and secondly, normalized mucosal TNF- α gene expression level [86]. In addition, UC is classified into three subgroups, Proctitis, Left-sided colitis, and Extensive colitis, according to the Montreal Classification [87]. The main symptoms associated with each of the subgroups is explained in Figure 3.

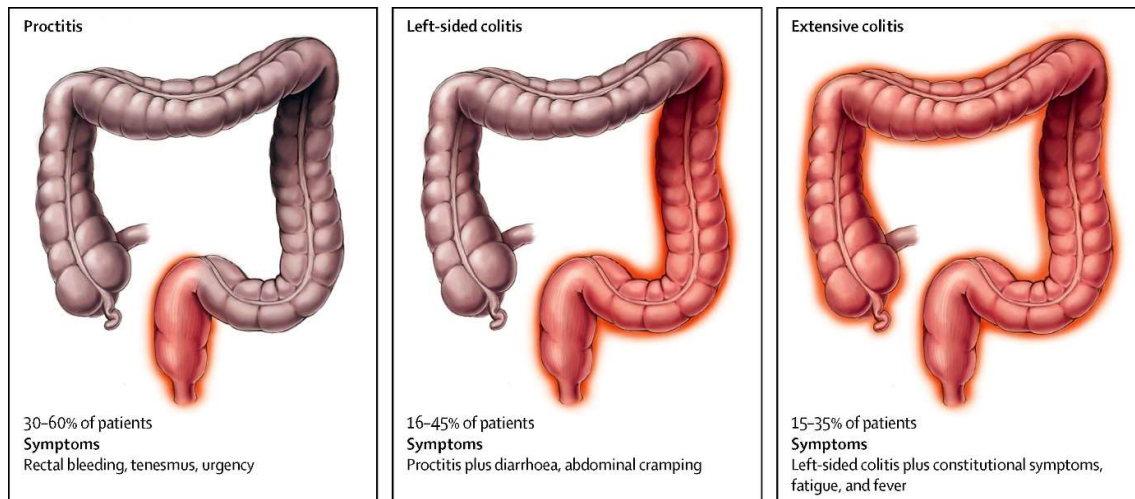


Figure 3. Disease extent, frequency, and symptoms by UC subgroups according to the Montreal classification. Used with permission from [88].

UC is treated based on the disease stage, severity and extent [88]. The treatment options range from topical and systematic treatments to surgery. The first line treatment for mild to moderate UC is 5-aminosalicylic acid (5-ASA) whereas, non-responders to 5-ASA are usually given glucocorticoids [89]. For remission maintenance, UC patients are kept on thiopurines, namely, azathioprine (AZA), and 6-mercaptopurine [88]. Moderate to severe UC, on the other hand, is treated by biologics targeting TNF. Currently used TNF antibodies are infliximab, adalimumab, and golimumab [90]. However, despite available treatment options, surgery is needed in 15% of UC patient [91]. The different treatment options in mild/moderate UC and moderate/severe UC according to the ECCO 2017 consensus [85] are explained in figures 4 and 5, respectively.

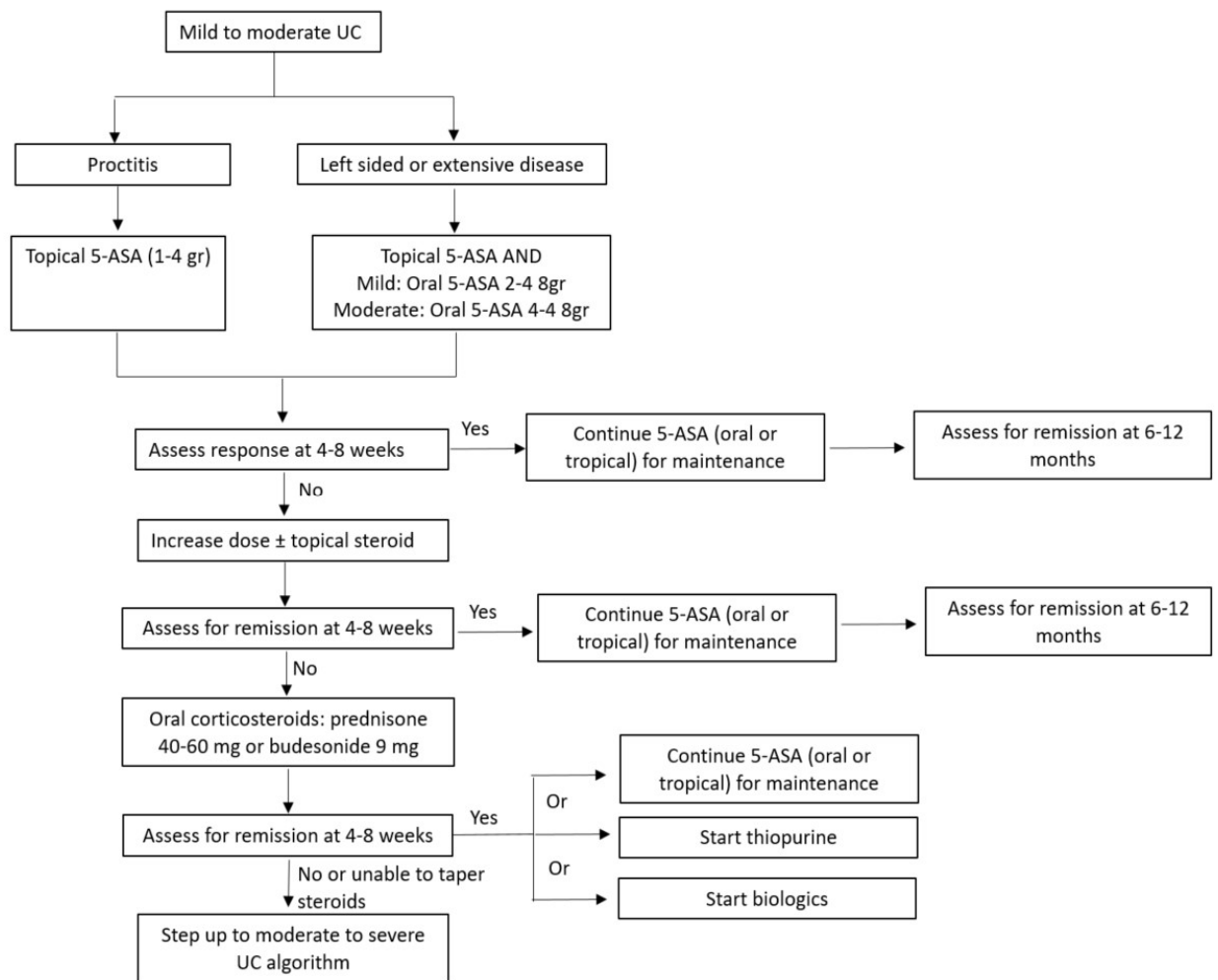


Figure 4. Flow chart for optimized treatment strategy, for mild to moderate UC, according to the ECCO 2017 consensus. Used with permission from [88].

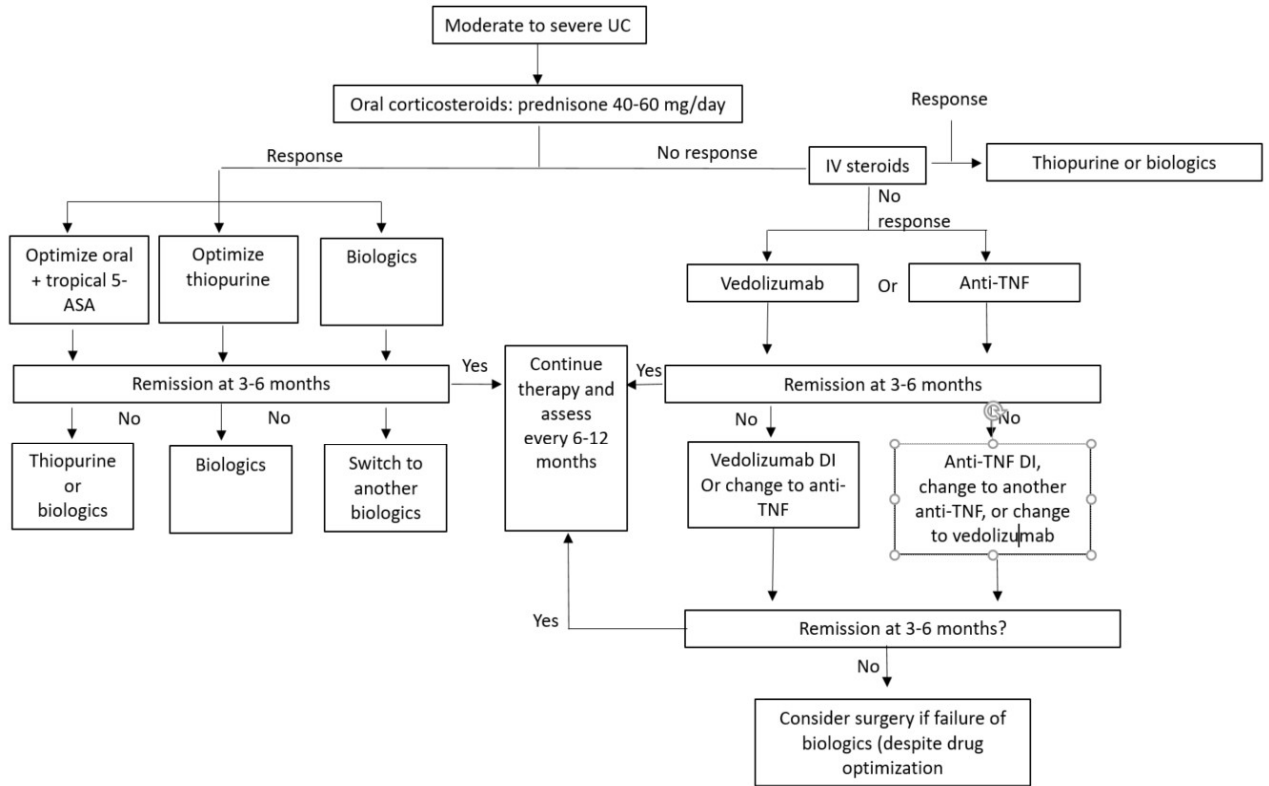


Figure 5. Flow chart for optimized treatment strategy, for moderate to severe UC, according to the ECCO 2017 consensus [88].

1.1.4 Biomarkers for UC

To date, there is no single, non-invasive biomarker for the diagnosis of UC [92]. The diagnosis is established based on a combination of clinical symptoms, laboratory findings, endoscopy, radiology and histopathology [93]. Most available biomarkers are only markers for ongoing inflammation, and serve as a support for diagnosis and initial severity assessment [93].

The best serological markers to differentiate between UC and CD are ASCA and ANCA, where the levels of the latter are higher in UC. However, both antibodies are not specific for IBD [67]. The C-reactive protein (CRP) is a marker for ongoing inflammation. Therefore, despite being non-specific, it can help in distinguishing between quiescent and active IBD [94]. So far, faecal calprotectin (FC) is the most frequently used marker in IBD with good correlation with clinical activity, endoscopic score, and even mucosal healing [92]. Other potential markers have been recently reported, such as serum levels of trefoil factor 3 (TFF3) [95], galectins-1 and -3 [96], and soluble suppression of tumourigenicity-2 (sST2) [97].

In a recent work by Bourgonje et al, the combination of four inflammatory biomarkers (serum amyloid A (SAA), Eotaxin-1, IL-6, IL-8) showed better prediction of UC disease activity than routine measures (CRP, FCal and SCCAI score) [98]. Furthermore, Biasci et al reported the first validated IBD prognostic biomarker [99] where the quantification of 17 genes in treatment naïve IBD patients could predict the need for more aggressive treatment regimen [99]. Moreover, Hamanaka et al found that serum levels of anti-poly ADP-ribose glycohydrolase, anti-transcription elongation factor A protein-like-1 antibodies are higher in patients with refractory UC than in patients with non-refractory UC [100]. Despite the potential clinical application of these markers, these results need to be assessed by large cohorts.

1.1.5 Clinical outcome

As previously mentioned in section 1.1.3, there is currently a lack of agreement on the treatment endpoint or ‘disease clearance’ [84]. Many UC patients relapse after de-escalating the medical treatment [101]. The Inflammatory Bowel South-Eastern Norway (IBSEN) cohort described four different scenarios for the UC clinical course based on a 10 years follow up study of 420 non-surgical UC patients [102]. According to those scenarios, 59% of the UC patients responded to treatment with declining UC activity whereas, 9% of the UC patients kept a chronic ongoing inflammation. Furthermore, 31% of the patients suffered from relapsing episodes followed by remission episodes, while 1% of the patients experienced an increase in the disease activity after treatment. The four UC activity scenarios, defined by IBSEN, are shown in Figure 6. This variation in the UC course requisites a biomarker that can predict the disease outcome, and improve the treatment strategy in the context of personalized medicine [103].

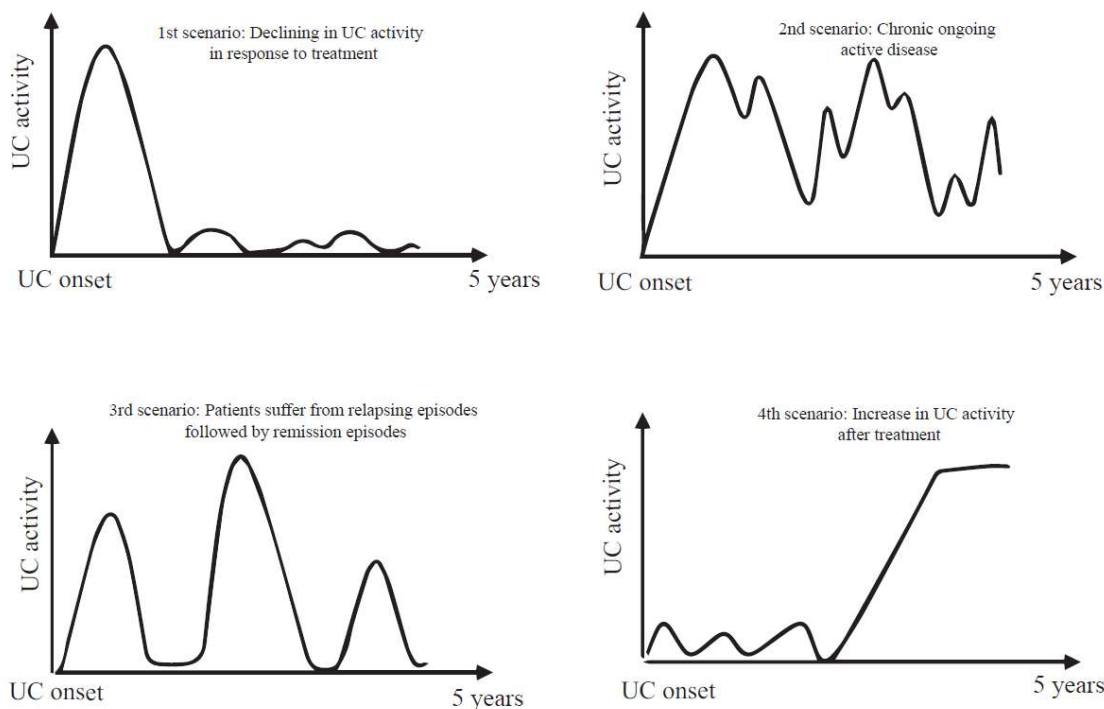


Figure 6. Defined scenarios describing the clinical course of UC in response to treatment after 5 years follow up according to the IBSEN cohort. Used with permission from [102].

Notably, there is an increase in large cohort studies in Europe and USA aiming to predict the onset of IBD, and improve the patients' stratification based on the outcome. One example is the PRoteomic Evaluation and Discovery in an IBD Cohort of Tri-service Subjects (PREDICTS) study [104]. PREDICTS is a retrospective cohort of 1000 UC and 1000 CD patients with 500 matched controls selected from an active duty US military personnel population. The goal of PREDICTS is to find novel serum biomarkers predicting disease risk by capturing pre-disease signals. Ultimately, the study aims to identify novel exposures that increase disease risk [104]. The Dutch IBD biobank study is another example in which, serum, DNA, biopsies and stool samples are collected from 3388 IBD patients [105]. The main intent of this study is to discover predictors (epidemiological risk factors and biomarkers) for individual disease course and treatment response [104]. In the UK, the PRognostic Effect of Environmental Factors in the Crohn's and Colitis (PREdiCCt) cohort is currently recruiting IBD patients [106]. The PREdiCCt objective is to develop a better understanding of the role of the environmental factors and the gut microbiota in IBD flare and recovery. In order to achieve this objective, PREdiCCt is collecting stool, blood, and saliva samples from more than 3000 IBD patients in the state of remission. These studies are a few examples highlighting the importance of big data collection and integration in the management of IBD [107].

1.1.6 ASIB study

The Advanced Study in Inflammatory Bowel Disease (ASIB) is a national and multiregional research project led by the Tromsø IBD group (Dr. Prof. J. Florholmen), and funded by the northern Norway regional health authority. The Tromsø IBD group has introduced a new treatment algorithm with an intensified induction course of biological therapy (anti-TNF) to achieve endoscopic remission, followed by discontinuation of anti-TNF treatment. ASIB, which started in 2016, is based on this treatment algorithm, and involves biopsy collection and follow up of IBD patients from 11 medical regional centers across Norway. ASIB focuses on developing a better understanding of the pathology of the IBD, prediction of severe outcome, and optimizing the treatment strategy. This objective is pursued through full-spectrum “omic” analysis, including tightly coordinated transcriptomic, proteomic and metabolomic profiling on well-stratified UC patients, such as treatment naïve, deep remission, nearly cured etc. Besides the current work, ASIB has reported the first full description of the mucosal proteome [108], and transcriptome [109] in treatment naïve UC as well as the transcriptome in deep remission UC [110]. Additionally, ASIB has highlighted the role of TNF-alpha as an inflammatory mediator in UC [111], and as a predictor of longstanding remission/near-cure of CD [112]. For instance, results from ASIB show that the measurement of the mucosal TNF mRNA at the onset of UC can predict the one year outcome, and provide a better marker to stop the treatment with anti TNF [113]. Thus, ASIB introduced the concept of immunological mucosal healing, defined by normalized TNF gene expression, as the new treatment goal in IBD [114]. In early 2020, ASIB has received additional funding from the northern Norway regional health authority with the aim of establishing specific diagnostics and personalized therapy.

This current work is a part of ASIB, in which we aim to provide the first description of the mucosal metabolome profile in treatment naïve UC. Results from this project, together with results from the transcriptomic and proteomic analysis, aim to dissect the IBD interactome in the context of system biology. This will offer comprehensive insights into molecular networks underlying genetic-microbial-immunological-environment interactions and help formulating data-driven hypotheses to guide personalized medicine.

1.2 Metabolomics and Lipidomics

1.2.1 Definition

The addition of the suffix “omics” to a molecular term implies global, high-throughput investigation of a set of molecules [115]. Therefore, “omics” technologies are the simultaneous assessment of all molecular components in the genome, epigenome, transcriptome, proteome, and metabolome [116]. For instance, metabolomics is the study of the metabolome, defined as the total small bio-molecules, known as metabolites, (<1,500 Da), within cells, biofluids, tissues or organisms [117]. The metabolome is resulted from the interaction between what has been encoded by the genome and modified by environmental factors [116]. Therefore, metabolomics provide information on the functional endpoint of the complex biological network known as the ‘omics cascade’ (Figure 7) [118]. Accordingly, it integrates the gene regulation, post-transcriptional modification, and pathway interactions [119]. Thus, metabolomics is a powerful framework within the context of cell biology, personalized medicine, and systems biology [120].

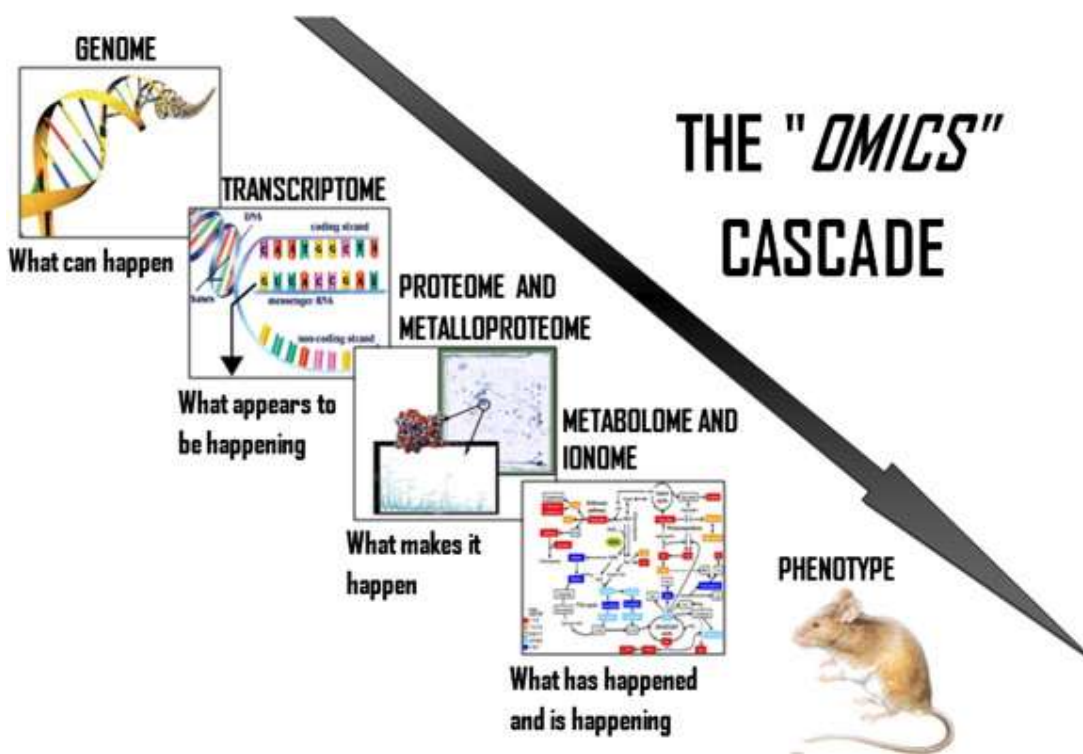


Figure 7. The role of metabolomics as the endpoint of the ‘omics cascade’. Used with permission from [121]

The term ‘metabolites’ constitutes many compounds, such as amino acids, lipids, short peptides, nucleic acids, organic acids, etc. These metabolites are produced endogenously during metabolism (catabolism

and anabolism) [122]. However, metabolites could also be xenobiotic compounds from dietary or environmental origin, such as bacterial byproducts, plant phytochemicals, pollutants, etc [122]. Therefore, the metabolic signature in humans refers highly to age, gender, lifestyle (diet, alcohol, smoking, drugs), and microbiota [123].

Lipidomics, a branch of metabolomics, is the comprehensive quantitative analysis of the lipidome, which consists of all bioactive molecules involved in lipid metabolism, lipid-lipid, and lipid-protein interaction. Lipids play a key role in cellular functions, including cellular membrane formation, signaling pathways, and energy depots [124]. In general, lipids are classified into eight categories: Fatty acids, glycerophospholipids, prenols, sterols, glycerolipides, saccharolipids, polyketides, and sphingolipids (SL), [125]. The corresponding structure for each lipid category is shown in Figure 8.

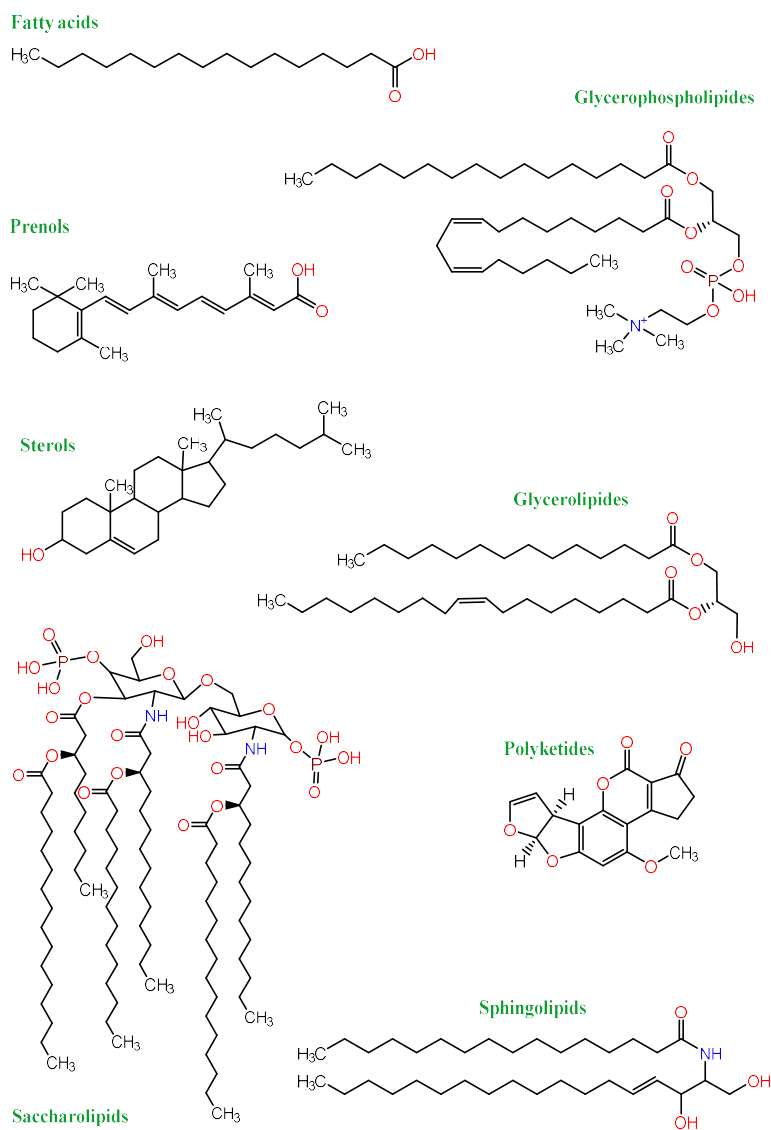


Figure 8. The eight lipid categories with one representative structure shown for each category. Figure made with ISIS/DraW

The first draft of the human metabolome database (HMDB) was published in 2007, in which 2180 human metabolites were characterized and annotated [126]. However, since then, the number of identified human metabolites has increased drastically to achieve 114 100 in the latest HMDB version. Though only 18 557 metabolites were detected and quantified [127]. On the other hand, the number of identified lipid species in the LIPID MAPS Structure Database [128] is 43600 lipids among which 22000 lipids are curated. Therefore, metabolomics and lipidomics analysis are very challenging techniques in terms of complexity, instrumentation, data acquisition, and results interpretation.

1.2.2 Analytical approaches for metabolomics

There are in principle two major kinds of metabolomic approaches which are targeted and untargeted metabolomics analysis [117]. These approaches are also known as metabolic profiling and metabolic finger printing, respectively [129]. The targeted approach focuses mainly on the analysis of a small set of related metabolites with respect to a specific metabolic pathway or to a class of compounds [129]. Thus, the targeted approach is hypothesis-driven, where the metabolites of interest are detected, identified and quantified [130]. Consequently, the targeted approach often reports the absolute concentration using internal standards (IS) [131]. Conversely, untargeted metabolomics are hypothesis-generating approaches intending to capture patterns or “fingerprints” of metabolites that change in response to phenomena (disease, toxin exposure, environmental or genetic alterations) [129]. Therefore, it aims to measure as many metabolites as possible, and provides semi quantitative data (relative abundance) [131]. In the strict, unbiased, untargeted analysis, the metabolites are not necessarily identified since the main objective is to capture all metabolic information. Accordingly, the metabolites are reported as chromatographic peaks “features”, compared through the set of samples, and if necessary, further identified [132]. In this case, usually high-resolution mass spectrometry (HRMS) is used, and several analytical platforms are combined to capture signals for as many metabolites as possible. In addition, statistical and chemometric data analysis approaches are often used to reveal the metabolites of interest [130]. However, a semi-targeted approach is also applicable, in which the metabolites are identified based on existing libraries, and one (or a few) IS are applied for multiple metabolites to provide the approximate concentration [131]. Since the untargeted approach cover a wide range of the metabolome, it is considered as a true ‘omics’ essay [129]. However, the targeted approach is more precise in terms of metabolite identification and quantitation [133].

1.2.3 Analytical platforms for metabolomics

Several analytical platforms are used for metabolomic analysis, such as nuclear magnetic resonance spectroscopy (NMR) [134], Fourier transform-infrared spectroscopy (FT-IR) [135] and mass spectrometry (MS) coupled to separation techniques, such as gas chromatography (GC), liquid chromatography (LC), and capillary electrophoresis (CE), or using direct flow injection [130].

Compared to NMR, MS shows much better sensitivity and ability for high-throughput applications, while NMR profits from a high reproducibility and non-distractive analysis [136]. Notably, MS is used on a larger scale in metabolomics. For targeted metabolomics, generally, all kind of MS devices, mainly triple quadrupole instruments, are applied, and multiple reaction monitoring (MRM) is used for data acquisition. For untargeted screening approaches, MS instruments with high-resolution mass measurements using full scan mode, such as time of flight (TOF) or orbitrap MS, are required [129]. However, it is well established that no single analytical platform is capable of capturing all metabolomic information in a single run [137].

Mainly, for MS-based metabolomics, the analytical workflow includes the following steps [129]:

- Sample preparation
- Sample analysis including metabolite separation and MS detection.
- Data processing
- Data analysis

Each of those steps will be further discussed. The focus will be on LC and GC as the separation technique, and the tissue-based metabolomics since it was applied in this thesis.

1.2.4 Sample preparation

Sample pre-treatment is a key step influencing the qualitative and the quantitative information obtained by the metabolomics analysis, as well as the constancy between different laboratories [138]. The main challenges of sample handling in metabolomics arise from the large diversity of chemical structures and physicochemical properties (such as polarity, stability, solubility, etc) of the metabolites [139]. Additionally, one should keep in mind the great differences in dynamic range (up to nine decades) of the metabolites present in a biological sample [140]. Thus, the tissue sampling procedure should be performed from the same part of the tissue through the whole experiment, and contamination with blood should be avoided [141].

Furthermore, the sampling process has a vast impact on the metabolite concentrations due to the high turnover rate (up to the order of 1 s for compounds like ATP and glucose 6-phosphate) [142]. Therefore, it is crucial to stop the enzymatic activity to ‘quench the metabolism’ [142]. This is usually achieved in tissue sampling by snap freezing using liquid nitrogen [143]. For cultured cells, quenching is done by the addition of hot or cold organic solvent [144, 145]. Additionally, in the clinical setting, the time between biofluid or tissue sampling and sample extraction or sample storage at low temperatures (-20 or -80°C) is a major source of bias in data reproducibility and interpretation [141]. Accordingly, thawing-freezing cycles should be avoided, since it increases the level of metabolites involved in cell degradation (purine and pyrimidine metabolism), such as fatty acids (FAs) and amino acids [146]. Conversely, levels of other metabolites seem to be decreased by thawing, such as taurine, myo-inositol-1-phosphate, pyruvic acid, *o*-phosphoethanolamine, adenosine-5-monophosphate, cholesterol,

galactonic acid, and monomethylphosphate [146]. The metabolite levels are also affected in thawed serum samples. However, the changes are less drastic than those occurring in tissue samples [147]. A few markers for sample pre-treatment quality has been suggested, such as lactate/glucose ratio for global metabolomics and phosphatidylcholine (PC) hydrolysis to lysophospholipid (LPC) for lipidomics [148].

In general, a sample preparation protocol for a metabolomics workflow contains a solvent extraction step, followed by ultrafiltration, and optionally, solid-phase extraction and a chemical derivatization step, which is followed by evaporation and reconstitution [149].

Sample pretreatment strategies differ depending on the analytical approach (targeted or untargeted). For instance, it is recommended that the sample handling should be minimal for the untargeted approach in order to prevent the loss of metabolites. Consequently, sample pre-treatment should include non-selective methods such as, “dilute and shoot” and solvent-protein precipitation [139]. Conversely, the sample pre-treatment for targeted approach can be less straightforward, as the goal is often to extract the compounds of interest while removing most of the background components. Therefore, a step including liquid liquid extraction (LLE) and/or solid phase extraction (SPE) is usually added in order to reduce matrix interfering effects, and to enrich the targeted metabolites [139]. Isotopically labelled IS are commonly added to correct for the metabolite loss during the sample preparation [131]. For targeted analysis, the ideal IS is a carbon and/or nitrogen isotope labelled version of the metabolite of interest, present at a concentration within the range of the expected metabolite concentrations. However, for semi targeted analysis, it is common to add a number of IS representing selected important metabolite groups [150].

The type of sample is also a defining factor for the sample treatment workflow. Tissue samples require homogenization using physical techniques such as ball grinding or cooled mortar and pestle [151], which makes the application of fully automated processes limited [152]. The next step is usually protein removal by organic solvent-based protein precipitation (PPT) followed by centrifugation, or membrane-based techniques, such as ultrafiltration [138]. However, the metabolites co-precipitation with proteins and/ or poor solubility in the selected extraction solvent may affect the reproducibility of the analysis and the coverage of the metabolome [153]. Therefore, the choice of solvent system has more influence on metabolite selection compared to the sample-homogenization methods [154]. Importantly, the ratio of solvent to tissue should be as identical as possible throughout all samples to assure a similar level of metabolite recovery [155].

In terms of solvent system, LLE methods are either monophasic (one miscible solvent system) or biphasic (two immiscible solvent layers) [156]. The monophasic extraction usually involves the use water/methanol or water/acetonitrile as solvent system providing a good coverage of the metabolome [156]. However, biphasic extractions, containing water and methanol with a non-polar solvent is better in terms of separating the water-soluble metabolites from the non-polar lipids. Therefore, for lipidomic

analysis, the solvents of choice are chloroform/methanol/water (Folch method), chloroform/methanol (modified Folch method), methyl tert-butyl ether (MTBE)/methanol/water (MTBE method), and butanol/methanol (BUME method) [157]. Recently, an MTBE-based extraction method was developed allowing the analysis of both polar and the non-polar metabolites. In this method, the whole sample preparation and analysis is within and from a single LC vial. Thus, it is called “in-vial dual extraction” [158].

It is common to add a SPE step for targeted metabolomics to increase the method selectivity, and to enrich the hydrophobic metabolites [139]. However, SPE based methods could also be applicable for untargeted metabolomics. For instance, a mixed-mode solid-phase (reversed-phase and anion-exchange) extraction method have been used to fractionate the metabolites into hydrophilic amine, hydrophobic amine/alcohol, and organic acid groups expanding the detected metabolite range in LC-MS [159]. Moreover, fractionation using a combined LLE, and SPE (NH₂) prior to the MS analysis proved to increase the coverage in untargeted metabolomics [160]. The last step of sample preparation is the evaporation and reconstitution. This allows increasing the concentration of metabolites while selecting a suitable solvent for the analysis [139].

Sample preparation for GC-MS involves a chemical derivatization, which is often required at a functional group to reduce polarity and increase thermal stability and volatility. Mostly, this is done via a two-stage process of oximation followed by trimethylsilylation (TMS) [139]. This is performed on the hydrogens in functional groups, such as -COOH, -OH, -NH, and -SH resulting in TMS ethers, TMS esters, TMS sulfides or TMS amines [129]. Silyl derivatives have a better thermal stability, lower boiling point, and produce more distinct MS spectra than their underivatized precursors [129]. However, extra care need to be taken to void contact with moist, and a drying step of the sample extract is required prior to the derivatization [129].

1.2.5 Metabolite separation

Several metabolomic methods utilizing direct injection into the MS have been reported previously [161, 162]. However, this technique is limited due to ion suppression, and poor separation of chemical isomers [129]. Therefore, it is common to use inline chromatography to overcome those analytical drawbacks, and to increase both sensitivity and specificity of the analysis of the metabolites [132]. Accordingly, LC-MS is the most frequently used separation method in global metabolomics [163]. However, one single LC run is not able to cover the wide range of metabolite polarities. For instance, reversed-phase (RP) chromatography, which is the most frequently used method for metabolomics, is not appropriate for highly polar and/or ionic species [136]. Conversely, the hydrophilic interaction chromatography (HILIC), used for polar metabolites (amino acid and organic acid), needs a longer re-equilibrium time, and shows retention time drifts [120]. Therefore, it is recommended to combine both RP and HILIC chromatography to achieve an acceptable coverage of the metabolome [164]. The introduction of ultra-

high-performance LC (UPLC) allows for the use of smaller particle size sub-2 μm , and high pressures up to 22 000 psi. This has led to improved peak width, shorter run times, increased peak capacity, and reduced mass spectral overlap. Consequently, UPLC leads to a better separation and identification of metabolites [165].

For RP separation, it is common to apply a gradient starting with a high aqueous content to a high organic phase. Additionally, buffer modifiers (formic acid, acetic acid, and ammonium acetate etc) can be added to improve the ionization and the separation [165]. In contrast, HILIC is based on the use of a polar stationary phase and a high proportion of organic mobile phase with at least 3 % water [165]. Recently, a combined dual HILIC and RP run was developed to merge lipidomic and metabolomic analysis [166], and an on-line HILIC and RP workflow was suggested to cover polar and non-polar lipids in one single run [167]. GC-MS is the method of choice for the analysis of volatile and semi volatile metabolites [168]. This is mainly due to the high-resolution and reproducible chromatographic separation, precise metabolite identification and quantification, and relatively low cost for maintenance [168]. However, GC-MS analysis is limited by a sufficient vapour pressure and thermal stability of the metabolites [129]. The preferred stationary phase for global metabolomics analysis is ionic liquid stationary since it exhibits “dual nature” retention behaviour. Accordingly, polar molecules are separated as if the stationary phase is polar, while nonpolar molecules are separated as if the stationary phase is nonpolar [169].

1.2.6 Metabolites detection and quantification by MS

The number and class of metabolites detected by MS depend on the choice of ionization mode. Therefore, due to the complexity of the metabolome, it is recommended to carry out the MS analysis using both positive and negative ionization modes under scan range of m/z 50–1000 [170].

Electrospray ionization (ESI) is a soft ionization technique where charged droplets are generated by applying a strong electric field on aerosol formed by passing the liquid through a capillary tube [171]. ESI is the most frequently used ionization technique in LC-MS based metabolomics due to the ability to produce intact molecular ions [170]. However, one limitation for ESI is ion suppression, which can occur when several metabolites are introduced simultaneously to the ionization source [129]. Bases, ketons, and ethers are ionized efficiently in positive mode and give good signal. Conversely, metabolites containing alcohol group alone, such as sugars, and organic acids are best detected in negative mode. Notably, acids containing a protonatable group such as amine or keton, are better detected in positive mode [172]. For lipid analysis, acylcarnitines, PC, LPC, phosphatidyl ethanolamine (PE), lysophosphatidyl ethanolamine (LPE), and sphingomyelins (SM) are ionized better with ESI in positive mode. In contrast, free FAs, phosphatidic acid, phosphatidylserine (PS), phosphatidylinositol, and phosphatidylglycerol are ionized better by negative mode ESI [129]. Atmospheric pressure chemical ionization (APCI) and atmospheric pressure photoionization (APPI) are used complementary to ESI, mainly for the analysis of non-polar and thermally stable metabolites such as lipids [170]. For instance,

the use of both APCI and ESI increased the coverage of the erythrocyte metabolome by 34 % [136]. APCI utilizes gas-phase ion-molecule reactions at atmospheric pressure. APPI, on the other hand, uses photoionization via a vacuum-ultraviolet lamp as source of photons [157]. The range of application for APCI, APPI, and ESI is shown in Figure 9.

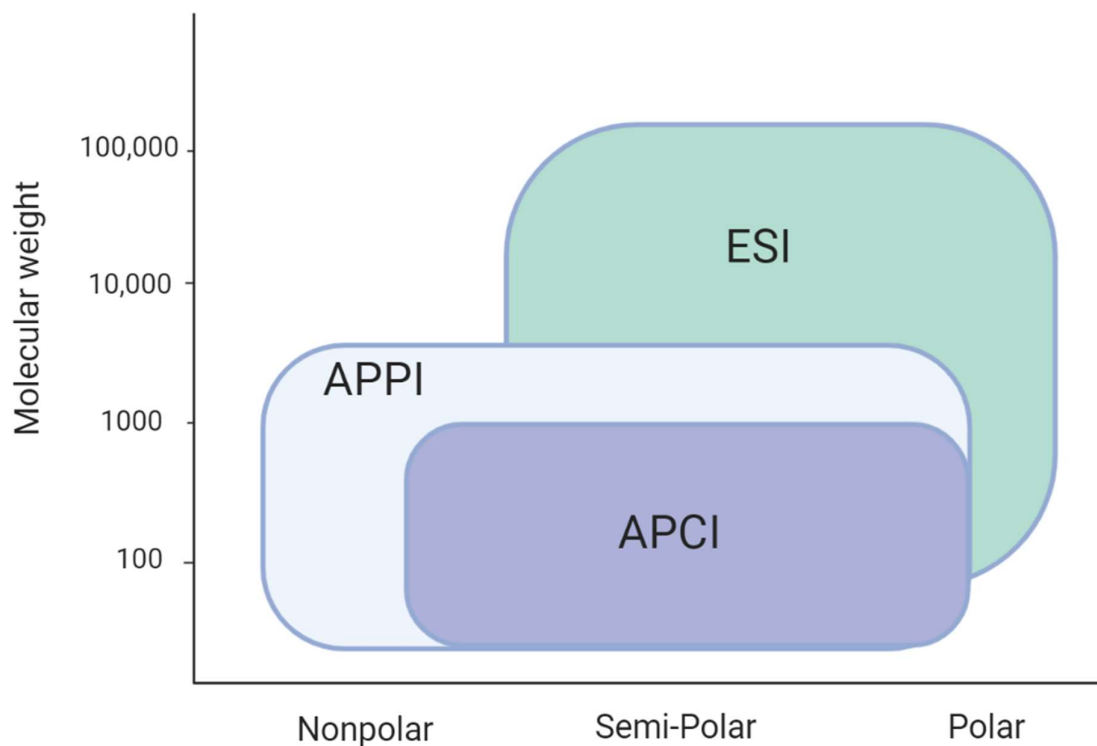


Figure 9. Range of application of APPI, APCI and ESI according to the polarity and the molecular weight of metabolites. Figure made with Biorender.

Electron impact (EI) is the ionization method of choice for GC-MS analysis. EI is a hard ionization method that causes a highly reproducible fragmentation of metabolites with minimal matrix effects [173]. The ionization and the fragmentation pattern are based on the nature of the metabolite. Therefore, EI is useful for distinguishing and identifying the metabolites using MS libraries [136] such as NIST [174].

Mass analysers can be categorized into low resolution MS such as quadrupole (Q) (also known as mass filter), linear ion trap (LIT), quadrupole ion trap (QIT), and into high resolution MS such as TOF, Fourier transform ion cyclotron resonance (FTICR) and orbitrap [173]. It is common to arrange mass analysers in a tandem configuration, such as triple quadrupole (TQ), quadrupole-TOF (Q-TOF), triple-quadrupole ion trap (QTrap), and the 'Orbitrap instruments family', which comes as quadrupole orbitrap (Qexecutive), ion trap orbitrap (Elite), and linear-quadrupole ion trap-Orbitrap (LTQ-Orbitrap), also known as Tribrid orbitrap (Fusion, Lumos, IDX). These techniques allow ion fragmentation by

collision-induced dissociation (CID) in either the quadrupole or ion trap [173]. The most frequently used mass analysers with GC for metabolomics are TQs or TOFs [173]. Q-TOF and LTQ-Orbitrap provide simultaneous MS/MS experiments for the structural elucidation and confirmation of the metabolites by screening for the neutral losses and characteristic ions [129]. In addition, Q-TOF, Qexective, and LTQ-Orbitrap achieve both high mass accuracy (1 ppm) and low detection limits (fg-pg) for the quantitation of metabolites. [170]. Consequently, Q-TOF, Qexective, and LTQ-Orbitrap are mostly used for untargeted LC-based metabolomics.

In the context of the identification of metabolites, two data acquisition techniques are available: data dependent acquisition (DDA) and data independent acquisition (DIA). In DDA, the instrument switches automatically to MS/MS based on the abundance of the precursor ion. However, this might miss low abundance metabolites, and can cause MS/MS overlap when several metabolites are included in the same mass window. On the other hand, DIA aims to obtain MS/MS data on all ions from all samples for metabolite identification. However, this generates complex spectra that complicates the linking with the precursor ion [175]. Sequential window acquisition of all theoretical fragment-ion spectra (SWATH) is the main DIA approach, which includes an isolation mass window of 20–50 Da and reduces the number of interfering ions [125]. Another DIA approach is all ion fragmentation (AIF) acquisition, which includes creating an MS/MS library with a focus on the retention time [176].

1.2.7 Data processing

The aim of data processing in untargeted and semi-targeted metabolomics is to convert the raw data into a standard and uniform format that facilitates the biochemical interpretation. Data processing workflow typically includes a peak-picking or peak deconvolution process followed by peak alignment, which ultimately yields a set of features across samples with a unique m/z and retention time [177]. The aligned peaks are integrated as peak area, and assigned to the corresponding feature in the data table. [178]. Various softwares are available to perform the processing, such as MarkerLynx (Waters), MassHunter (Agilent), MarkerView (AB Sciex), XCMS, MZmine, and Progenesis QI (Waters) [179]. When open access softwares are used, it is common to convert the raw data file from manufacturer format (such as .d) to a universal form that can be ‘read’ by different open access software. The widest used form is network common data form (NetCDF) which is a binary data format [129]. Several pre-processing steps are usually needed to reduce the size of the raw data file such as ‘centroiding’, and ‘data binning’. Data compression by ‘centroiding’ reduces the MS file size by combining multiple data points from the same peak into a single data point with one m/z and intensity value [180]. In ‘data binning’, the m/z axis is divided into equally sized ‘bins’, which transforms of raw data into an (x,y) matrix, retention times in the rows (x-direction) and m/z values in the columns (y-direction) [180].

Semi-targeted metabolomics involves similar approaches. However, it includes a final step for metabolite identification (or annotation). This step uses an in-house library, or external library, to

annotate the extracted features [180]. There are four levels for metabolite identification defined by Metabolites Standards Initiative [181]. Level 1 is the definitive identification using authentic chemical standards analysed under identical analytical methodology. Level 2 and 3 refer to identification by comparison against literature and data sets. Level 4 refers to unknown compounds [181].

1.2.8 Data normalization and scaling

Metabolomic data are usually pretreated prior to statistical analysis to reduce the systematic bias in the data. Thus, data pretreatment strategies are mainly data normalization and data scaling [180]. Notably, normalizing the data reduces the difference between samples (or within chromatograms) whereas, scaling the data allows comparing the metabolites (or chromatograms) [180].

Sample normalization is usually performed using chemical or mathematical approaches. The chemical approach is based on the use of single or multiple IS. Mathematical normalization uses computation models based on the quality control samples (QCs) [180]. Each variable is individually corrected according to its value in the neighboring QCs [182], or based on the average or on the median of the QCs [183]. A simpler normalization strategy is done by calculating the relative abundance of metabolites with respect to all other metabolite peaks in the same sample (e.g. unit normalization [184] or median intensities normalization [185]).

Scaling strategies are based on dividing each variable by a variable-specific factor, the scaling factor. This aims to reduce the magnitude of difference between metabolites by converting the data into relative concentrations with respect to the scaling factor [186]. The most frequently used scaling method is autoscaling, which provides equal variance to each variable. Additionally, transformation methods, such as log transformation and power transformation, provide a pseudo scaling effect, and reduce the data heteroscedasticity [186].

1.2.9 Data analysis

A metabolomics data set can include up to hundreds (or even thousands) of features. Thus, it is important to choose statistical test carefully. Multivariate data analysis (MVA) offers a powerful tool for the analysis of complex metabolomics data. Principle component analysis (PCA) is an effective, unsupervised dimension reduction tool that is used to detect outliers and to spot trends in the data [187]. Hierarchical clustering, which is also an unsupervised clustering method, is useful to spot clustering patterns in high dimensional space [188]. To identify the most interesting molecular features, Partial least squares (PLS) is frequently used as supervised learning methods. PLS can be used as a predictive and descriptive modelling method as well as for classification [189]. In this context, it is called partial least squares discriminant analysis (PLS-DA) [190]. Orthogonal projections to latent structures (O-PLS) is an extension to PLS with addition of an orthogonal signal correction filter [191]. In OPLS, systematic variation from X (descriptor variables) that is orthogonal to Y (property variables) is filtered out. This

means the removal of variation in X that is not correlated to Y to improve the interpretational ability of the data [192]. Both OPLS and PLS rank the variables according to the variable influence on projection (VIP), which facilitate the data interpretation [193].

1.2.10 Biomedical interpretation

The ultimate step for an ideal untargeted metabolomics workflow is putting the identified metabolites of interest into biological context. Therefore, pathway analysis is performed to better understand the biological relevance of the metabolite alteration [180]. However, this step might not be required for targeted metabolomics in which the metabolic alteration is predicted, and the analysis lead to confirming (or discarding) this prediction [180]. Several open access tools are available for integrated pathway analysis such as metaboanalyst [194], which is based on HMDB and Kyoto Encyclopedia of Genes and Genomes (KEEG) [195]. Nevertheless, there is lack in pathway analysis tools for lipidomics data, since the available softwares group several lipid species “as one node” under the same lipid class.

1.2.11 Metabolomics in IBD

Multiomics approaches were suggested to tackle the overwhelming complexity of the IBD interactome. Accordingly, integrating genomic, epigenomic, transcriptomic, proteomic, metabolomic and microbiome information could map the molecular landscape of IBD [16]. In this context, genomics and proteomics data provide mainly extensive information regarding the genotype, whereas metabolomics reflects the effects of gene regulation, post-transcriptional regulation and pathway interactions [196]. In addition, depending on the chosen matrix, metabolomics capture the host-microbiome interaction signatures [197]. For instance, gut microbiota composition is reflected mostly in the faecal metabolome, which explains approx. 68% of microbial variance [198]. Notably, the metabolite profile is related to age, gender, lifestyle, medication, and many other environmental factors [123]. Therefore, metabolomics is a core component in unravelling IBD interactome and improving the stratification of patients into IBD subtypes toward personalized treatment. However, results from metabolomic studies in IBD are inconstant and inconclusive. For instance, Kolho et al [199] described the metabolic changes in pediatric UC patients compared to healthy controls by analyzing serum and fecal samples. Fecal metabolomics showed alterations in several pathways especially the taurine and hypotaurine metabolism. The serum metabolomic profile, on the other hand, revealed alterations in several amino acid metabolism pathways such as tryptophan (Trp), serine, and methionine. Additionally, it has been reported alterations in bile acid biosynthesis and sphingosine metabolism. Surprisingly, Daniluk et al [200] only found perturbation in phospholipid (PL) related metabolites in the serum of pediatric UC patients compared with controls. Bjerrum et al [201] performed faecal metabolomic analysis on treated UC patients, and found increased levels of amino acids and decreased levels of SCFA. Interestingly, the urine metabolome of IBD patients showed significant changes in amino acids, hippurates, and citric acid

cycle intermediates [202]. However, these results were less consistent with the serum metabolome profile in UC patients described by other studies. For instance, Scoville et al [203] reported only 5 significantly altered metabolites in UC patients' serum compared with healthy controls. These metabolites were related to bile acid metabolism and SL metabolism. Similarly, there are disagreement among results from lipid analysis in UC. For instance, Fenling et al [204] found only 5 lipid species within the PL class that changed significantly in UC patients serum compared to healthy controls. In contrast, Bazarganipour [205] reported major disruption in ceramides (Cer) and SM which correspond to UC activity and severity. Murgia et al [206] reported significant perturbations in FAs, PC, and LPC in IBD patients' serum compared to control.

Besides the differences in reported characteristic metabolic changes in IBD, most of the studies were able to differentiate between CD and UC patients regardless of the biological matrix [196]. However, other metabolomics studies failed to distinguish between inactive and active IBD based on urine [207] and breath [208] samples. Conversely, Hisamatsu et al [209] distinguished between active and quiescent IBD based on plasma amino acid profiles. Finally, there is a lack of studies correlating the metabolomic profile with the ongoing disease activity with only one study linking the faecal metabolome in IBD patients with the severity score. However, patients included in this study were undergoing different treatment regimens [210].

The integration of the faecal metabolome and metagenome profiles can provide insight into the gut microbiome composition and function in IBD. For instance, a large cohort of 161 IBD patients and healthy controls revealed association between differentially abundant bacterial species and differentially abundant metabolites [211]. For instance, IBD-associated metabolites, such as ω -3 and ω -6 PUFAs were negatively associated with control-associated species, such as *Eubacterium ventriosum* and positively associated with IBD-associated species, such as *Ruminococcus gnavus* [211]. Furthermore, the faecal metabolome in IBD patients was characterized by increased amino acids, SL, PC and bile acids, and decreased LCFA, triacylglycerols and tetrapyrroles [211].

In another large cohort, Lloyd-Price et al performed integrated multi-omic analysis (metagenomics, metatranscriptomics, metaproteomics and metabolomics) on stool, colon biopsies, and blood samples collected from 67 CD patients, 38 UC patients, and 27 healthy controls [212]. Metabolite profiling demonstrated decreased levels of SCFAs and secondary bile acids in dysbiosis. Moreover, dysregulation of acylcarnitine levels were particularly highly correlated with dysbiosis. Metabolite changes during periods of disease showed increased levels of PUFAs (adrenate and arachidonate), while nicotinuric acid was exclusively found in stool samples of IBD patients [211]. Network analysis identified key dysbiosis-associated network hubs including bacterial species, such as *F. prausnitzii*, unclassified *Subdoligranulum*, *Alistipes*, *Escherichia coli* and members belonging to *Roseburia*, as well as metabolites, such as SCFAs, octanoyl carnitine and several lipids [212]. Furthermore, Bjerrum et al performed metabolomics and transcriptomics on colon biopsies taken from 22 active UC patients, 21

UC remission patients, and 15 healthy controls. The combination of the two omics datasets was able to discriminate between active UC, remission UC, and controls; as well as between early or late disease onset [118].

A recent review article on integrating omics in IBD has marked the lack of multi omics integration approaches, and the insufficiency of molecular signatures that can differentiate between IBD subtypes or between disease relapse and remission [213]. Moreover, the available omics data in IBD are inconsistent, probably due to differences in methodological approaches, design of experiments, lack of stratification of patients, and biological material used for analysis [123, 214]. Notably, there is a scarcity in studies on the mucosal metabolomic profile in IBD even though it is well established that tissues are under greater homeostatic regulation than plasma [215], which can provide a better understanding of the molecular basis of diseases [216]. In addition, a description of the mucosal lipid status in UC is lacking despite the important role of the membrane bioactive lipids in modulating the immune response during inflammation [217].

2. Aims of the study

The main hypothesis of the current work is that the onset of UC is characterized by metabolic signatures leading to the induction of inflammatory response. Therefore, by capturing these signatures in inflamed mucosa from treatment naïve patients we can improve the understanding of the IBD interactome. Additionally, the identification of the key molecular drivers in UC would be valuable in achieving precise (personalized) treatment via patients stratification based on disease activity, response to treatment, and clinical outcome. Thus, the objectives of this work are as follows:

- To describe the mucosal metabolic landscape in treatment-naïve UC patients.
- To assess the ability of metabolomics and lipidomics in discriminating between treatment-naïve UC patients, deep remission UC patients and healthy controls.
- To map the mucosal changes in bioactive omega-3 and omega-6 polyunsaturated fatty acid metabolites in treatment-naïve UC patients compared to deep remission UC.
- Identify metabolic bio-signatures of potential clinical value in defining the severity of the inflammation and predicting the disease outcome.

3. Methods

3.1. Biopsies collection

In the current work, colon biopsies were obtained from the ASIB study's biobank at the University hospital of North Norway (UNN). The study and the storage of biological material were approved by The Regional Committee of Medical Ethics of North Norway and the Norwegian Social Science Data Services under the number (REK NORD 2012/1349). All enrolled subjects have signed an informed consent form, and the study was conducted according to the declaration of Helsinki.

Only treatment-naïve UC patients were included in the active UC group, while UC patients in deep remission induced by treatment with biologics were considered in the UC remission group (as described in session 1.1.3). Subjects undergoing endoscopy for colonic cancer screening examination with normal findings (no ulcer, no redness) and normal colonic histological results, served as healthy controls. In order to evaluate the degree of the inflammation activity, the mucosal TNF- α mRNA expression levels in all enrolled subjects were measured by real-time Polymerase chain reaction (PCR), as previously described [111]. All biopsies were acquired from the rectum except few samples from the treatment-naïve patients that were obtained from the sigmoid. In active UC patients, biopsies were obtained from the inflamed mucosa. The biopsies' dry weight ranged from 2–8 mg. After collection, all biopsies were snapped frozen immediately at -80 °C, and kept at this temperature until further analysis.

3.2. Global metabolomics by GC-MS

Metabolite extraction was performed using a mix of methanol:water (8:1) as described previously [218]. 150 μ L was pooled from each extract for GC-MS analysis. Prior to the analysis, a derivatization step was carried out by an oximation step using methoxyamine solution in pyridine, followed by trimethylsilylation using TMS and a methyl-N-(trimethylsilyl) trifluoroacetamide MSTFA [219]. Metabolite analysis was done by means of GC-TOF-MS as previously described [219]. The GC system was an Agilent 6890 GC equipped with a DB 5-MS capillary column (10 m \times 0.18 mm I.D.), and coupled to a Pegasus III TOF-MS system. Data processing was done as follows; A Matlab based in-house script was used for baseline correction, chromatogram alignment, and peak deconvolution. Metabolites were identified based on the retention index values and MS spectra from the in-house mass spectra library. Furthermore, GC-MS metabolites were normalized by internal standards, and submitted to data analysis.

3.3. Global metabolomics by LC-MS

Metabolites extraction was performed using a mix of methanol:water (8:1) as described previously [218]. 200 μ L was pooled from each extract for LC-MS analysis. Metabolite analysis was done by means of UPLC-QTOF-MS/MS as previously described [219]. The UPLC system was an Infinity 1290

Agilent equipped with an Acquity C18 column (HSS T3, 2.1 × 50 mm, 1.8 μm), and coupled to an Agilent 6550 QTOF MS. Each sample was injected twice in positive and negative ionization mode. Data processing was carried out using Agilent MassHunter ProFinder software, whereas in-house databases with exact masses and experimental retention times were used for identification. UPLC–MS metabolites were normalized by the total peak areas, and submitted to data analysis.

3.3. Global lipidomics by LC-MS

Lipids extraction was carried out using a mixture of chloroform:methanol 2:1 according to the modified Folch extraction method [220]. Lipids were analysed by means of UPLC-QTOF-MS/MS as previously described [220]. The UPLC system was an Infinity 1290 Agilent equipped with an Acquity C18 column (CSH, 2.1× 50 mm, 1.7 μm), and coupled to an Agilent 6550 QTOF MS. Each sample was injected twice in positive and negative ionization mode. Data processing was performed by Agilent MassHunter ProFinder software. An in-house databases with exact masses and experimental retention times were used for lipid identification. Prior to data analysis, peak areas of individual lipid species were normalized by the sum of peak areas of all detected lipid species in the same lipid class.

3.4. Targeted metabolomics by LC-MS

For the targeted oxylipin and endocannabinoid (eCB) analysis, the extraction was done using methanol, followed by SPE protocol (using OASIS-HBL-EA cartridge) developed by Gouveia et al [221]. Targeted analysis was performed using UPLC-TQ-MS/MS based method [222]. The UPLC system was an Agilent UPLC system (Infinity 1290) equipped by an Acquity C18 column (BEH 2.1 mm × 150 mm, 1.7-μm), and coupled to an Agilent 6490 triple quadrupole. Each sample was injected twice for UPLC-ESI-MS as follows: positive ionization mode for eCBs, negative ionization mode for oxylipins. Data were acquired by a MRM method that is described elsewhere [221]. The absolute quantification (as pg/mg of colon tissue) was carried out using a 8-point calibration curve with pure standards. For each of the targeted compound, a suitable labelled IS was selected based on structural similarities. Hence, a total of 13 labelled IS were used.

3.5. Data analysis

For the global metabolomics and lipidomics, differences in the mean relative concentration among the study groups were identified using Kruskal–Wallis test followed by dunn test [223] as post hoc test. Acquired P values were adjusted using Benjamini and Hochberg false discovery rate (FDR) method [224]. For targeted data, significant differences in the mean concentration of metabolites were identified by Mann-Whitney U test at a fold change (FC) of 2 and FDR cut-off of 0.1.

MVA was applied on auto scaled and mean-centred data. The quality of the built OPLS-DA model was assessed by R^2X_{cum} , R^2Y_{cum} and Q^2_{cum} , whereas, R^2X_{cum} is the cumulative modeled variation in X , R^2Y_{cum} is the amount of variation in X correlated to Y (response matrix) and Q^2_{cum} is the cumulative predicted ability of the model. Pathway analysis was performed using MetaboAnalyst 4.0, a web tool for metabolomics data analysis [225]. Metabolites were annotated according to HMDB and linked to a metabolic pathway according to the KEGG database [226]. For targeted oxylipin and eCB data, pairwise Spearman's rank correlation coefficients between metabolites, cytokine transcripts, and between metabolites and transcripts were computed and presented in a heatmap. This was done using RStudio: Integrated Development Environment (version 1.0.143); and R package “corrplot”: Visualization of a Correlation Matrix (version 0.84; <https://github.com/taiyun/corrplot>).

4. Summary of results

4.1 Paper I

‘A Quantitative Analysis of Colonic Mucosal Oxylipins and Endocannabinoids in Treatment-Naïve and Deep Remission Ulcerative Colitis Patients and the Potential Link With Cytokine Gene Expression’[227]

Joseph Diab, Rania Al-Mahdi, Sandra Gouveia-Figueira, Terkel Hansen, Einar Jensen, Rasmus Goll Thomas Moritz, Jon Florholmen, and Guro Forsdahl. *Inflammatory bowel diseases*, 2019. **25**(3): p. 490-497.

In this work, we quantified thirty-five oxylipins and eleven eCBs, by means of UPLC-TQ-MS/MS, in colon biopsies taken from treatment naïve UC patient (n=15), UC patients in deep remission (n=5) and healthy subjects (n=10). As shown in Figure 10, we included oxylipin derivates from three main ω -6 PUFAs: AA (C:20:4), and linoleic acid (LA (C18:2)), and dihomo-gamma-linolenic acid (DGLA (C20:3)), and two main ω -3 PUFAs: EPA (C20:5), and DHA (C22:6). These oxylipins are produced by three main enzymatic pathways: cyclooxygenase (*COX*), lipoxygenase (*LOX*), and cytochrome P450 (*CYP450*). Similarly, we measured the mucosal gene expression of 10 cytokines. This was achieved by measuring the level of mRNA of the cytokines by PCR. To date, this is the only absolute quantification of such a large number of ω -6 and ω -3 related oxylipins and eCBs in UC patients’ inflamed and healed mucosa. Levels of ω -6-related oxylipins, specifically PGE₂, LTB₄, Thromboxane (TXB₂), and 12-Hydroxy-eicosatetraenoic acid (12-HETE), were significantly elevated compared to healthy controls. Conversely, levels of ω -3-related eCBs, mainly, docosahexaenoyl ethanolamine (DHEA) and Eicosapentaenoyl ethanolamine (EPEA) were significantly lower in the UC patients’ inflamed mucosa compared to healed and healthy mucosa (Figure 11.A). Gene expression of all studied cytokines was higher in the inflamed mucosa compared to healed and healthy mucosa. Additionally, we reported a positive association between cytokine gene expression and the levels of ω -6 related oxylipins, and a negative association between cytokine gene expression and the levels of ω -3 eCBs (Figure 11.B). These findings pinpoint the imbalance between the pro-inflammatory oxylipins and anti-inflammatory eCBs in inflamed mucosa in UC patients. Furthermore, it highlights the importance of PUFA metabolism in mediating the inflammatory response in UC. Additionally, it suggests that targeting the eCBs system in UC patients’ mucosa could be beneficial in resolving the inflammation in UC mucosa.

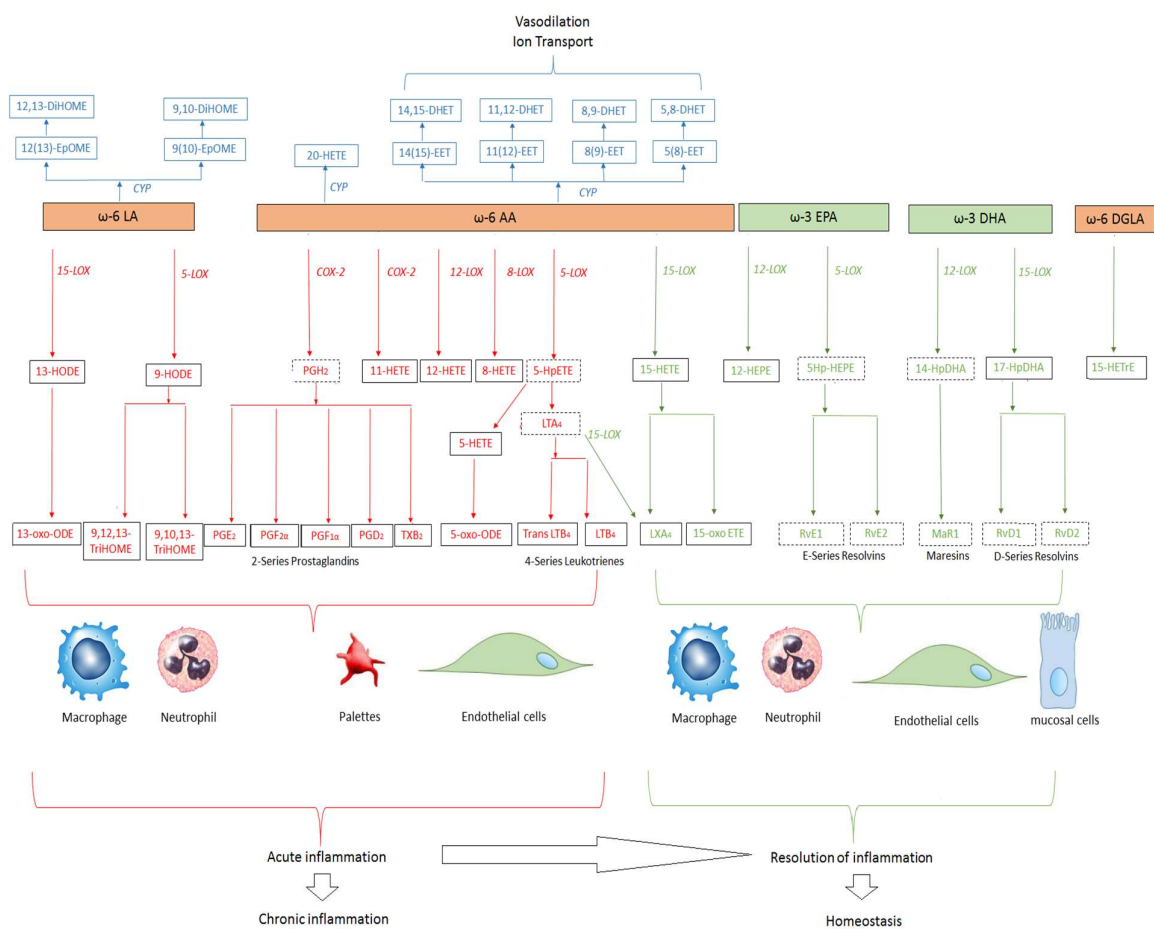


Figure 10. A summary of the biosynthetic pathways the oxylipins quantified in this study, which are metabolites of the following PUFAs: AA, LA, DHA, EPA, and DGLA. Three main enzymatic pathways are involved in their synthesis: cyclooxygenase (COX), lipoxygenase (LOX), and cytochrome P450 (CYP450). For the simplicity of the visualization, oxylipins are coloured according to the potential role in provoking (red) or resolving (green) the inflammation [228], whereas oxylipins produced via the CYP pathway are coloured in blue. Oxylipin that were not investigated within this study are in dashed boxes. Pathways are based on KEGG databases. The full list of oxylipin names is provided in Appendix 1.

4.2 Paper II

'Lipidomics in Ulcerative Colitis Reveal Alteration in Mucosal Lipid Composition Associated With the Disease State' [229]

Joseph Diab, Terkel Hansen, Rasmus Goll, Hans Stenlund, Maria Ahnlund, Einar Jensen, Thomas Moritz, Jon Florholmen, and Guro Forsdahl. *Inflammatory bowel diseases*, 2019, **25**(11), p.1780-1787.

Here we explored the mucosal lipid profile in treatment-naïve UC patients and deep remission UC patients compared with healthy subjects. A comprehensive lipidomic analysis was performed on colon biopsies collected from treatment-naïve UC patients (n = 21), UC patients in deep remission (n = 12), and healthy volunteers (n = 14). This was the first reported lipid profiling from inflamed and healed mucosa from UC patients. In total, 220 lipids from 11 lipid classes were identified and relatively quantified. The relative concentration of 122 and 36 lipids was changed in UC treatment-naïve patients and UC remission patients, respectively, compared with healthy controls. The most prominent changes were found in the PC, ceramide (Cer), and SM composition. The PCA score plot (Figure 12.A) revealed a clear separation between treatment-naïve UC patients and healthy controls, indicating a specific lipidomic profile for active UC patients. We further built two OPLS-DA models to discriminate between UC patients (in active and remission state) and healthy controls. Consequently, we have identified the main distinctive lipid signature in inflamed, healed, and normal mucosa. Notably, PE(38:3) is exclusively present in UC patients' colonic mucosa. Furthermore, very long fatty acid chain (VLFC) ceramides, such as Cer(d18:1/24:0), and Cer(d18:1/24:2), seem to increase in a stepwise manner from control to remission, and active UC (Figure 12.B). Thus, these lipids are candidates for the disease progress monitoring and potential predictors of the outcome. Additionally, the reported mucosal lipid composition changes reflect the role of lipid metabolism during active UC and treatment-induced deep remission UC.

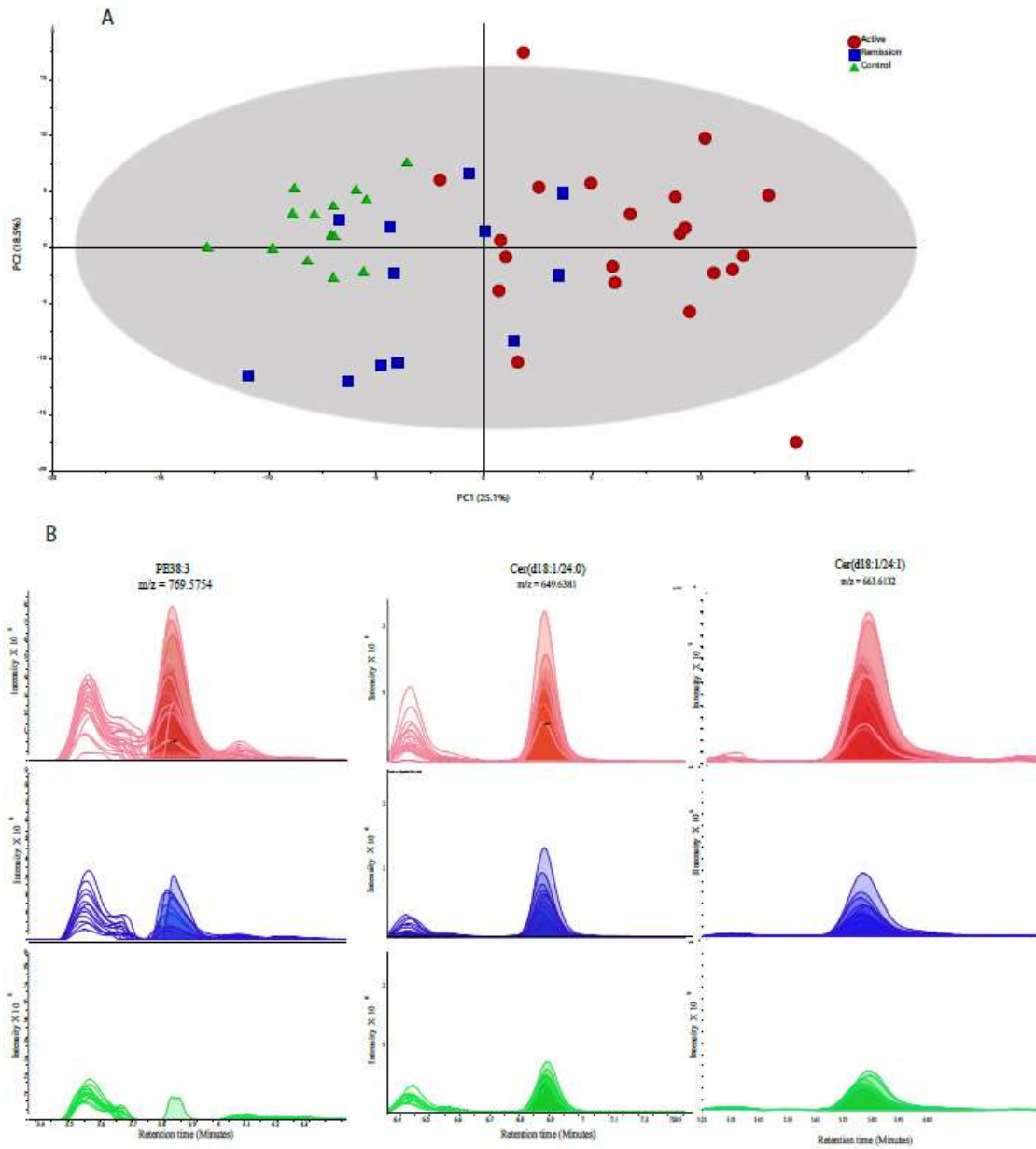


Figure 12. Summary of the main results from paper II; A, PCA score plots; the variation explained by PC1 and PC2 were 25.1% and 18.5%, respectively. Each subject was labelled according to the corresponding study group. B, Represents the extracted ion chromatograms of PE(38:3), Cer(d18:1/24:0), and Cer(d18:1/24:2). The peaks are aligned and coloured according to the study group. Red is the treatment-naïve UC group, blue is UC deep remission group, and green is healthy control group. Used with permission from [229].

4.3 Paper III

‘Mucosal Metabolomic Profiling and Pathway Analysis Reveal the Metabolic Signature of Ulcerative Colitis’[230]

Joseph Diab, Terkel Hansen, Rasmus Goll, Hans Stenlund, Einar Jensen, Thomas Moritz, Jon Florholmen, and Guro Forsdahl. *Metabolites*, 2019. 9(12): p. 291.

In this work, we mapped the mucosal metabolic landscape in treatment-naïve UC patients. Colon biopsies from treatment-naïve UC patients (n = 18), UC patients in deep remission (n = 10), and healthy volunteers (n = 14) were collected during endoscopy. Metabolomic analysis of these biopsies was performed by GC-TOF-MS and UPLC-QTOF-MS analysis. Furthermore, 177 metabolites from 50 metabolic pathways were identified and relatively quantified. Alterations in the LPC profile and amino acids profile were found discriminative between the study groups according to OPLS-DA. Integrative pathway analysis revealed the metabolic disruption during the onset of UC ranging from amino acid metabolism (such as Trp metabolism, and alanine, aspartate and glutamate metabolism) to long- and short-chain fatty acid (LCFA and SCFA) metabolism, namely linoleic metabolism and butyrate metabolism (Figure 13). To our knowledge, this paper was the first description of the mucosal metabolome in untreated newly diagnosed and deep remission UC patients. The reported perturbed pathways are of a high value unravelling the UC interactome signatures. In addition, these pathways might be candidates to assess the severity of the inflammation and the response to treatment.

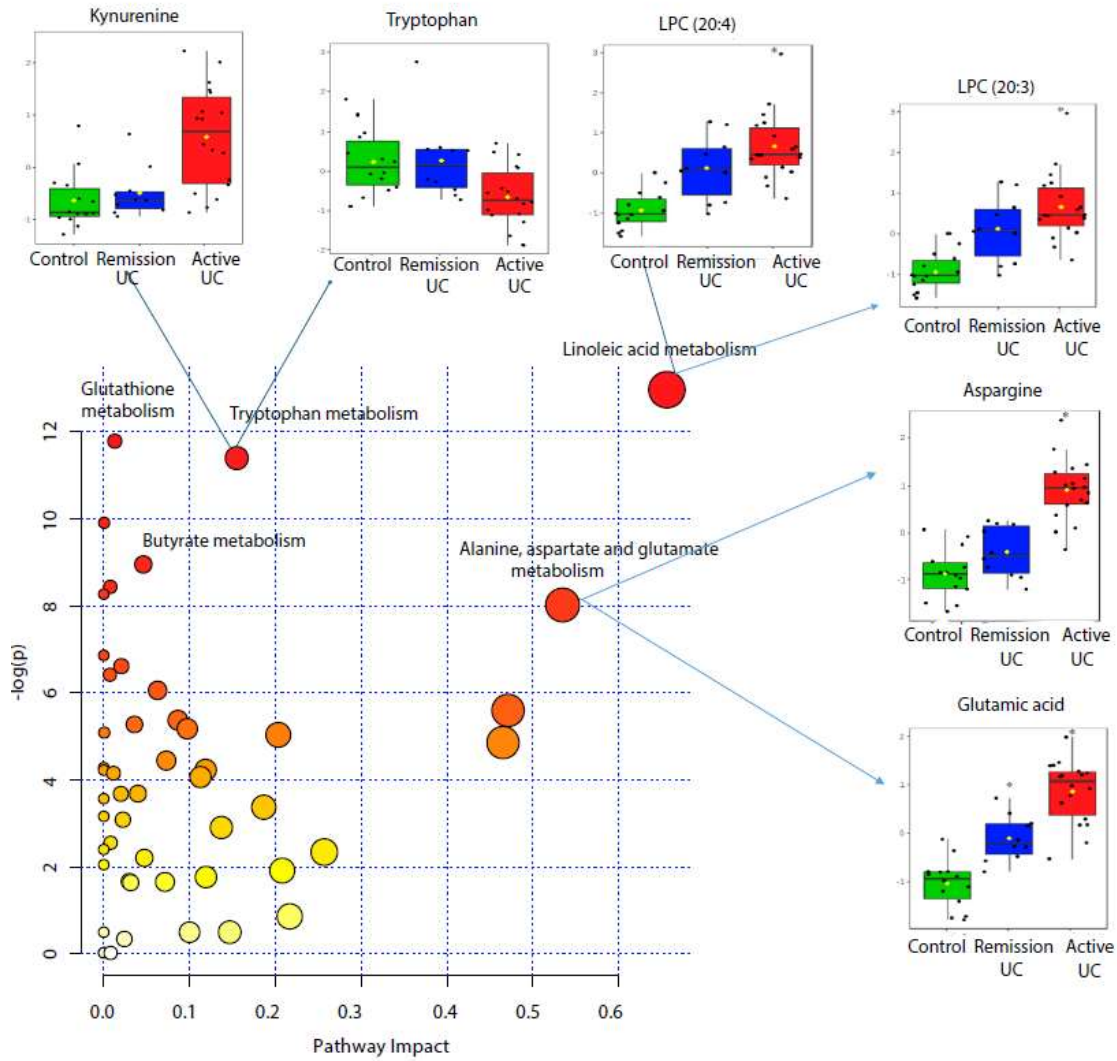


Figure 13. Summary of the main results from paper III. Pathway analysis, combining pathway enrichment and pathway topology analysis, of annotated metabolites in UC treatment-naïve patients and healthy controls. The x-axis marks the pathway impact and the y-axis represents the pathway enrichment. Each node marks a pathway. Larger sizes and darker colours represent higher pathway impact values and higher pathway enrichment. Mucosal levels of representative metabolites from the top 3 high impact pathways are reported as jitter box plots. Used with permission from [230].

5. Discussion

5.1 Methodological considerations

5.1.1 Study design

In this work, the mucosal metabolomic and lipidomic profile in treatment naïve UC patients provides a unique snapshot of the metabolic landscape in the onset of UC. The inclusion of only treatment naïve UC patients rules out any bias resulting from metabolic changes caused by different treatment regimens. Previous data have shown that common UC treatment, such as biologics, have short- and long-term side effects on the immune response [231]. Moreover, according to the treatment algorithm followed by Tromsø IBD group, only moderate to severe patients are receiving biologics. Therefore, given the fact the deep remission patients have been treated with biologics for different periods, it is difficult to assign the metabolic signature in those subjects to either the effects of the treatment duration or the mucosal healing process. Consequently, we excluded the UC remission patients from the pathway analysis. Furthermore, there was a difference in the UC disease activity score among treatment naïve UC patients. However, the small study group size and the fact that we did not observe clustering according to UC severity in PCAs preclude the subgroup analysis.

We aimed to select the study groups with similar subject characteristics regarding gender and age distribution. However, the age is skewed towards a higher age in the healthy controls compared to UC patients since colon cancer screening is less common among young subjects. In addition, although the gender ratio female/male is similar between the study groups, the number of male subjects is higher than the number of female subjects. It would have been preferable to include sex- and age-matched healthy controls, but the selection was restricted to samples available in the biobank. Notably, the biggest difference in sex and age among participants is in the study described in paper 1 as only males were enrolled in the UC remission group. However, we nearly found no difference in the levels of PUFA's derivative between the UC remission group and healthy controls. Hence, we tend to believe that the reported findings were not influenced by the subject sex.

The biopsies in the biobank were acquired in Norwegian hospitals. Accordingly, the ethnicity, life-style and diet of the subjects correspond to the Norwegian society. This could imply that our results might not apply to other populations. However, one can argue that the subjects were clustered in PCA according to their corresponding study groups, which means that the differences according to age, sex, and other subject characteristics are minor. In future studies, it would still be preferable, to collect data on ethnicity, body mass index, family history with IBD, and detailed dietary habits, since the selection of a homogenous study group could reduce the noise in the data.

Finally, we could not account for bias in our findings from the unreported self-medication. For instance, although the use of Non Steroidal Anti-Inflammatory Drugs (NSAID) is contraindicated in IBD [232], and self-medication with steroids is common among IBD patients [233].

5.1.2 Mucosal biopsies

As described in section 3.1, biopsies were collected during endoscopy. Notably there was a large variation in the dry weight of these biopsies. Therefore, for the targeted analysis, the concentration of the reported metabolites was corrected by the dry weight of the samples, and the final concentrations of oxylipins and eCBs were reported as pg in mg of tissue sample. Furthermore, the amount of the extraction solution was adjusted for each sample based on the sample weight. The relative abundances of the metabolites from the GC-MS analysis and the UPLC-MS were normalized by the peak area of the IS, and the total sum of peak area of all metabolites, respectively. However, a drawback of using colon biopsies is the heterogeneity of cellular content, especially when comparing inflamed and non-inflamed mucosa [234]. Additionally, biopsies were acquired exclusively from the rectum in the healthy controls, while biopsies were obtained from the rectum and the sigmoid in the active UC and remission UC groups. Although samples were clustered in the PCA according to their respective study group, we cannot rule out bias in our data from the different collection sites and cellular content. Recently, single cell metabolomics have emerged as a powerful tool to overcome the cellular heterogeneity in metabolomic experiments, which makes this approach worth considering in future analysis [235].

5.1.3 Metabolomics and lipidomics analysis

In the current work, combining two analytical platforms (GC-MS and UPLC-MS), and performing metabolomics/lipidomics workflows allowed for a high coverage of metabolites and lipids in different polarity and molecular weight ranges. This approach enabled gaining a deeper prospective of the metabolome and increased coverage of metabolic pathways [236]. Notably, we have used in house libraries for the identification of metabolites, and thus only identified metabolites were included in the data analysis. An untargeted approach generates thousands of unknown ‘features’, which doesn’t necessarily correspond to unique endogenous metabolites, and could refer to an exogenous metabolite, a salt adduct, a degradation product, or even a fragment produced during ionization [132]. Therefore, a fully untargeted approach was avoided since the focus of the current study is to study the changes in the mucosal metabolome and endogenous metabolites. However, with the increased interest in studying the gut microbial-derived metabolites [237], our raw data could be valuable in future studies using untargeted data processing or microbial metabolites based targeted processing. Recently, Olaisen et al, published the first metagenome data on the mucosa-associated microbiome in the inflamed and non-inflamed ileum in CD [238]. This emphasizes the importance of mucosal metabolomics analysis in future studies on IBD.

5.2 The mucosal metabolic landscape in treatment-naïve UC

5.2.1 Mucosal lipid profiles in treatment-naïve UC

It seems that the altered PL profile, mainly, PC, PS and PE is the hallmark of UC lipidome. For instance, according to our data from the lipidomics analysis, from the 55 quantified PCs, 40 PCs were found significantly changed in treatment naïve UC compared with control. PCs are known to play a vital role in immune cell biology, including proliferation, migration, differentiation, and cytokine release [239]. Furthermore, PLs present in the mucosal epithelial cells and in the mucus as liposome-like aggregates form a hydrophobic barrier protecting the intestinal mucosal cells [240]. Thus, altered PC profile is linked to the impairment in the mucus barrier during IBD. Our findings were confirmed by Murgia et al, whom separated lipid classes in fraction by performing SPE on serum samples from UC patients prior to LC-MS analysis [206]. Accordingly, they reported significant increase in several PCs, such as PC18:2/18:0, PC22:5/16:0, PC20:3/18:0, and PC16:0/18:2. PLs constitute a large part of the lipids forming the cell membranes [239]. Different PLs are characterized by FA substitution at the *sn1* and *sn2* positions of the glycerol backbone. Accordingly, *sn1* FAs are saturated or monounsaturated, whereas *sn2* FAs are polyunsaturated with longer acyl chains [239]. Phospholipases A1 (PLA₁) and Phospholipases A2 (PLA₂) hydrolyse the carboxylic esters at the *sn-1* and *sn-2* positions of glycerol backbones, respectively [241]. Consequently, PC and PE hydrolysis result in LPC and LPE, respectively, and a free FA. Interestingly, based on metabolomics data, the mucosal levels of LPC(20:3), LPC(20:4), hydroxylinoleoyl-carnitine (C18:2-OH), and hydroxyoctadecenoyl carnitine (C18:1-OH) were higher in treatment naïve UC compared with healthy control, which comes in alignment with Murgia et al findings. The released LPC promotes the inflammation by increased pro-inflammatory cytokines release, such as IL-1 β , IL-6, and TNF- α , and increased B cells and macrophages activation [242].

Another key finding in our data is the altered SL metabolism, mainly Cer and SM. It is well established that pro-inflammatory cytokines modulate SL metabolism in the membranes of intestinal mucosal cells by stimulating the SM hydrolysis to Cer, which is metabolised further to sphingosine [243]. Cer and sphingosine act as pro-apoptotic mediator triggering the cell death, and stimulate the inflammatory response in IBD [244]. For instance, Cer generation by TNF leads to increased activity of PLA₂, and induce COX-2 expression [245]. This could explain the elevated levels of oxylipins produced via COX-2 according to our targeted quantification data [227]. Similarly, SM phosphorylation to S1P, which mediate pro-inflammatory responses in neutrophils, monocytes, platelets, and endothelial cells [243]. Additionally, S1P results in increased T_H17-cell differentiation, and regulates immune cell trafficking and tissue localization [246]. Recently, Groesch et al mapped the SL metabolism in UC by comparing the lipids profile and the gene expression of enzymes from SL metabolism pathway in colon biopsies taken from the inflamed and non-inflamed mucosa [247]. However, they did not find any significant

changes in the mucosal Cer, sphingosine, and SL metabolism related gene expression profile. This could be explained by either that, nearly all included UC patients were being treated, or that they have included non-inflamed mucosa from the same patients.

5.2.2 Mucosal metabolic signature in treatment-naïve UC reflects the state of dysbiosis

Changes in the mucosal SL profile might mirror the changes in microbiota during IBD [248]. For instance, galactosylceramide (GalCer), produced by intestinal *Bacteroidetes* can modulate the mucosal immune response, and act as a protective molecules against colitis [249]. In addition, fecal lipid profiles in IBD patients were characterized by a decreased level of *Bacteroides*-derived SL and increased levels of host SL [250]. According to our data, the level of nearly all GalCer lipids were lower in treatment-naïve patients, and several GalCer species were highly discriminative and exclusively present in healthy control mucosa.

The reported mucosal metabolic signature in this work is a result of the interaction between the mucosal inflammation and the state of dysbiosis in the gut. For instance, the disruption in the acyl carnitine profile could indicate energy impairment during inflammation since intestinal endothelial cells utilize carnitine as a transporter of long-chain fatty acids into the mitochondria for β -oxidation [251]. Indeed, Polymorphisms in OCTN2 gene, encoding for the carnitine transporter, is a known risk factor for IBD [252]. Additionally, changes in the mucosal acyl carnitine profile pinpoint the state of dysbiosis in the gut during IBD as reported recently [212]. Moreover, we reported significant changes in the mucosal level of several amino acids, which come in agreement with previously published data on the serum amino acid profile in UC patients [253]. Notably, we marked an increase in Trp metabolism, which has been linked to increased IBD severity [254]. Conversely, the mucosal levels of glutamic acid and asparagine were low in non-inflamed mucosa, and were gradually elevated in UC remission patients and active UC patients. This increase might underline the increase in urease activity and amino acid synthesis caused by gut microbiota dysbiosis, as suggested previously [255]. Furthermore, altered SCFA metabolism, namely butyrate metabolism, underlines the changes in the gut microbiome composition. For instance, previous published data demonstrated a decrease in the number of SCFAs/butyrate-producing bacteria during active UC, such as *Roseburia hominis* and *Faecalibacterium prausnitzii* [256].

5.3 Discriminative lipids and metabolites for the UC state

MVA was applied to assess the ability of mucosal lipidomic and metabolomic profiles to discriminate between treatment-naïve active UC patients, deep remission UC patients and healthy controls. Accordingly, PCA revealed a clear separation between naïve-treatment UC patients and healthy controls indicating a specific lipidomic and metabolomic profile for active UC patients. In addition, although UC remission patients were selected based on well-defined criteria (normalized TNF gene expression,

histologic, and endoscopic healing), those patients were not separated, and clustered between active UC patients and healthy controls. On the other hand, OPLS DA models were able to achieve a maximum separation between the study groups with acceptable predictive ability. Therefore, this demonstrates the power of metabolomics and lipidomics to optimize the current scoring systems, and to improve the stratification of IBD patients towards implementing personalized treatment strategies. The relatively small data set precludes discriminant analysis based on disease severity score and outcome. However, PCA did not reveal separation between enrolled subjects based on the metabolomic and lipidomic profile according to age, sex or activity score.

According to our data, PE(38:3) was exclusively detected in UC patients mucosa, and its level increased significantly in active UC compared with remission UC. Notably, high levels of PE(38:3) in serum has previously been linked with diabetes and prediabetes [257]. Moreover, previous data shows that levels of PE(38:3) are increased in endothelial cells in response to oxidative stress [258]. Therefore, PE(38:3) is potentially a good marker for the mucosal inflammatory state in active and quiescent UC. In addition, very long chain fatty acid (VLCFAs) sphingolipids, namely (C22:0, C22:1, C24:0, and C24:1) ceramides, were found highly discriminative according to our data. For instance, the mucosal levels Cer(d18:1/24:1) and Cer(d18:1/24:0) increased on a step wise manner from control to remission to active UC patients. The accumulation of VLCFA ceramides has been shown to induce autophagy, mitochondrial dysfunction, and oxidative stress [259]. Additionally, higher levels of VLCFA ceramide have been linked to several inflammatory disease, such as, rheumatoid arthritis [260] and Alzheimer's disease [261]. Interestingly, C24:0 and C24:1 ceramides were among the most significantly increased lipids in mucosal biopsies taken from irritable bowel syndrome (IBS) patients compared with healthy control [262]. Therefore, this might explain the mucosal inflammation at the microscopic and molecular level in IBS and the overlapping symptoms between IBS and IBD [263]. The mucosal levels of LPC(20:3), LPC(20:4) were discriminative between inflamed mucosa UC, healed mucosa in quiescent UC, and normal mucosa in healthy controls. The high level of these metabolites in active UC suggests that UC patients' mucosa is characterized by a higher proportion of ω -6 AA, and ω -6 DGLA in their PLs. This finding is supported by results from the oxylipins analysis where we reported higher levels of bio-active lipids derived from ω -6 AA and ω -6 DGLA in active UC patients mucosa [227]. Additionally, a previous study found that SNPs in fatty acid desaturase (FADS1) which converts DGLA to AA increase the risk for IBD [264]. Furthermore, levels of amino acids, such as glutamic acids and asparagine, seem to vary according to the disease state, and discriminate between treatment naïve UC, remission UC, and healthy controls. This finding aligns with a previous report from urinary amino acid profiling in IBD patients, and could correspond to altered microbial composition during dysbiosis [265].

5.4 Mucosal bioactive lipid mediators in UC

5.4.1 The imbalance between pro- and anti-inflammatory molecules during UC

The quantitative analysis of the mucosal oxylipins and eCBs provides a detailed description of the mucosal bioactive lipid status during UC. Accordingly, levels of ω -6 AA related pro-inflammatory oxylipins, specifically PGE₂, LTB₄, TXB₂, and 12-HETE, were significantly higher in treatment naïve UC compared to healthy controls. Conversely, levels of ω -3 EPA and ω -3 DHA related anti-inflammatory eCBs, EPEA and DHEA, were lower. This supports the hypothesis describing the inflammatory state during IBD as an imbalance between pro- and anti-inflammatory molecules and a deficiency in inflammation resolving bioactive lipids [44]. While increased levels of ω -6 AA related oxylipins in UC patients were reported previously [266], we described the status of ω -3 PUFA related eCBs in IBD for the first time. Notably, It was demonstrated that DHEA exhibits an anti-inflammatory effect by competitive inhibition of COX, and reduction of oxylipins production, such as PGE₂ and TXB₂ [267]. Moreover, data suggest that DHEA has more potent anti-inflammatory properties than its precursor DHA [268]. Notably, we reported no significant change in the levels of the primary eCBs, such as arachidonoyl ethanolamine (AEA), and 2-arachidonoylglycerol (2-AG). This was recently confirmed by Grill et al, who analyzed the mucosal gene expression of endocannabinoid system (ECS) in UC, and reported no significant change compared with healthy controls [269].

Furthermore, according to our data, the oxylipin derived from ω -6 DGLA, known as 15-hydroxy-eicosatrienoic acid (15-HETrE), was significantly increased in UC remission mucosa compared with healthy controls. It is well established that 15-HETrE plays a protective role by suppressing the production of AA related pro-inflammatory oxylipins via LOX and COX [270, 271]. Thus, this finding pinpoints the potential role of 15-HETrE in healed mucosa in preventing relapse. However, due to the small number of UC patients in the state of remission included in this work, this finding need to be confirmed in a larger cohort, and include biopsies taken from non-inflamed mucosa of active UC patients.

5.4.2 The association between oxylipins and eCBs profile and cytokines gene expression

We studied the correlation between the cytokines gene expression and the mucosal levels of oxylipins and eCBs. Accordingly, a positive correlation was found between cytokine gene expression and nearly all ω -6 AA related oxylipins suggesting that AA is being metabolised at a higher rate via LOX and COX pathways during active UC. Previously, Weise et al found a negative correlation between mucosal cytokine levels and AA serum levels [45]. Conversely, the correlation matrix revealed a negative correlation between the cytokine profile and the eCB profile, especially regarding EPEA and DHEA. This could be explained by the previously reported role of EPEA and DHEA in inhibiting the production of pro-inflammatory cytokines such as, IL-6, and promoting the production of anti-inflammatory

cytokines such as IL-10 [272]. Another explanation might be the high levels of ω -6 PUFA in intestinal epithelial cells in UC patients as suggested by the results from the metabolomic analysis. However, the effectiveness of increased ω -3 dietary supplementation in the prevention and treatment of UC is doubtful [273]. Notably, increasing the mucosal level of eCBs family members, such as AEA [274] and 2-AG [275] has reduced the inflammation in experimentally induced colitis. Moreover, despite the positive association between the increased cytokines gene expression and increased levels of pro-inflammatory oxylipins in active UC, there was a negative association with anti-inflammatory ω -6 AA related oxylipins, such as lipoxine (LXA₄) and prostacyclin (PGI₂).

5.5 Metabolic signatures with potential clinical utility

5.5.1 Fatty acid metabolism

Despite the explanatory nature of this work, we believe that several findings have potentially clinical value as marker for predicting the UC outcome, and monitoring the response to treatment. For instance, the altered balance between pro-and anti-inflammatory lipid mediators correlates with the severity of inflammation, and may be considered as potential targets for intervention. Pathway analysis suggests the LA pathway to have the highest impact on the onset of UC suggesting higher conversation rate of anti-inflammatory ω -6 LA to pro-inflammatory ω -6 AA. This is supported by previous data that found lower levels of ω -6 LA and ω -6 eicosadienoic acid (EDA) and higher levels of ω -6 AA in UC patients serum compared with healthy controls [271]. Therefore, the AA/EDA ratio was suggested as a marker for response to treatment, since an increased AA/EDA ratio correlates with reducing the symptoms of UC as reported in a previous clinical trial [276]. In the current work, we have studied the correlation between mucosal cytokine gene expression at the transcriptional level, and the PUFA related metabolites at the metabolic level. However, a protein quantification of the mucosal cytokines could give a better insight on the changes in the cytokines at translational level [277]. Therefore, for future work, we suggest absolute quantification of the mucosal cytokines using a MRM-based proteomic approach [278]. In addition, altered butyrate metabolism supports the clinical utility of fatty acids profiling. In fact, previous data have shown that the anti-inflammatory effect of *F. prausnitzii* by maintaining T_H17/T_{reg} balance is mediated by butyrate [279]. Consequently, a recent clinical trial showed the efficacy of supplementation of butyrate to 5-ASA in active UC treatment. Accordingly, 85% of UC patients in the butyrate in addition to 5-ASA group demonstrated significant improvement in UC symptoms by day 14, compared with only 55% in the 5-ASA alone group [280]. Thus, low faecal levels of SCFA and butyrate producing capacity by the microbiota (determined by butyryl-CoA acetate CoA-transferase (BCoAT) gene expression) in UC patients could indicate that these patients may benefit from butyrogenic therapy.

5.5.2 Phosphatidylethanolamine and sphingomyelin composition

Data from the lipid analysis unravel several potential prognostic and diagnostic markers for UC. For instance, PE38:3 was exclusively found in UC patients mucosa, and was decreased in healed mucosa in deep remission UC compared with inflamed mucosa in active UC. Notably, PE has been suggested as a target for cell death imaging and a marker for TNF-induced inflammation [281]. However, further analysis needs to be done in order to identify the fatty acid composition on the *sn1* and *sn2* position. Several approaches could be used in future analysis to achieve this objective, such as fragmentation using CID [282], coupling charged surface hybrid (CSH) column with ion mobility-TOF MS [283], and tribrid LTQ-Orbitrap [284].

Furthermore, the disruption in SL composition suggest a plausible role for SM as candidate biomarker and/or therapeutic target. Recently, the S1P signaling pathway has emerged as a new treatment strategy for the modulation of several cellular processes during IBD [285]. For instance, S1P singling blockage attenuates the intestinal inflammation by modulating lymphocyte and dendritic cell migration, and restoring vascular barrier function [286]. Thus, promising results were obtained from clinical trials evaluating the efficacy of S1P receptor agonist in treating UC [287].

5.5.3 Tryptophan metabolism

Our results showed that the Trp metabolism is a key aspect of the impaired metabolism in the onset of UC. Accordingly, Trp is converted to kynurenine (Kyn) at a higher rate in treatment naïve UC patients compared to UC remission patients and healthy controls. Notably, a large cohort study consisting of 148 UC patients has concluded that increased Trp metabolism is associated with UC activity where Trp levels were significantly lower in patients who had to undergo surgery [254]. This indicates that studying Trp metabolism in the intestinal mucosa could be of a great clinical use is the assessment of UC severity and prognosis. Tryptophan metabolism has gained a lot of interest as the hub of host–microbiota crosstalk since the metabolism of Trp to serotonin, Kyn, and indole derivatives is under the direct or indirect control of the microbiota [288]. While the Kyn:Trp ratio is considered as a systemic inflammatory marker [289], indole derivatives play an anti-inflammatory role [290]. This is mainly achieved by acting as ligands for the aryl hydrocarbon receptor (AHR) and inducing the production of anti-inflammatory IL-22 and IL-17, which maintain intestinal homeostasis, promotes immune defense and tissue repair [291, 292]. Therefore, we suggest exploring the mucosal Trp metabolism in UC using targeted analytical methods to assess its full clinical relevance [293].

6. Conclusion

This work presents a comprehensive mapping of the mucosal metabolome and the lipidome in UC. The inclusion of well-stratified treatment naïve UC patients and UC patients in deep remission allowed capturing the main metabolic characteristics of the IBD interactome. It seems that the inflammatory response in UC is characterized by an altered balance between pro- and anti-inflammatory lipid mediators. In addition, several metabolic fingerprints of the IBD could be linked to the microbiota dysbiosis, such as altered SCFA and amino acids metabolism, and altered galactosylceramide composition. Furthermore, this work suggests several candidates of clinical value as diagnostic and prognostic markers for the severe disease outcome, such as Trp metabolites, ω -6 and ω -3 PUFA derivatives, PE38:3, and VLCFA ceramides. However, those markers need to be further investigated in larger cohorts using targeted analytical approaches.

References

1. Nishida, A., et al., *Gut microbiota in the pathogenesis of inflammatory bowel disease*. Clinical Journal of Gastroenterology, 2018. **11**(1): p. 1-10.
2. Gajendran, M., et al., *A comprehensive review and update on Crohn's disease*. Disease-a-Month, 2018. **64**(2): p. 20-57.
3. Gajendran, M., et al., *A comprehensive review and update on ulcerative colitis*. Disease-a-Month, 2019. **65**(12): p. 100851.
4. Owczarek, D., et al., *Diet and nutritional factors in inflammatory bowel diseases*. World journal of gastroenterology, 2016. **22**(3): p. 895-905.
5. Kornbluth, A., D.B. Sachar, and a.T.P.P.C.o.t.A.C.o. Gastroenterology, *Ulcerative Colitis Practice Guidelines in Adults: American College of Gastroenterology, Practice Parameters Committee*. American Journal of Gastroenterology, 2010. **105**(3): p. 501-523.
6. Wilks, S., *Morbid appearances in the intestine of Miss Bankes*. Med Times Gazette, 1859. **2**(2): p. 264-265.
7. Crohn, B.B., L. Ginzburg, and G.D. Oppenheimer, *Regional ileitis: a pathologic and clinical entity*. Journal of the American Medical Association, 1932. **99**(16): p. 1323-1329.
8. Alatab, S., et al., *The global, regional, and national burden of inflammatory bowel disease in 195 countries and territories, 1990-2017: a systematic analysis for the Global Burden of Disease Study 2017*. The Lancet Gastroenterology & Hepatology, 2020. **5**(1): p. 17-30.
9. Ng, S.C., et al., *Worldwide incidence and prevalence of inflammatory bowel disease in the 21st century: a systematic review of population-based studies*. The Lancet, 2017. **390**(10114): p. 2769-2778.
10. Kaplan, G.G. and S.C. Ng, *Understanding and Preventing the Global Increase of Inflammatory Bowel Disease*. Gastroenterology, 2017. **152**(2): p. 313-321.e2.
11. Festen, E.A.M., C. Wijmenga, and R.K. Weersma, *Inflammatory Bowel Disease*, in *Genomic and Personalized Medicine (Second Edition)*, G.S. Ginsburg and H.F. Willard, Editors. 2013, Academic Press. p. 863-878.
12. Rosen, M.J., A. Dhawan, and S.A. Saeed, *Inflammatory Bowel Disease in Children and Adolescents*. JAMA Pediatrics, 2015. **169**(11): p. 1053-1060.
13. Lee, S.H., J.E. Kwon, and M.-L. Cho, *Immunological pathogenesis of inflammatory bowel disease*. Intestinal research, 2018. **16**(1): p. 26-42.
14. Sun, Y., et al., *Stress Triggers Flare of Inflammatory Bowel Disease in Children and Adults*. Frontiers in Pediatrics, 2019. **7**(432).
15. Wiens, J., J.A. Rankin, and K.L. Then, *Arthropathies in Inflammatory Bowel Disease: A Review for Clinicians*. Gastroenterology Nursing, 2017. **40**(6): p. 496-503.
16. de Souza, H.S.P., C. Fiocchi, and D. Iliopoulos, *The IBD interactome: an integrated view of aetiology, pathogenesis and therapy*. Nat Rev Gastroenterol Hepatol, 2017. **14**(12): p. 739-749.
17. Sartor, R.B., *Mechanisms of Disease: pathogenesis of Crohn's disease and ulcerative colitis*. Nature Clinical Practice Gastroenterology & Hepatology, 2006. **3**(7): p. 390-407.
18. Jostins, L., et al., *Host-microbe interactions have shaped the genetic architecture of inflammatory bowel disease*. Nature, 2012. **491**(7422): p. 119-124.
19. Parkes, M., et al., *Genetic insights into common pathways and complex relationships among immune-mediated diseases*. Nat Rev Genet, 2013. **14**(9): p. 661-73.
20. Duerr, R.H., et al., *A Genome-Wide Association Study Identifies IL23R as an Inflammatory Bowel Disease Gene*. Science, 2006. **314**(5804): p. 1461-1463.
21. Glas, J., et al., *Analysis of IL12B gene variants in inflammatory bowel disease*. PloS one, 2012. **7**(3): p. e34349-e34349.
22. De Vries, L.C.S., et al., *The Future of Janus Kinase Inhibitors in Inflammatory Bowel Disease*. Journal of Crohn's & colitis, 2017. **11**(7): p. 885-893.

23. Häuser, F., et al., *Macrophage-stimulating protein polymorphism rs3197999 is associated with a gain of function: implications for inflammatory bowel disease*. *Genes & Immunity*, 2012. **13**(4): p. 321-327.
24. Ellinghaus, D., et al., *The genetics of Crohn's disease and ulcerative colitis – status quo and beyond*. *Scandinavian Journal of Gastroenterology*, 2015. **50**(1): p. 13-23.
25. Barrett, J.C., et al., *Genome-wide association study of ulcerative colitis identifies three new susceptibility loci, including the HNF4A region*. *Nature Genetics*, 2009. **41**(12): p. 1330-1334.
26. Waller, S., et al., *Evidence for association of OCTN genes and IBD5 with ulcerative colitis*. *Gut*, 2006. **55**(6): p. 809-814.
27. Schwab, M., et al., *Association between the C3435T MDR1 gene polymorphism and susceptibility for ulcerative colitis*. *Gastroenterology*, 2003. **124**(1): p. 26-33.
28. Hasler, R., et al., *A functional methylome map of ulcerative colitis*. *Genome Res*, 2012. **22**(11): p. 2130-7.
29. Childers, R.E., et al., *Family history of inflammatory bowel disease among patients with ulcerative colitis: A systematic review and meta-analysis*. *Journal of Crohn's and Colitis*, 2014. **8**(11): p. 1480-1497.
30. Schiff, E.R., et al., *A New Look at Familial Risk of Inflammatory Bowel Disease in the Ashkenazi Jewish Population*. *Digestive diseases and sciences*, 2018. **63**(11): p. 3049-3057.
31. Wang, M.H., et al., *A novel approach to detect cumulative genetic effects and genetic interactions in Crohn's disease*. *Inflamm Bowel Dis*, 2013. **19**(9): p. 1799-808.
32. Cleynen, I. and S. Vermeire, *The genetic architecture of inflammatory bowel disease: past, present and future*. *Current Opinion in Gastroenterology*, 2015. **31**(6): p. 456-463.
33. Gismera, C.S. and B.S. Aladrén, *Inflammatory bowel diseases: a disease (s) of modern times? Is incidence still increasing?* *World journal of gastroenterology*, 2008. **14**(36): p. 5491-5498.
34. Wijmenga, C., *Expressing the differences between Crohn disease and ulcerative colitis*. *PLoS medicine*, 2005. **2**(8): p. e230-e304.
35. Danese, S., M. Sans, and C. Fiocchi, *Inflammatory bowel disease: the role of environmental factors*. *Autoimmunity Reviews*, 2004. **3**(5): p. 394-400.
36. Rogler, G. and S. Vavricka, *Exposome in IBD: Recent Insights in Environmental Factors that Influence the Onset and Course of IBD*. *Inflammatory Bowel Diseases*, 2014. **21**(2): p. 400-408.
37. Rizzello, F., et al., *Implications of the Westernized Diet in the Onset and Progression of IBD*. *Nutrients*, 2019. **11**(5): p. 1033.
38. Statovci, D., et al., *The Impact of Western Diet and Nutrients on the Microbiota and Immune Response at Mucosal Interfaces*. *Front Immunol*, 2017. **8**: p. 838.
39. Hou, J.K., B. Abraham, and H. El-Serag, *Dietary intake and risk of developing inflammatory bowel disease: a systematic review of the literature*. *Am J Gastroenterol*, 2011. **106**(4): p. 563-73.
40. Andersen, V., et al., *Fibre intake and the development of inflammatory bowel disease: A European prospective multi-centre cohort study (EPIC-IBD)*. *J Crohns Colitis*, 2018. **12**(2): p. 129-136.
41. Ricciotti, E. and G.A. FitzGerald, *Prostaglandins and inflammation*. *Arteriosclerosis, thrombosis, and vascular biology*, 2011. **31**(5): p. 986-1000.
42. Wallace, J.L., *Prostaglandin biology in inflammatory bowel disease*. *Gastroenterol Clin North Am*, 2001. **30**(4): p. 971-980.
43. Serhan, C.N. and N.A. Petasis, *Resolvins and Protectins in Inflammation-Resolution*. *Chem Rev*, 2011. **111**(10): p. 5922-5943.
44. Das, U.N., *Inflammatory bowel disease as a disorder of an imbalance between pro- and anti-inflammatory molecules and deficiency of resolution bioactive lipids*. *Lipids Health Dis*, 2016. **15**: p. 11-18.

45. Wiese, D.M., et al., *Serum Fatty Acids Are Correlated with Inflammatory Cytokines in Ulcerative Colitis*. PLoS One, 2016. **11**(5): p. e0156387.
46. Scaioli, E., E. Liverani, and A. Belluzzi, *The Imbalance between n-6/n-3 Polyunsaturated Fatty Acids and Inflammatory Bowel Disease: A Comprehensive Review and Future Therapeutic Perspectives*. International Journal of Molecular Sciences, 2017. **18**(12): p. 2619.
47. de Souza, H.S.P. and C. Fiocchi, *Immunopathogenesis of IBD: current state of the art*. Nature Reviews Gastroenterology & Hepatology, 2016. **13**(1): p. 13-27.
48. Brazil, J.C., N.A. Louis, and C.A. Parkos, *The role of polymorphonuclear leukocyte trafficking in the perpetuation of inflammation during inflammatory bowel disease*. Inflamm Bowel Dis, 2013. **19**(7): p. 1556-65.
49. Gren, S.T. and O. Grip, *Role of Monocytes and Intestinal Macrophages in Crohn's Disease and Ulcerative Colitis*. Inflammatory Bowel Diseases, 2016. **22**(8): p. 1992-1998.
50. Duerr, R.H., et al., *Neutrophil cytoplasmic antibodies: a link between primary sclerosing cholangitis and ulcerative colitis*. Gastroenterology, 1991. **100**(5 Pt 1): p. 1385-91.
51. Abraham, C. and J.H. Cho, *Inflammatory Bowel Disease*. New England Journal of Medicine, 2009. **361**(21): p. 2066-2078.
52. Fujino, S., et al., *Increased expression of interleukin 17 in inflammatory bowel disease*. Gut, 2003. **52**(1): p. 65-70.
53. Kempski, J., et al., *T(H)17 Cell and Epithelial Cell Crosstalk during Inflammatory Bowel Disease and Carcinogenesis*. Frontiers in immunology, 2017. **8**: p. 1373-1373.
54. Veltkamp, C., et al., *Apoptosis of regulatory T lymphocytes is increased in chronic inflammatory bowel disease and reversed by anti-TNFalpha treatment*. Gut, 2011. **60**(10): p. 1345-53.
55. Wang, P., W. Han, and D. Ma, *Electronic Sorting of Immune Cell Subpopulations Based on Highly Plastic Genes*. J Immunol, 2016. **197**(2): p. 665-73.
56. Facchin, S., et al., *Discrimination between ulcerative colitis and Crohn's disease using phage display identified peptides and virus-mimicking synthetic nanoparticles*. Nanomedicine: Nanotechnology, Biology and Medicine, 2017. **13**(6): p. 2027-2036.
57. Tontini, G.E., et al., *Differential diagnosis in inflammatory bowel disease colitis: state of the art and future perspectives*. World journal of gastroenterology, 2015. **21**(1): p. 21-46.
58. Maul, J. and R. Duchmann, *Can loss of immune tolerance cause IBD?* Inflammatory Bowel Diseases, 2008. **14**(suppl_2): p. S115-S116.
59. Lidar, M., P. Langevitz, and Y. Shoenfeld, *The role of infection in inflammatory bowel disease: initiation, exacerbation and protection*. Isr Med Assoc J, 2009. **11**(9): p. 558-63.
60. Gong, D., et al., *Involvement of Reduced Microbial Diversity in Inflammatory Bowel Disease*. Gastroenterology research and practice, 2016. **2016**: p. 6951091-6951091.
61. Frank, D.N., et al., *Molecular-phylogenetic characterization of microbial community imbalances in human inflammatory bowel diseases*. Proceedings of the National Academy of Sciences of the United States of America, 2007. **104**(34): p. 13780-13785.
62. Gevers, D., et al., *The Treatment-Naive Microbiome in New-Onset Crohn's Disease*. Cell Host & Microbe, 2014. **15**(3): p. 382-392.
63. Kostic, A.D., R.J. Xavier, and D. Gevers, *The Microbiome in Inflammatory Bowel Disease: Current Status and the Future Ahead*. Gastroenterology, 2014. **146**(6): p. 1489-1499.
64. Ohkusa, T., et al., *Commensal bacteria can enter colonic epithelial cells and induce proinflammatory cytokine secretion: a possible pathogenic mechanism of ulcerative colitis*. Journal of Medical Microbiology, 2009. **58**(5): p. 535-545.
65. Kamada, N., et al., *Role of the gut microbiota in immunity and inflammatory disease*. Nature Reviews Immunology, 2013. **13**(5): p. 321-335.
66. Varela, E., et al., *Colonisation by Faecalibacterium prausnitzii and maintenance of clinical remission in patients with ulcerative colitis*. Aliment Pharmacol Ther, 2013. **38**(2): p. 151-61.

67. Bennike, T., et al., *Biomarkers in inflammatory bowel diseases: Current status and proteomics identification strategies*. World Journal of Gastroenterology : WJG, 2014. **20**(12): p. 3231-3244.
68. Morgan, X.C., et al., *Dysfunction of the intestinal microbiome in inflammatory bowel disease and treatment*. Genome Biol, 2012. **13**(9): p. R79.
69. Rowan, F., et al., *Desulfovibrio bacterial species are increased in ulcerative colitis*. Dis Colon Rectum, 2010. **53**(11): p. 1530-6.
70. Paramsothy, S., et al., *Faecal Microbiota Transplantation for Inflammatory Bowel Disease: A Systematic Review and Meta-analysis*. J Crohns Colitis, 2017. **11**(10): p. 1180-1199.
71. Abraham, B. and E.M.M. Quigley, *Antibiotics and probiotics in inflammatory bowel disease: when to use them?* Frontline Gastroenterology, 2020. **11**(1): p. 62.
72. Levine, A., R. Sigall Boneh, and E. Wine, *Evolving role of diet in the pathogenesis and treatment of inflammatory bowel diseases*. Gut, 2018. **67**(9): p. 1726.
73. Martinez-Medina, M., et al., *Western diet induces dysbiosis with increased E coli in CEABAC10 mice, alters host barrier function favouring AIEC colonisation*. Gut, 2014. **63**(1): p. 116-124.
74. David, L.A., et al., *Diet rapidly and reproducibly alters the human gut microbiome*. Nature, 2014. **505**(7484): p. 559-563.
75. Rubin, D.T., et al., *ACG Clinical Guideline: Ulcerative Colitis in Adults*. American Journal of Gastroenterology, 2019. **114**(3): p. 384-413.
76. Hindryckx, P., V. Jairath, and G. D'Haens, *Acute severe ulcerative colitis: from pathophysiology to clinical management*. Nat Rev Gastroenterol Hepatol, 2016. **13**(11): p. 654-664.
77. Atreya, R. and M.F. Neurath, *Current and Future Targets for Mucosal Healing in Inflammatory Bowel Disease*. Visceral medicine, 2017. **33**(1): p. 82-88.
78. Walmsley, R.S., et al., *A simple clinical colitis activity index*. Gut, 1998. **43**(1): p. 29.
79. Walsh, A. and S. Travis, *Assessing disease activity in patients with ulcerative colitis*. Gastroenterology & hepatology, 2012. **8**(11): p. 751-754.
80. Jauregui-Amezaga, A., et al., *A Simplified Geboes Score for Ulcerative Colitis*. Journal of Crohn's and Colitis, 2016. **11**(3): p. 305-313.
81. Kirchgessner, J., et al., *Nancy Index Scores of Chronic Inflammatory Bowel Disease Activity Associate With Development of Colorectal Neoplasia*. Clin Gastroenterol Hepatol, 2020. **18**(1): p. 150-157.e1.
82. Magro, F., et al., *Comparing the Continuous Geboes Score With the Robarts Histopathology Index: Definitions of Histological Remission and Response and their Relation to Faecal Calprotectin Levels*. Journal of Crohn's and Colitis, 2020. **14**(2): P. 169–175.
83. Ungaro, R., et al., *A Treat-to-Target Update in Ulcerative Colitis: A Systematic Review*. American Journal of Gastroenterology, 2019. **114**(6): p. 874-883.
84. Danese, S., G. Roda, and L. Peyrin-Biroulet, *Evolving therapeutic goals in ulcerative colitis: towards disease clearance*. Nature Reviews Gastroenterology & Hepatology, 2020. **17**(1): p. 1-2.
85. Magro, F., et al., *Third European Evidence-based Consensus on Diagnosis and Management of Ulcerative Colitis. Part 1: Definitions, Diagnosis, Extra-intestinal Manifestations, Pregnancy, Cancer Surveillance, Surgery, and Ileo-anal Pouch Disorders*. J Crohns Colitis, 2017. **11**(6): p. 649-670.
86. Johnsen, K.M., et al., *Repeated intensified infliximab induction - results from an 11-year prospective study of ulcerative colitis using a novel treatment algorithm*. Eur J Gastroenterol Hepatol, 2017. **29**(1): p. 98-104.
87. Satsangi, J., et al., *The Montreal classification of inflammatory bowel disease: controversies, consensus, and implications*. Gut, 2006. **55**(6): p. 749-753.
88. Ungaro, R., et al., *Ulcerative colitis*. The Lancet, 2017. **389**(10080): p. 1756-1770.
89. Sutherland, L.R., et al., *5-Aminosalicylic acid enema in the treatment of distal ulcerative colitis, proctosigmoiditis, and proctitis*. Gastroenterology, 1987. **92**(6): p. 1894-1898.

90. Meier, J. and A. Sturm, *Current treatment of ulcerative colitis*. World journal of gastroenterology, 2011. **17**(27): p. 3204-3212.
91. Frolkis, A.D., et al., *Risk of surgery for inflammatory bowel diseases has decreased over time: a systematic review and meta-analysis of population-based studies*. Gastroenterology, 2013. **145**(5): p. 996-1006.
92. Nakov, R., *New markers in ulcerative colitis*. Clinica Chimica Acta, 2019. **497**: p. 141-146.
93. Iskandar, H.N. and M.A. Ciorba, *Biomarkers in inflammatory bowel disease: current practices and recent advances*. Translational research : the journal of laboratory and clinical medicine, 2012. **159**(4): p. 313-325.
94. Chang, S., L. Malter, and D. Hudesman, *Disease monitoring in inflammatory bowel disease*. World journal of gastroenterology, 2015. **21**(40): p. 11246-11259.
95. Nakov, R., et al., *Trefoil Factor 3 is Highly Predictive of Complete Mucosal Healing Independently and in Combination with C-Reactive Protein in Patients with Ulcerative Colitis*. J Gastrointestin Liver Dis, 2019. **28**: p. 169-174.
96. Yu, T.B., et al., *Serum galectins as potential biomarkers of inflammatory bowel diseases*. PLoS one, 2020. **15**(1): p. e0227306-e0227306.
97. Díaz-Jiménez, D., et al., *Soluble ST2 is a sensitive clinical marker of ulcerative colitis evolution*. BMC Gastroenterology, 2016. **16**(1): p. 103.
98. Bourgonje, A.R., et al., *A Combined Set of Four Serum Inflammatory Biomarkers Reliably Predicts Endoscopic Disease Activity in Inflammatory Bowel Disease*. Frontiers in Medicine, :2019. **6**(251).
99. Biasci, D., et al., *A blood-based prognostic biomarker in IBD*. Gut, 2019. **68**(8): p. 1386-1395.
100. Hamanaka, S., et al., *Investigation of novel biomarkers for predicting the clinical course in patients with ulcerative colitis*. Journal of Gastroenterology and Hepatology, 2018. **33**(12): p. 1975-1983.
101. Bryant, R.V., et al., *Systematic review: Histological remission in inflammatory bowel disease. Is 'complete' remission the new treatment paradigm? An IOIBD initiative*. Journal of Crohn's and Colitis, 2014. **8**(12): p. 1582-1597.
102. Henriksen, M., et al., *Ulcerative colitis and clinical course: results of a 5-year population-based follow-up study (the IBSEN study)*. Inflamm Bowel Dis, 2006. **12**(7): p. 543-50.
103. Siegel, C.A., *Refocusing IBD Patient Management: Personalized, Proactive, and Patient-Centered Care*. Am J Gastroenterol, 2018. **113**(10): p. 1440-1443.
104. Porter, C.K., et al., *Cohort profile of the PRoteomic Evaluation and Discovery in an IBD Cohort of Tri-service Subjects (PREDICTS) study: Rationale, organization, design, and baseline characteristics*. Contemporary clinical trials communications, 2019. **14**: p. 100345-100345.
105. Spekhorst, L.M., et al., *Cohort profile: design and first results of the Dutch IBD Biobank: a prospective, nationwide biobank of patients with inflammatory bowel disease*. BMJ Open, 2017. **7**(11): p. e016695.
106. <https://www.clinicaltrials.gov/ct2/show/NCT03282903>. (Last access 6/16/2020).
107. Olivera, P., et al., *Big data in IBD: a look into the future*. Nature Reviews Gastroenterology & Hepatology, 2019. **16**(5): p. 312-321.
108. Schniers, A., *Ulcerative colitis: functional analysis of the in-depth proteome*. Vol. 16. 2019.
109. Taman, H., et al., *Transcriptomic Landscape of Treatment-Naive Ulcerative Colitis*. J Crohns Colitis, 2018. **12**(3): p. 327-336.
110. Fenton, C.G., et al., *Transcriptional Signatures That Define Ulcerative Colitis in Remission*. Inflammatory Bowel Diseases, 2020.
111. Olsen, T., et al., *Tissue levels of tumor necrosis factor-alpha correlates with grade of inflammation in untreated ulcerative colitis*. Scand J Gastroenterol, 2007. **42**(11): p. 1312-1320.
112. Rismo, R., et al., *Normalization of mucosal cytokine gene expression levels predicts long-term remission after discontinuation of anti-TNF therapy in Crohn's disease*. Vol. 48. 2013.

113. Rasmus, G., et al., *Mucosal Gene Transcript of Tumor Necrosis Factor in Personalized Medicine of Inflammatory Bowel Disease: P-037*. American Journal of Gastroenterology, 2018. **113**: p. S9.
114. Olsen, T., et al., *Normalization of mucosal tumor necrosis factor- α : A new criterion for discontinuing infliximab therapy in ulcerative colitis*. Cytokine, 2016. **79**: p. 90-95.
115. Hasin, Y., M. Seldin, and A. Lusic, *Multi-omics approaches to disease*. Genome Biology, 2017. **18**(1): p. 83.
116. Debnath, M., G.B.K.S. Prasad, and P.S. Bisen, *Omics Technology*, in *Molecular Diagnostics: Promises and Possibilities*, M. Debnath, G.B.K.S. Prasad, and P.S. Bisen, Editors. 2010, Springer Netherlands: Dordrecht. p. 11-31.
117. Steuer, A.E., L. Brockbals, and T. Kraemer, *Metabolomic Strategies in Biomarker Research—New Approach for Indirect Identification of Drug Consumption and Sample Manipulation in Clinical and Forensic Toxicology?* Frontiers in Chemistry, 2019. **7**(319).
118. Rantalainen, M., et al., *Integrative Transcriptomic and Metabonomic Molecular Profiling of Colonic Mucosal Biopsies Indicates a Unique Molecular Phenotype for Ulcerative Colitis*. Journal of Proteome Research, 2015. **14**(1): p. 479-490.
119. De Preter, V. and K. Verbeke, *Metabolomics as a diagnostic tool in gastroenterology*. World journal of gastrointestinal pharmacology and therapeutics, 2013. **4**(4): p. 97-107.
120. Aretz, I. and D. Meierhofer, *Advantages and Pitfalls of Mass Spectrometry Based Metabolome Profiling in Systems Biology*. International journal of molecular sciences, 2016. **17**(5): p. 632.
121. García-Sevillano, M.Á., et al., *Omics technologies and their applications to evaluate metal toxicity in mice *M. spretus* as a bioindicator*. Journal of Proteomics, 2014. **104**: p. 4-23.
122. Wishart, D.S., *Metabolomics for Investigating Physiological and Pathophysiological Processes*. Physiological Reviews, 2019. **99**(4): p. 1819-1875.
123. Filimoniuk, A., et al., *Metabolomic profiling in children with inflammatory bowel disease*. Advances in Medical Sciences, 2020. **65**(1): p. 65-70.
124. Wang, R., et al., *A lipidomics investigation into the intervention of celastrol in experimental colitis*. Mol Biosyst, 2016. **12**(5): p. 1436-44.
125. Züllig, T., M. Trötzmüller, and H.C. Köfeler, *Lipidomics from sample preparation to data analysis: a primer*. Analytical and Bioanalytical Chemistry, 2020. **412**: p. 2191–2209.
126. Wishart, D.S., et al., *HMDB: the Human Metabolome Database*. Nucleic Acids Research, 2007. **35**(suppl_1): p. D521-D526.
127. Wishart, D.S., et al., *HMDB 4.0: the human metabolome database for 2018*. Nucleic Acids Research, 2017. **46**(D1): p. D608-D617.
128. Sud, M., et al., *LMSD: LIPID MAPS structure database*. Nucleic Acids Res, 2007. **35**(Database issue): p. D527-32.
129. Dettmer, K., P.A. Aronov, and B.D. Hammock, *Mass spectrometry-based metabolomics*. Mass Spectrometry Reviews, 2007. **26**(1): p. 51-78.
130. Ghanbari, R. and S. Sumner, *Using Metabolomics to Investigate Biomarkers of Drug Addiction*. Trends in Molecular Medicine, 2018. **24**(2): p. 197-205.
131. Broadhurst, D., et al., *Guidelines and considerations for the use of system suitability and quality control samples in mass spectrometry assays applied in untargeted clinical metabolomic studies*. Metabolomics, 2018. **14**(6): p. 72.
132. Gertsman, I. and B.A. Barshop, *Promises and pitfalls of untargeted metabolomics*. Journal of inherited metabolic disease, 2018. **41**(3): p. 355-366.
133. Ribbenstedt, A., H. Ziarrusta, and J.P. Benskin, *Development, characterization and comparisons of targeted and non-targeted metabolomics methods*. PLOS ONE, 2018. **13**(11): p. e0207082.
134. Nicholson, J.K. and I.D. Wilson, *Opinion: understanding 'global' systems biology: metabonomics and the continuum of metabolism*. Nat Rev Drug Discov, 2003. **2**(8): p. 668-76.

135. Johnson, H.E., et al., *High-throughput metabolic fingerprinting of legume silage fermentations via Fourier transform infrared spectroscopy and chemometrics*. Appl Environ Microbiol, 2004. **70**(3): p. 1583-92.
136. Emwas, A.-H.M., *The Strengths and Weaknesses of NMR Spectroscopy and Mass Spectrometry with Particular Focus on Metabolomics Research*, in *Metabolomics: Methods and Protocols*, J.T. Bjerrum, Editor. 2015, Springer New York: New York, NY. p. 161-193.
137. Dinis-Oliveira, R.J., *Metabolomics of drugs of abuse: a more realistic view of the toxicological complexity*. Bioanalysis, 2014. **6**(23): p. 3155-9.
138. Hyötyläinen, T., *Critical evaluation of sample pretreatment techniques*. Analytical and Bioanalytical Chemistry, 2009. **394**(3): p. 743-758.
139. Raterink, R.-J., et al., *Recent developments in sample-pretreatment techniques for mass spectrometry-based metabolomics*. TrAC Trends in Analytical Chemistry, 2014. **61**: p. 157-167.
140. Krug, S., et al., *The dynamic range of the human metabolome revealed by challenges*. The FASEB Journal, 2012. **26**(6): p. 2607-2619.
141. Kirwan, J.A., et al., *Preanalytical Processing and Biobanking Procedures of Biological Samples for Metabolomics Research: A White Paper, Community Perspective (for "Precision Medicine and Pharmacometabolomics Task Group"—The Metabolomics Society Initiative)*. Clinical Chemistry, 2020. **64**(8): p. 1158-1182.
142. Lu, W., et al., *Metabolite Measurement: Pitfalls to Avoid and Practices to Follow*. Annual review of biochemistry, 2017. **86**: p. 277-304.
143. Palladino, G.W., J.J. Wood, and H.J. Proctor, *Modified freeze clamp technique for tissue assay*. J Surg Res, 1980. **28**(2): p. 188-90.
144. Winder, C.L., et al., *Global metabolic profiling of Escherichia coli cultures: an evaluation of methods for quenching and extraction of intracellular metabolites*. Anal Chem, 2008. **80**(8): p. 2939-48.
145. Gonzalez, B., J. Francois, and M. Renaud, *A rapid and reliable method for metabolite extraction in yeast using boiling buffered ethanol*. Yeast, 1997. **13**(14): p. 1347-55.
146. Torell, F., et al., *Tissue sample stability: thawing effect on multi-organ samples*. Metabolomics, 2015. **12**(2): p. 19.
147. Torell, F., et al., *The effects of thawing on the plasma metabolome: evaluating differences between thawed plasma and multi-organ samples*. Metabolomics : Official journal of the Metabolomic Society, 2017. **13**(6): p. 66-66.
148. Jobard, E., et al., *A Systematic Evaluation of Blood Serum and Plasma Pre-Analytics for Metabolomics Cohort Studies*. International Journal of Molecular Sciences, 2016. **17**(12): p. 2035.
149. Kuehnbaum, N.L. and P. Britz-McKibbin, *New advances in separation science for metabolomics: resolving chemical diversity in a post-genomic era*. Chem Rev, 2013. **113**(4): p. 2437-68.
150. Theodoridis, G.A., Gika, H.G. and Wilson, I.D, *LC-MS-Based Nontargeted Metabolomics*, in *Metabolomics in Practice*, M.L.a.W. Weckwerth, Editor. 2013, Wiley. p. 93-115.
151. Römisch-Margl, W., et al., *Procedure for tissue sample preparation and metabolite extraction for high-throughput targeted metabolomics*. Metabolomics, 2012. **8**(1): p. 133-142.
152. Vuckovic, D., *Current trends and challenges in sample preparation for global metabolomics using liquid chromatography–mass spectrometry*. Analytical and Bioanalytical Chemistry, 2012. **403**(6): p. 1523-1548.
153. Boensen, K.O., S. Gatzek, and G. Imbert, *Controlled Protein Precipitation in Combination with Chip-Based Nanospray Infusion Mass Spectrometry. An Approach for Metabolomics Profiling of Plasma*. Analytical Chemistry, 2005. **77**(22): p. 7255-7264.
154. Geier, F.M., et al., *Cross-Platform Comparison of Caenorhabditis elegans Tissue Extraction Strategies for Comprehensive Metabolome Coverage*. Analytical Chemistry, 2011. **83**(10): p. 3730-3736.

155. Wu, H., et al., *High-throughput tissue extraction protocol for NMR- and MS-based metabolomics*. *Anal Biochem*, 2008. **372**(2): p. 204-12.
156. Chetwynd, A.J., W.B. Dunn, and G. Rodriguez-Blanco, *Collection and Preparation of Clinical Samples for Metabolomics*, in *Metabolomics: From Fundamentals to Clinical Applications*, A. Sussulini, Editor. 2017, Springer International Publishing. p. 19-44.
157. Yang, K. and X. Han, *Lipidomics: Techniques, Applications, and Outcomes Related to Biomedical Sciences*. *Trends in biochemical sciences*, 2016. **41**(11): p. 954-969.
158. Whiley, L., et al., *In-Vial Dual Extraction for Direct LC-MS Analysis of Plasma for Comprehensive and Highly Reproducible Metabolic Fingerprinting*. *Analytical Chemistry*, 2012. **84**(14): p. 5992-5999.
159. Wu, Q., et al., *Enhancing coverage in LC-MS-based untargeted metabolomics by a new sample preparation procedure using mixed-mode solid-phase extraction and two derivatizations*. *Analytical and Bioanalytical Chemistry*, 2019. **411**(23): p. 6189-6202.
160. Yang, Y., et al., *New sample preparation approach for mass spectrometry-based profiling of plasma results in improved coverage of metabolome*. *Journal of Chromatography A*, 2013. **1300**: p. 217-226.
161. Fuhrer, T., et al., *High-throughput, accurate mass metabolome profiling of cellular extracts by flow injection-time-of-flight mass spectrometry*. *Analytical chemistry*, 2011. **83**(18): p. 7074-7080.
162. Castrillo, J.I., et al., *An optimized protocol for metabolome analysis in yeast using direct infusion electrospray mass spectrometry*. *Phytochemistry*, 2003. **62**(6): p. 929-37.
163. Patti, G.J., *Separation strategies for untargeted metabolomics*. *Journal of Separation Science*, 2011. **34**(24): p. 3460-3469.
164. Theodoridis, G.A., et al., *Liquid chromatography-mass spectrometry based global metabolite profiling: A review*. *Analytica Chimica Acta*, 2012. **711**: p. 7-16.
165. Ren, J.-L., et al., *Advances in mass spectrometry-based metabolomics for investigation of metabolites*. *RSC Advances*, 2018. **8**(40): p. 22335-22350.
166. Schwaiger, M., et al., *Merging metabolomics and lipidomics into one analytical run*. *Analyst*, 2019. **144**(1): p. 220-229.
167. Rampler, E., et al., *Simultaneous non-polar and polar lipid analysis by on-line combination of HILIC, RP and high resolution MS*. *Analyst*, 2018. **143**(5): p. 1250-1258.
168. Deda, O., et al., *GC-MS-Based Metabolic Phenotyping*, in *The Handbook of Metabolic Phenotyping*, J.C. Lindon, J.K. Nicholson, and E. Holmes, Editors. 2019, Elsevier. p. 137-169.
169. Anderson, J.L., D.W. Armstrong, and G.-T. Wei, *Ionic Liquids in Analytical Chemistry*. *Analytical Chemistry*, 2006. **78**(9): p. 2892-2902.
170. Zhou, B., et al., *LC-MS-based metabolomics*. *Molecular bioSystems*, 2012. **8**(2): p. 470-481.
171. Joshi, K. and D. Patil, *Proteomics*, in *Innovative Approaches in Drug Discovery*, B. Patwardhan and R. Chaguturu, Editors. 2017, Academic Press: Boston. p. 273-294.
172. Kamleh, M.A., J.A.T. Dow, and D.G. Watson, *Applications of mass spectrometry in metabolomic studies of animal model and invertebrate systems*. *Briefings in Functional Genomics*, 2008. **8**(1): p. 28-48.
173. Gowda, G.A.N. and D. Djukovic, *Overview of mass spectrometry-based metabolomics: opportunities and challenges*. *Methods in molecular biology (Clifton, N.J.)*, 2014. **1198**: p. 3-12.
174. Babushok, V.I., et al., *Development of a database of gas chromatographic retention properties of organic compounds*. *J Chromatogr A*, 2007. **1157**(1-2): p. 414-21.
175. Barbier Saint Hilaire, P., et al., *Comparative Evaluation of Data Dependent and Data Independent Acquisition Workflows Implemented on an Orbitrap Fusion for Untargeted Metabolomics*. *Metabolites*, 2020. **10**(4): p. 158.
176. Tada, I., et al., *Creating a Reliable Mass Spectral-Retention Time Library for All Ion Fragmentation-Based Metabolomics*. *Metabolites*, 2019. **9**(11): p. 251.

177. Domingo-Almenara, X. and G. Siuzdak, *Metabolomics Data Processing Using XCMS*, in *Computational Methods and Data Analysis for Metabolomics*, S. Li, Editor. 2020, Springer US: New York, NY. p. 11-24.
178. Jonsson, P., et al., *Extraction, interpretation and validation of information for comparing samples in metabolic LC/MS data sets*. *The Analyst*, 2005. **130**(5): p. 701-707.
179. Karaman, I., *Preprocessing and Pretreatment of Metabolomics Data for Statistical Analysis*, in *Metabolomics: From Fundamentals to Clinical Applications*, A. Sussulini, Editor. 2017, Springer International Publishing: Cham. p. 145-161.
180. Gorrochategui, E., et al., *Data analysis strategies for targeted and untargeted LC-MS metabolomic studies: Overview and workflow*. *TrAC Trends in Analytical Chemistry*, 2016. **82**: p. 425-442.
181. Sumner, L.W., et al., *Proposed minimum reporting standards for chemical analysis*. *Metabolomics*, 2007. **3**(3): p. 211-221.
182. Dunn, W.B., et al., *The importance of experimental design and QC samples in large-scale and MS-driven untargeted metabolomic studies of humans*. *Bioanalysis*, 2012. **4**(18): p. 2249-2264.
183. van der Kloet, F.M., et al., *Analytical Error Reduction Using Single Point Calibration for Accurate and Precise Metabolomic Phenotyping*. *Journal of Proteome Research*, 2009. **8**(11): p. 5132-5141.
184. Scholz, M., et al., *Metabolite fingerprinting: detecting biological features by independent component analysis*. *Bioinformatics*, 2004. **20**(15): p. 2447-2454.
185. Wang, W., et al., *Quantification of Proteins and Metabolites by Mass Spectrometry without Isotopic Labeling or Spiked Standards*. *Analytical Chemistry*, 2003. **75**(18): p. 4818-4826.
186. van den Berg, R.A., et al., *Centering, scaling, and transformations: improving the biological information content of metabolomics data*. *BMC Genomics*, 2006. **7**: p. 142.
187. Wold, S., K. Esbensen, and P. Geladi, *Principal component analysis*. *Chemometrics and Intelligent Laboratory Systems*, 1987. **2**(1): p. 37-52.
188. Stanimirova, I. and M. Daszykowski, *Exploratory Analysis of Metabolomic Data*, in *Comprehensive Analytical Chemistry*, J. Jaumot, C. Bedia, and R. Tauler, Editors. 2018, Elsevier. p. 227-264.
189. Shi, L., et al., *Variable selection and validation in multivariate modelling*. *Bioinformatics*, 2018. **35**(6): p. 972-980.
190. Lee, L.C., C.-Y. Liong, and A.A. Jemain, *Partial least squares-discriminant analysis (PLS-DA) for classification of high-dimensional (HD) data: a review of contemporary practice strategies and knowledge gaps*. *Analyst*, 2018. **143**(15): p. 3526-3539.
191. Bylesjö, M., et al., *OPLS discriminant analysis: combining the strengths of PLS-DA and SIMCA classification*. *Journal of Chemometrics*, 2006. **20**(8-10): p. 341-351.
192. Trygg, J. and S. Wold, *Orthogonal projections to latent structures (O-PLS)*. *Journal of Chemometrics*, 2002. **16**(3): p. 119-128.
193. Galindo-Prieto, B., L. Eriksson, and J. Trygg, *Variable influence on projection (VIP) for OPLS models and its applicability in multivariate time series analysis*. *Chemometrics and Intelligent Laboratory Systems*, 2015. **146**: p. 297-304.
194. Chong, J., et al., *MetaboAnalyst 4.0: towards more transparent and integrative metabolomics analysis*. *Nucleic Acids Research*, 2018. **46**(W1): p. W486-W494.
195. Kanehisa, M., et al., *KEGG: new perspectives on genomes, pathways, diseases and drugs*. *Nucleic Acids Res*, 2017. **45**(D1): p. 353-361.
196. De Preter, V., *Metabolomics in the Clinical Diagnosis of Inflammatory Bowel Disease*. *Dig Dis*, 2015. **33** (Suppl 1): p. 2-10.
197. Mayneris-Perxachs, J. and J.-M. Fernández-Real, *Exploration of the microbiota and metabolites within body fluids could pinpoint novel disease mechanisms*. *The FEBS Journal*. 2020. **287**(5): p. 856-865.

198. Zierer, J., et al., *The fecal metabolome as a functional readout of the gut microbiome*. Nature genetics, 2018. **50**(6): p. 790-795.
199. Kolho, K.L., et al., *Faecal and Serum Metabolomics in Paediatric Inflammatory Bowel Disease*. J Crohns Colitis, 2017. **11**(3): p. 321-334.
200. Daniluk, U., et al., *Untargeted Metabolomics and Inflammatory Markers Profiling in Children With Crohn's Disease and Ulcerative Colitis-A Preliminary Study*. Inflamm Bowel Dis, 2019. **25**(7): p. 1120-1128.
201. Bjerrum, J.T., et al., *Metabonomics of human fecal extracts characterize ulcerative colitis, Crohn's disease and healthy individuals*. Metabolomics, 2015. **11**: p. 122-133.
202. Stephens, N.S., et al., *Urinary NMR metabolomic profiles discriminate inflammatory bowel disease from healthy*. J Crohns Colitis, 2013. **7**(2): p. e42-8.
203. Scoville, E.A., et al., *Alterations in Lipid, Amino Acid, and Energy Metabolism Distinguish Crohn's Disease from Ulcerative Colitis and Control Subjects by Serum Metabolomic Profiling*. Metabolomics, 2018. **14**(1): p. 17.
204. Fan, F., et al., *Lipidomic Profiling in Inflammatory Bowel Disease: Comparison Between Ulcerative Colitis and Crohn's Disease*. Inflamm Bowel Dis, 2015. **21**(7): p. 1511-8.
205. Bazarganipour, S., et al., *The Lipid Status in Patients with Ulcerative Colitis: Sphingolipids are Disease-Dependent Regulated*. Journal of Clinical Medicine, 2019. **8**(7): p. 971.
206. Murgia, A., et al., *Italian cohort of patients affected by inflammatory bowel disease is characterised by variation in glycerophospholipid, free fatty acids and amino acid levels*. Metabolomics, 2018. **14**(10): p. 140.
207. Bjerrum, J.T., et al., *Metabonomics in Ulcerative Colitis: Diagnostics, Biomarker Identification, And Insight into the Pathophysiology*. Journal of Proteome Research, 2010. **9**(2): p. 954-962.
208. Patel, N., et al., *Metabolomic analysis of breath volatile organic compounds reveals unique breathprints in children with inflammatory bowel disease: a pilot study*. Aliment Pharmacol Ther, 2014. **40**(5): p. 498-507.
209. Hisamatsu, T., et al., *Novel, Objective, Multivariate Biomarkers Composed of Plasma Amino Acid Profiles for the Diagnosis and Assessment of Inflammatory Bowel Disease*. PLOS ONE, 2012. **7**(1): p. e31131.
210. De Preter, V., et al., *Faecal metabolite profiling identifies medium-chain fatty acids as discriminating compounds in IBD*. Gut, 2015. **64**(3): p. 447.
211. Franzosa, E.A., et al., *Gut microbiome structure and metabolic activity in inflammatory bowel disease*. Nature microbiology, 2019. **4**(2): p. 293-305.
212. Lloyd-Price, J., et al., *Multi-omics of the gut microbial ecosystem in inflammatory bowel diseases*. Nature, 2019. **569**(7758): p. 655-662.
213. Kumar, M., M. Garand, and S. Al Khodor, *Integrating omics for a better understanding of Inflammatory Bowel Disease: a step towards personalized medicine*. Journal of Translational Medicine, 2019. **17**(1): p. 419.
214. Marigorta, U.M., *Genetic Risk Prediction in IBD*, in *Molecular Genetics of Inflammatory Bowel Disease*, C. Hedin, J.D. Rioux, and M. D'Amato, Editors. 2019, Springer International Publishing: Cham. p. 141-156.
215. Viant, M.R., C. Ludwig, and U. Günther, *1D and 2D NMR Spectroscopy: From Metabolic Fingerprinting to Profiling*. RSC Biomolecular Sciences, 2007: p. 44-70.
216. Gowda, G.A.N., et al., *Metabolomics-based methods for early disease diagnostics*. Expert review of molecular diagnostics, 2008. **8**(5): p. 617-633.
217. Shores, D.R., et al., *New Insights into the Role of Fatty Acids in the Pathogenesis and Resolution of Inflammatory Bowel Disease*. Inflammatory bowel diseases, 2011. **17**(10): p. 2192-2204.
218. Trygg, J., et al., *Extraction and GC/MS analysis of the human blood plasma metabolome*. Anal Chem, 2005. **77**(24): p. 8086-94.

219. Karimpour, M., et al., *Postprandial metabolomics: A pilot mass spectrometry and NMR study of the human plasma metabolome in response to a challenge meal*. *Anal Chim Acta*, 2016. **908**: p. 121-31.
220. Nygren, H., et al., *Liquid chromatography-mass spectrometry (LC-MS)-based lipidomics for studies of body fluids and tissues*. *Methods Mol Biol*, 2011. **708**: p. 247-57.
221. Gouveia-Figueira, S. and M.L. Nording, *Validation of a tandem mass spectrometry method using combined extraction of 37 oxylipins and 14 endocannabinoid-related compounds including prostamides from biological matrices*. *Prostaglandins Other Lipid Mediat*, 2015. **121**(Pt A): p. 110-121.
222. Wu, J., et al., *Oxylipins, endocannabinoids, and related compounds in human milk: Levels and effects of storage conditions*. *Prostaglandins Other Lipid Mediat*, 2016. **122**: p. 28-36.
223. Dunn, O.J., *Multiple Comparisons among Means*. *Journal of the American Statistical Association*, 1961. **56**(293): p. 52-64.
224. Vinaixa, M., et al., *A Guideline to Univariate Statistical Analysis for LC/MS-Based Untargeted Metabolomics-Derived Data*. *Metabolites*, 2012. **2**(4): p. 775-795.
225. Xia, J. and D.S. Wishart, *Using MetaboAnalyst 3.0 for Comprehensive Metabolomics Data Analysis*. *Curr Protoc Bioinformatics*, 2016. **55**: p. 14101-141091.
226. Kanehisa, M., et al., *KEGG: new perspectives on genomes, pathways, diseases and drugs*. *Nucleic Acids Res*, 2017. **45**(D1): p. D353-d361.
227. Diab, J., et al., *A Quantitative Analysis of Colonic Mucosal Oxylipins and Endocannabinoids in Treatment-Naïve and Deep Remission Ulcerative Colitis Patients and the Potential Link With Cytokine Gene Expression*. *Inflammatory bowel diseases*, 2019. **25**(3): p. 490-497.
228. Gabbs, M., et al., *Advances in Our Understanding of Oxylipins Derived from Dietary PUFAs*. *Advances in nutrition (Bethesda, Md.)*, 2015. **6**(5): p. 513-540.
229. Diab, J., et al., *Lipidomics in Ulcerative Colitis Reveal Alteration in Mucosal Lipid Composition Associated With the Disease State*. *Inflammatory Bowel Diseases*, 2019. p.1780–1787
230. Diab, J., et al., *Mucosal Metabolomic Profiling and Pathway Analysis Reveal the Metabolic Signature of Ulcerative Colitis*. *Metabolites*, 2019. **9**(12): p. 291.
231. D'Haens, G., *Risks and benefits of biologic therapy for inflammatory bowel diseases*. *Gut*, 2007. **56**(5): p. 725-32.
232. Klein, A. and R. Eliakim, *Non Steroidal Anti-Inflammatory Drugs and Inflammatory Bowel Disease*. *Pharmaceuticals (Basel, Switzerland)*, 2010. **3**(4): p. 1084-1092.
233. Filipe, V., P.B. Allen, and L. Peyrin-Biroulet, *Self-medication with steroids in inflammatory bowel disease*. *Dig Liver Dis*, 2016. **48**(1): p. 23-6.
234. Goldman, S.L., et al., *The Impact of Heterogeneity on Single-Cell Sequencing*. *Frontiers in Genetics*, 2019. **10**(8).
235. Minakshi, P., et al., *Single-Cell Metabolomics: Technology and Applications*, in *Single-Cell Omics*, D. Barh and V. Azevedo, Editors. 2019, Academic Press. p. 319-353.
236. Shulaev, V., *Metabolomics technology and bioinformatics*. *Briefings in Bioinformatics*, 2006. **7**(2): p. 128-139.
237. Mayneris-Perxachs, J. and J.-M. Fernández-Real, *Exploration of the microbiota and metabolites within body fluids could pinpoint novel disease mechanisms*. *The FEBS Journal*, 2020. **287**(5): p. 856-865.
238. Olaisen, M., et al., *Bacterial Mucosa-associated Microbiome in Inflamed and Proximal Noninflamed Ileum of Patients With Crohn's Disease*. *Inflammatory Bowel Diseases*, 2020.
239. O'Donnell, V.B., J. Rossjohn, and M.J. Wakelam, *Phospholipid signaling in innate immune cells*. *The Journal of clinical investigation*, 2018. **128**(7): p. 2670-2679.
240. Eehalt, R., et al., *Phosphatidylcholine and lysophosphatidylcholine in intestinal mucus of ulcerative colitis patients. A quantitative approach by nanoelectrospray-tandem mass spectrometry*. *Scandinavian Journal of Gastroenterology*, 2004. **39**(8): p. 737-742.

241. Haas, E. and D.W. Stanley, *Phospholipases*, in *xPharm: The Comprehensive Pharmacology Reference*, S.J. Enna and D.B. Bylund, Editors. 2007, Elsevier: New York. p. 1-3.
242. Law, S.H., et al., *An Updated Review of Lysophosphatidylcholine Metabolism in Human Diseases*. *Int J Mol Sci*, 2019. **20**(5).
243. Sukocheva, O.A., et al., *Sphingolipids as mediators of inflammation and novel therapeutic target in inflammatory bowel disease*, in *Advances in Protein Chemistry and Structural Biology*, R. Donev, Editor. 2020, Academic Press. p. 123-158.
244. Wang, J., X.-W. Lv, and Y.-G. Du, *Potential Mechanisms Involved in Ceramide-induced Apoptosis in Human Colon Cancer HT29 Cells*. *Biomedical and Environmental Sciences*, 2009. **22**(1): p. 76-85.
245. Nixon, G.F., *Sphingolipids in inflammation: pathological implications and potential therapeutic targets*. *British Journal of Pharmacology*, 2009. **158**(4): p. 982-993.
246. Rivera, J., R.L. Proia, and A. Olivera, *The alliance of sphingosine-1-phosphate and its receptors in immunity*. *Nature Reviews Immunology*, 2008. **8**(10): p. 753-763.
247. Bazarganipour, S., et al., *The Lipid Status in Patients with Ulcerative Colitis: Sphingolipids are Disease-Dependent Regulated*. *J Clin Med*, 2019. **8**(7).
248. Sitkin, S., et al., *Altered Sphingolipid Metabolism and its Interaction With the Intestinal Microbiome Is Another Key to the Pathogenesis of Inflammatory Bowel Disease*. *Inflamm Bowel Dis*, 2019. **25**(12): p. e157-e158.
249. An, D., et al., *Sphingolipids from a symbiotic microbe regulate homeostasis of host intestinal natural killer T cells*. *Cell*, 2014. **156**(1-2): p. 123-33.
250. Brown, E.M., et al., *Bacteroides-Derived Sphingolipids Are Critical for Maintaining Intestinal Homeostasis and Symbiosis*. *Cell Host & Microbe*, 2019. **25**(5): p. 668-680.e7.
251. Rinaldo, P., D. Matern, and M.J. Bennett, *Fatty acid oxidation disorders*. *Annu Rev Physiol*, 2002. **64**: p. 477-502.
252. Barrett, J.C., et al., *Genome-wide association defines more than 30 distinct susceptibility loci for Crohn's disease*. *Nat Genet*, 2008. **40**(8): p. 955-62.
253. Xin, L., et al., *An analysis of amino acid metabolic profile and its clinical significance in ulcerative colitis*. *Zhonghua nei ke za zhi*, 2015. **54**(3): p. 210-213.
254. Nikolaus, S., et al., *Increased Tryptophan Metabolism Is Associated With Activity of Inflammatory Bowel Diseases*. *Gastroenterology*, 2017. **153**(6): p. 1504-1516.e2.
255. Ni, J., et al., *A role for bacterial urease in gut dysbiosis and Crohn's disease*. *Science Translational Medicine*, 2017. **9**(416): p. eaah6888.
256. Machiels, K., et al., *A decrease of the butyrate-producing species Roseburia hominis and Faecalibacterium prausnitzii defines dysbiosis in patients with ulcerative colitis*. *Gut*, 2014. **63**(8): p. 1275-83.
257. Meikle, P.J., et al., *Plasma Lipid Profiling Shows Similar Associations with Prediabetes and Type 2 Diabetes*. *PLOS ONE*, 2013. **8**(9): p. e74341.
258. Colombo, S., et al., *Phospholipidome of endothelial cells shows a different adaptation response upon oxidative, glycative and lipoxidative stress*. *Scientific Reports*, 2018. **8**(1): p. 12365.
259. Law, B.A., et al., *Lipotoxic very-long-chain ceramides cause mitochondrial dysfunction, oxidative stress, and cell death in cardiomyocytes*. *The FASEB Journal*, 2018. **32**(3): p. 1403-1416.
260. Kosinska, M.K., et al., *Sphingolipids in human synovial fluid--a lipidomic study*. *PLoS One*, 2014. **9**(3): p. e91769.
261. Mielke, M.M., et al., *Serum ceramides increase the risk of Alzheimer disease: The Women's Health and Aging Study II*. *Neurology*, 2012. **79**(7): p. 633-641.
262. Kajander, K., et al., *Elevated pro-inflammatory and lipotoxic mucosal lipids characterise irritable bowel syndrome*. *World journal of gastroenterology*, 2009. **15**(48): p. 6068-6074.

263. Ng, Q.X., et al., *The role of inflammation in irritable bowel syndrome (IBS)*. Journal of inflammation research, 2018. **11**: p. 345-349.
264. Mesbah-Uddin, M., et al., *In-silico analysis of inflammatory bowel disease (IBD) GWAS loci to novel connections*. PLoS one, 2015. **10**(3): p. e0119420-e0119420.
265. Martin, F.P., et al., *Urinary metabolic insights into host-gut microbial interactions in healthy and IBD children*. World J Gastroenterol, 2017. **23**(20): p. 3643-3654.
266. Masoodi, M., et al., *Altered colonic mucosal Polyunsaturated Fatty Acid (PUFA) derived lipid mediators in ulcerative colitis: new insight into relationship with disease activity and pathophysiology*. PLoS One, 2013. **8**(10): p. e76532.
267. Meijerink, J., et al., *Inhibition of COX-2-mediated eicosanoid production plays a major role in the anti-inflammatory effects of the endocannabinoid N-docosahexaenoylethanolamine (DHEA) in macrophages*. Br J Pharmacol, 2015. **172**(1): p. 24-37.
268. Meijerink, J., et al., *The ethanolamide metabolite of DHA, docosahexaenoylethanolamine, shows immunomodulating effects in mouse peritoneal and RAW264. 7 macrophages: evidence for a new link between fish oil and inflammation*. British journal of nutrition, 2011. **105**(12): p. 1798-1807.
269. Grill, M., et al., *Members of the endocannabinoid system are distinctly regulated in inflammatory bowel disease and colorectal cancer*. Sci Rep, 2019. **9**(1): p. 2358.
270. Pham, H., T. Banerjee, and V.A. Ziboh, *Suppression of cyclooxygenase-2 overexpression by 15S-hydroxyeicosatrienoic acid in androgen-dependent prostatic adenocarcinoma cells*. Int J Cancer, 2004. **111**(2): p. 192-197.
271. Sergeant, S., E. Rahbar, and F.H. Chilton, *Gamma-linolenic acid, dihommo-gamma linolenic, eicosanoids and inflammatory processes*. European journal of pharmacology, 2016. **785**: p. 77-86.
272. McDougle, D.R., et al., *Anti-inflammatory omega-3 endocannabinoid epoxides*. Proc Natl Acad Sci U S A, 2017. **114**(30): p. 6034-6043.
273. Ungaro, F., et al., *Actors and Factors in the Resolution of Intestinal Inflammation: Lipid Mediators As a New Approach to Therapy in Inflammatory Bowel Diseases*. Frontiers in Immunology, 2017. **8**(1331).
274. Engel, M.A., et al., *Ulcerative colitis in AKR mice is attenuated by intraperitoneally administered anandamide*. J Physiol Pharmacol, 2008. **59**(4): p. 673-89.
275. Alhouayek, M., et al., *Increasing endogenous 2-arachidonoylglycerol levels counteracts colitis and related systemic inflammation*. Faseb j, 2011. **25**(8): p. 2711-21.
276. Sitkin, S. and J. Pokrotnieks, *Alterations in Polyunsaturated Fatty Acid Metabolism and Reduced Serum Eicosadienoic Acid Level in Ulcerative Colitis: Is There a Place for Metabolomic Fatty Acid Biomarkers in IBD?* Digestive Diseases and Sciences, 2018. **63**(9): p. 2480-2481.
277. Kays, I. and B.E. Chen, *Protein and RNA quantification of multiple genes in single cells*. BioTechniques, 2019. **66**(1): p. 15-21.
278. Foster, M.W., et al., *Quantitative Proteomics of Bronchoalveolar Lavage Fluid in Idiopathic Pulmonary Fibrosis*. Journal of Proteome Research, 2015. **14**(2): p. 1238-1249.
279. Zhou, L., et al., *Faecalibacterium prausnitzii Produces Butyrate to Maintain Th17/Treg Balance and to Ameliorate Colorectal Colitis by Inhibiting Histone Deacetylase 1*. Inflamm Bowel Dis, 2018. **24**(9): p. 1926-1940.
280. Sitkin, S. and J. Pokrotnieks, *Clinical Potential of Anti-inflammatory Effects of Faecalibacterium prausnitzii and Butyrate in Inflammatory Bowel Disease*. Inflamm Bowel Dis, 2019. **25**(4): p. e40-e41.
281. Delvaeye, T., et al., *Noninvasive Whole-Body Imaging of Phosphatidylethanolamine as a Cell Death Marker Using (99m)Tc-Duramycin During TNF-Induced SIRS*. J Nucl Med, 2018. **59**(7): p. 1140-1145.

282. Huynh, K., et al., *High-Throughput Plasma Lipidomics: Detailed Mapping of the Associations with Cardiometabolic Risk Factors*. *Cell Chem Biol*, 2019. **26**(1): p. 71-84.e4.
283. Damen, C.W., et al., *Enhanced lipid isomer separation in human plasma using reversed-phase UPLC with ion-mobility/high-resolution MS detection*. *J Lipid Res*, 2014. **55**(8): p. 1772-83.
284. Almeida, R., et al., *Comprehensive Lipidome Analysis by Shotgun Lipidomics on a Hybrid Quadrupole-Orbitrap-Linear Ion Trap Mass Spectrometer*. *Journal of the American Society for Mass Spectrometry*, 2015. **26**(1): p. 133-148.
285. Danese, S., F. Furfaro, and S. Vetrano, *Targeting S1P in Inflammatory Bowel Disease: New Avenues for Modulating Intestinal Leukocyte Migration*. *Journal of Crohn's and Colitis*, 2017. **12**(suppl_2): p. S678-S686.
286. Karuppuchamy, T., et al., *Sphingosine-1-phosphate receptor-1 (S1P1) is expressed by lymphocytes, dendritic cells, and endothelium and modulated during inflammatory bowel disease*. *Mucosal immunology*, 2017. **10**(1): p. 162-171.
287. Sandborn, W.J., et al., *Ozanimod Induction and Maintenance Treatment for Ulcerative Colitis*. *New England Journal of Medicine*, 2016. **374**(18): p. 1754-1762.
288. Agus, A., J. Planchais, and H. Sokol, *Gut Microbiota Regulation of Tryptophan Metabolism in Health and Disease*. *Cell Host Microbe*, 2018. **23**(6): p. 716-724.
289. Chen, Y. and G.J. Guillemin, *Kynurenine pathway metabolites in humans: disease and healthy states*. *International Journal of Tryptophan Research*, 2009. **2**: p. IJTR. S2097.
290. da Silva Guerra, A.S.H., et al., *Anti-inflammatory and antinociceptive activities of indole-imidazolidine derivatives*. *International Immunopharmacology*, 2011. **11**(11): p. 1816-1822.
291. Ramirez, J.M., et al., *Activation of the aryl hydrocarbon receptor reveals distinct requirements for IL-22 and IL-17 production by human T helper cells*. *Eur J Immunol*, 2010. **40**(9): p. 2450-9.
292. Mizoguchi, A., et al., *Clinical importance of IL-22 cascade in IBD*. *J Gastroenterol*, 2018. **53**(4): p. 465-474.
293. Whiley, L., et al., *Ultrahigh-Performance Liquid Chromatography Tandem Mass Spectrometry with Electrospray Ionization Quantification of Tryptophan Metabolites and Markers of Gut Health in Serum and Plasma—Application to Clinical and Epidemiology Cohorts*. *Analytical Chemistry*, 2019. **91**(8): p. 5207-5216.

Appendix

Table 1. The list of investigated oxylipins in this thesis

Abbreviation	Full name
PGD ₂	Prostaglandin D ₂
α-keto PGF1a	α-Keto prostaglandin F1a
PGE ₂	Prostaglandin E ₂
PGF 2a	Prostaglandin F2a ethanolamide
TXB ₂	Thromboxane B ₂
5-HETE	5-Hydroxy-eicosatetraenoic acid
5-oxo-ODE	5-Oxo-octadecadienoic acid
8-HETE	15-Hydroxy-eicosatetraenoic acid
12-HETE	12-Hydroxy-eicosatetraenoic acid
12-oxo-ETE	2-Oxo-eicosatetraenoic acid
15-HETE	15-Hydroxy-eicosatetraenoic acid
15-oxo-ETE	5-Oxo-eicosatetraenoic acid
20-HETE	20-Hydroxy-eicosatetraenoic acid
9-HODE	9-Hydroxy-octadecadienoic acid
13-HODE	13-Hydroxy-octadecadienoic acid
13-oxo-ODE	13-Oxo-octadecadienoic acid
LTB ₄	Leukotriene B ₄
trans-LTB ₄	Trans-leukotriene B ₄
9,10,13-TriHOME	Trihydroxyoctadecenoic acid
9,12,13-TriHOME	Trihydroxyoctadecenoic acid
12S-HEPE	12-Hydroxy-eicosapentaenoic acid
9(10)-EpOME	9,10-Epoxy-octadecenoic acid
12(13)-EpOME	12,13-Epoxy-octadecenoic acid
9,10-DiHOME	9,10-Dihydroxy-octadecenoic acid
12,13-DiHOME	12,13-Dihydroxy-octadecenoic acid
17R-HDoHE	17-Hydroxydocosahexaenoic acid
15s-HETrE	15S-Hydroxy-eicosatrienoic acid
5,6- EpETrE	5,6-Epoxy-eicosatrienoic acid
5,6-DHET	5,6-Dihydroxy-eicosatrienoic acid
8,9- EpETrE	8,9-Epoxy-eicosatrienoic acid
8,9-DHET	8,9-Dihydroxy-eicosatrienoic acid
11(12)- EpETrE	11,12-Epoxy-eicosatrienoic acid
11,12-DHET	11,12-Dihydroxy-eicosatrienoic acid
14(15)- EpETrE	14,15-Epoxy-eicosatrienoic acid
14,15-DHET	14,15-Dihydroxy-eicosatrienoic acid

Table 2. The list of investigated endocannabinoids in this study

Abbreviation	Full name
AEA	N-arachidonylethanolamine
2AG	2-arachidonoylglycerol
NAGLy	N-arachidonoyl glycine
POEA	N-palmitoleoyl-ethanolamine
SEA	Stearoylethanolamide
PEA	Palmitoylethanolamide
EPEA	Eicosapentaenoyl ethanolamide
DHEA	Docosahexanoyl ethanolamide
OEA	Oleoyl-ethanolamine
LEA	Dihomo- γ -linolenylethanolamine
DEA	Docosatetraenylethanolamide

Paper I

Diab, J., Al-Mahdi, R., Gouveia-Figueira, S., Hansen, T., Jensen, E., Goll, R., ... Forsdahl, G. (2019). A Quantitative Analysis of Colonic Mucosal Oxylipins and Endocannabinoids in Treatment-Naïve and Deep Remission Ulcerative Colitis Patients and the Potential Link with Cytokine Gene Expression. *Inflammatory bowel diseases*, 25(3), 490-497.

<https://doi.org/10.1093/ibd/izy349>

A Quantitative Analysis of Colonic Mucosal Oxylipins and Endocannabinoids in Treatment-Naïve and Deep Remission Ulcerative Colitis Patients and the Potential Link With Cytokine Gene Expression

Joseph Diab, MSc,* Rania Al-Mahdi, PhD,[†] Sandra Gouveia-Figueira, PhD,[‡] Terkel Hansen, PhD,* Einar Jensen, PhD,* Rasmus Goll, PhD,[†] Thomas Moritz, PhD,[‡] Jon Florholmen, PhD,[†] and Guro Forsdahl, PhD*

Background: The bioactive metabolites of omega 3 and omega 6 polyunsaturated fatty acids (ω -3 and ω -6) are known as oxylipins and endocannabinoids (eCBs). These lipid metabolites are involved in prompting and resolving the inflammatory response that leads to the onset of inflammatory bowel disease (IBD). This study aims to quantify these bioactive lipids in the colonic mucosa and to evaluate the potential link to cytokine gene expression during inflammatory events in ulcerative colitis (UC).

Methods: Colon biopsies were taken from 15 treatment-naïve UC patients, 5 deep remission UC patients, and 10 healthy controls. Thirty-five oxylipins and 11 eCBs were quantified by means of ultra-high-performance liquid chromatography coupled with tandem mass spectrometry. Levels of mRNA for 10 cytokines were measured by reverse transcription polymerase chain reaction.

Results: Levels of ω -6-related oxylipins were significantly elevated in treatment-naïve patients with respect to controls, whereas the levels of ω -3 eCBs were lower. 15S-Hydroxy-eicosatrienoic acid (15S-HETrE) was significantly upregulated in UC deep remission patients compared with controls. All investigated cytokines had significantly higher mRNA levels in the inflamed mucosa of treatment-naïve UC patients. Cytokine gene expression was positively correlated with several ω -6 arachidonic acid-related oxylipins, whereas negative correlation was found with lipoxin, prostacyclin, and the eCBs.

Conclusions: Increased levels of ω -6-related oxylipins and decreased levels of ω -3-related eCBs are associated with the debut of UC. This highlights the altered balance between pro- and anti-inflammatory lipid mediators in IBD and suggests potential targets for intervention.

Key Words: EPEA, DHEA, IBD, PUFA, eicosanoids

INTRODUCTION

Inflammatory bowel disease (IBD) is a chronic, relapsing inflammatory disorder in the gastrointestinal tract that affects up to 0.5% of the population of the Western world.¹ The 2 major forms of IBD, ulcerative colitis (UC) and Crohn's

disease (CD), are characterized by a dysregulated mucosal immune response triggered by intestinal commensal flora.² The onset of IBD symptoms appears to be caused by an imbalance between pro- and anti-inflammatory molecules.³ However, several factors might be involved in the chronic inflammatory state observed in IBD. These include cytokines, interleukins (ILs), nitric oxide (NO), free radicals, activated Toll-like receptors, oxylipins, and microbiota.³ Furthermore, it has previously been shown that colitis is associated with a disruption in the lipid metabolism.⁴

Oxylipins are bioactive derivatives mainly from omega 3 and omega 6 polyunsaturated fatty acids (ω -3 and ω -6 PUFAs) such as ω -6 arachidonic acid (AA), ω -6 linoleic acid (LA), ω -3 eicosapentaenoic acid (EPA), and ω -3 docosahexaenoic acid (DHA).⁵ Oxylipins are synthesized through 3 main enzymatic pathways, namely cyclooxygenase (COX), lipoxigenase (LOX), and cytochrome P450 (CYP450), resulting in more than 100 active mediators. The AA-derived oxylipins, also known as eicosanoids, are involved in chemotaxis and promoting the recruitment of neutrophils to the site of inflammation. The role of oxylipins in IBD is very complex and not completely understood; for example, prostaglandin E₂ (PGE₂) induces epithelial proliferation in response to

Received for publications May 15, 2018; Editorial Decision October 11, 2018.

From the *Natural Products and Medicinal Chemistry Research Group, Department of Pharmacy, and [†]Research Group of Gastroenterology and Nutrition, Department of Clinical Medicine, Faculty of Health Sciences, University of Tromsø–The Arctic University of Norway, Tromsø, Norway; [‡]Swedish Metabolomics Center, Swedish University of Agricultural Sciences, Umeå, Sweden

Supported by: This project was funded by University of Tromsø–The Arctic University of Norway and Helse Nord RHF (SFP-1134-13).

Address correspondence to: Guro Forsdahl, PhD, Department of Pharmacy, University of Tromsø–The Arctic University of Norway, Tromsø, Norway (guro.forsdahl@uit.no).

© 2018 Crohn's & Colitis Foundation. Published by Oxford University Press on behalf of Crohn's & Colitis Foundation.

This is an Open Access article distributed under the terms of the Creative Commons Attribution Non-Commercial License (<http://creativecommons.org/licenses/by-nc/4.0/>), which permits non-commercial re-use, distribution, and reproduction in any medium, provided the original work is properly cited. For commercial re-use, please contact journals.permissions@oup.com

doi: 10.1093/ibd/izy349

Published online 22 November 2018

mucosal damage and suppresses the release of tumor necrosis factor (TNF) from macrophages.⁶ Leukotriene B₄ (LTB₄) has chemotactic effects by stimulating leucocyte activation and adhesion to the vascular endothelium and promotes the production of inflammatory cytokines.⁷ Furthermore, inflammation-resolving oxylipins termed resolvins, lipoxins, protectins, and maresins are produced from AA, EPA, and DHA.⁸

The endocannabinoids (eCBs) are a family of bioactive lipids that are biosynthesized from membrane glycerophospholipids and bind to cannabis receptors (CB), specifically, CB1 and CB2.⁹ The primary eCBs are arachidonoyl ethanolamine, known as anandamide (AEA), and 2-arachidonoylglycerol (2-AG). The secondary or “atypical” eCBs, such as docoheptaenoic ethanolamine (DHEA) and eicosapentaenoic ethanolamine (EPEA), play an important synergistic role to AEA.¹⁰ CB1 receptors are highly expressed in several brain regions that mediate the psychoactive effects of cannabinoids, whereas CB2 receptors are found in a number of immune cells and in a few neurons.¹¹ It has been shown that eCBs regulate immune homeostasis in the gut–pancreas axis. For instance, eCBs inhibit the release of a wide class of pro-inflammatory mediators, including IL-1 β , TNF, and NO.^{9, 12} Some studies have reported changes in endocannabinoid system expression during UC.¹³ However, a previous targeted analysis of eCBs in inflamed mucosa in IBD was inconclusive and was restricted to ω -6 AA derivatives.^{14–17}

A quantitative analysis of all bioactive lipid metabolites in UC colon biopsies is needed to fully understand their involvement in promoting and resolving the inflammatory event in IBD. Therefore, in this study, we have quantified 35 nonesterified oxylipins and 11 eCB metabolites (Supplementary Table 1) simultaneously in colon biopsies taken from 3 different groups, namely treatment-naïve UC patients in the debut of the disease, deep remission UC patients, and healthy subjects. We have further analyzed the cytokine profile in colon biopsies from the same patients to evaluate a potential link between the lipid profile and the inflammatory events mediated by pro- and anti-inflammatory cytokines.

METHODS

Collection of Biopsies

Mucosal biopsies were collected from newly diagnosed treatment-naïve UC patients and UC patients in deep remission. UC diagnosis was established based on clinical, endoscopic, and histological criteria defined by European Crohn's and Colitis Organization (ECCO) guidelines.¹⁸ Furthermore, the degree of inflammation was evaluated during colonoscopy using the scoring system of the Ulcerative Colitis Disease Activity Index (UCDAI).¹⁹ Moreover, TNF mRNA levels were measured by real-time reverse transcription polymerase chain reaction (RT-PCR) to assess the level of UC activity.²⁰ Deep remission was defined by endoscopically healed mucosa (Mayo

score = 0) and a normalized mucosal TNF gene expression level induced by anti-TNF treatment.²¹ Subjects admitted for a cancer screening and with normal colonoscopy histological findings served as healthy controls. None of the recruited subjects suffered from irritable bowel syndrome, and they were not taking nonsteroidal anti-inflammatory drugs (NSAIDs) before the colonoscopy. The patients in deep remission were on regular UC medications including 5-aminosalicylic acid (5-ASA), azathioprine, and anti-TNF. From each study participant, 2 adjacent biopsies were obtained from the inflamed mucosa, and 1 biopsy was immediately immersed in RNAlater (Qiagen, Hilden, Germany). The second biopsy was immediately frozen in a dry cryotube tube at -70°C . The biopsies from both UC patients and the UC remission group were obtained from the rectum or sigmoid colon, whereas biopsies from the control group were obtained from the rectum area only. The dry weight of the biopsies ranged from 2 to 8 mg. All biopsies were kept at -70°C until further analysis.

Chemical and Reagents

The eCB analytical standards, the oxylipin analytical standards, and 12-(cyclohexylamino)carbonyl[amino]-dodecanoic acid (CUDA) were purchased from Cayman Chemicals (Ann Arbor, MI, USA). Acetonitrile (ACN) and methanol (MeOH) were acquired from Merck (Darmstadt, Germany). Isopropanol was obtained from VWR PROLABO (Fontenay-sous-Bois, France). Acetic acid was purchased from Aldrich Chemical Company, Inc. (Milwaukee, WI, USA). All solvents were of HPLC grade or higher. Water was purified by a Milli-Q Gradient system (Millipore, Milford, MA, USA). Oasis HLB cartridges (3 cc, 60 mg) were obtained from Waters (Milford, MA, USA).

Endocannabinoid and Oxylipin Quantification

Analysis of eCBs and nonesterified oxylipins was performed by a previously published method.²² Briefly, 500 μL of methanol and a tungsten bead were added to each sample; the samples were then mixed in Qiagen plates (Qiagen, Valencia, CA, USA) for 3 minutes at a speed of 30 Hz. After removing the beads, the samples were centrifuged for 3 minutes at a speed of 14,000 rpm ($2125 \times g$) and $+4^{\circ}\text{C}$. The metabolites were extracted by a solid phase extraction (SPE) protocol described elsewhere.²³ In brief, the samples were spiked with 10 μL of the following internal standard solution: 50 ng/mL 12,13-DiHOME-d₄ and 12,13-EPOME-d₄, 25 ng/mL 9-HODE-d₄, PGE₂-d₄, 5-HETE-d₈, 20-HETE-d₆ and TXB₂-d₄, 800 ng/mL 2-AG-d₈, 40 ng/mL PGF_{2 α} -EA-d₄ and PGE₂-EA-d₄, 20 ng/mL AEA-d₄, OEA-d₄, and SEA-d₃. Then, the samples were applied to the SPE columns and washed by a mix of 5% MeOH and 0.1% acetic acid, before eluting the metabolites with 3 mL of ACN and 2 mL of MeOH. Finally, the samples were dried using a vacuum concentrator (MIVac, SP, Warminster,

PA, USA), reconstituted in 100 μ L of MeOH, and spiked with 10 μ L of the recovery standard CUDA (0.025 μ g/mL). The analysis was conducted using an Agilent UPLC system (Infinity 1290) coupled with an electrospray ionization source (ESI) to an Agilent 6490 triple quadrupole system equipped with iFunnel Technology (Agilent Technologies, Santa Clara, CA, USA). Metabolite separation was performed using a Waters BEH C18 column (2.1 mm \times 150 mm, 130 \AA , 1.7- μ m particle size). A flow rate of 300 μ L/min and 10- μ L injection volume were employed for each run. Separate injections were used for subsequent ionization in positive (eCB) and negative (oxylipin) mode. The mobile phase consisted of (1) 0.1% acetic acid in MilliQ water and (2) acetonitrile:isopropanol (90:10). The gradient and ESI applied conditions were optimized and have been described elsewhere.²³ MassHunter Workstation software was used to control the instrument and to integrate all peaks manually.

An 8-point calibration curve was constructed using pure standards. Furthermore, the recovery of each internal standard was calculated by adding the recovery standard CUDA to each sample as quality control.

Quantification of Cytokine mRNA Using Real-time PCR

Total RNA was isolated from patient biopsies using the Allprep DNA/RNA Mini Kit (Qiagen, Hilden, Germany, Cat No: 80204) and the automated QIAcube instrument (Qiagen, Hilden, Germany) according to the manufacturer's recommendations. Quantity and purity of the extracted RNA were determined using the Qubit 3 Fluorometer (Cat No: Q33216; Invitrogen by Thermo Fisher Scientific, Waltham, MA, USA). Reverse transcription of the total RNA was performed using the QuantiTect Reverse Transcription Kit (Cat. No: 205314; Qiagen, Hilden, Germany). Levels of mRNA for IL-1 β , IL-4, IL-5, IL-6, IL-10, IL-12, IL-17, IL-23, IFN- γ , TNF, and the housekeeping gene β -actin were quantified by a previously published method.²⁴ The primers and probe sequences are shown in [Supplementary Table 3](#). Cytokine mRNA expression was reported according to the Δ CT and $\Delta\Delta$ CT method described by Schmittgen, with fold change as $2^{-\Delta\Delta\text{CT}}$.²⁵ For the TNF assay, we used an in-house absolute standard based on a serially diluted PCR product. By using this standard curve, we derived a copy number per μ g of total RNA for each sample.

Statistical Analysis

The concentration of each metabolite was normalized by sample weight, and the results were reported as pg/mg of colon tissue. Statistical analysis was carried out using MetaboAnalyst 3.0, a web tool for metabolomics data analysis (<http://www.metaboanalyst.ca/>).²⁶ Two samples had extremely low and high concentrations (below/higher than the mean plus/minus 3 standard deviations) of 60% of the metabolites and were consequently excluded. One percent of reported metabolites were below the

level of detection. Therefore, they were replaced by a small value (half of the minimum positive value in the original data).

First, metabolite concentrations were autoscaled to reduce differences in magnitude.²⁷ Second, the Shapiro-Wilk test for normality was run. The data were found to be non-normally distributed, and nonparametric univariate analysis (Mann-Whitney *U* test) was performed. Differences in the mean concentration of metabolites between the study groups were identified at a fold change (FC) of 2 and a false discovery rate (FDR; Benjamini Hochberg) cutoff of 0.1, as previously described.²⁸ The 2-FC cutoff was chosen to minimize the effects of biological variation, whereas the FDR cutoff was set to 0.1 due to the exploratory nature of our study, and the low risk of reporting false positivity. Finally, significant variation in the metabolite concentrations among the 3 study groups was detected by Kruskal-Wallis nonparametric analysis of variance. For multiple testing correction, acquired *P* values were adjusted using the Benjamini and Hochberg method. Adjusted *P* values <0.05 were considered significant.

Frequency distribution analysis and tests of normality (Shapiro Wilk) were run on Δ CT values from RT-PCR analyses. The data were found to be normally distributed, and cytokine gene expression differences between the study groups were compared using a 2-tailed Student *t* test. To account for the multiple group testing, acquired *P* values were adjusted by the Dunnett post hoc test. Adjusted *P* values <0.05 were considered significant.

Pair-wise Spearman's rank correlation coefficients between metabolites, transcripts, and between metabolites and transcripts (autoscaled values) were computed and are presented in a heatmap. This was done using RStudio: Integrated Development Environment (version 1.0.143); and R package "corrplot": Visualization of a Correlation Matrix (version 0.84; <https://github.com/taiyun/corrplot>).

Ethical Considerations

The Regional Committee of Medical Ethics of North Norway and the Norwegian Social Science Data Services approved the study and the storage of biological material under the number REK NORD 2012/1349. In addition, all enrolled subjects have signed an informed written consent.

RESULTS

Subjects Characteristic

In total, 15 newly diagnosed treatment-naïve UC patients with mild to severe disease activity, 5 UC patients in deep remission, and 10 healthy controls were enrolled in this study. The study group characteristics are described in [Table 1](#). Ulcerative colitis patients' disease activity ranged from mild to severe; a UCDAI score of 3 to 6 was defined as mild, 7 to 10 as moderate,

and 11 to 12 as severe UC. Accordingly, 7 patients had mild UC, 4 patients had moderate UC, and 4 patients had severe UC.

Mucosal eCB and Oxylipin Profiles in Treatment-Naïve UC Patients, UC Remission Patients, and Controls

The concentrations of eCBs and oxylipins in colon biopsies from treatment-naïve UC and deep remission UC patients were compared with controls. As seen in [Figure 1A](#), the volcano plot shows that the mucosal levels of PGE₂, thromboxane (TXB₂), trans-leukotriene (trans-LTB₄), and 12-Hydroxy-eicosatetraenoic acid (12-HETE) were significantly upregulated (FDR ≤ 0.1) in colon biopsies taken from treatment-naïve patients. The mean concentrations of these oxylipins were increased by 7-, 3-, 8-, and 5-fold, respectively. In contrast, DHEA and EPEA were significantly downregulated. The mean concentration was decreased by 3-fold for both eCBs, with respect to the control group.

The comparison between the mucosal concentration of the investigated metabolites in deep remission UC patients and healthy controls is demonstrated in [Figure 1B](#). Only 15S-Hydroxy-eicosatrienoic acid (15s-HETrE) was significantly upregulated by 2-fold in deep remission UC patients compared with healthy controls.

Furthermore, the Kruskal-Wallis test was used to compare the metabolite mucosal profiles between all 3 groups, as shown in [Figure 2A](#). The metabolites that showed significant variance between the study groups were 1 ω-3 eCB, specifically DHAE ([Fig. 1D, C](#)), and 1 ω-6 AA oxylipin, specifically HETE-12 ([Fig. 1D](#)). The mean concentration of DHAE decreased in a stepwise manner from UC-naïve treatment patients to UC remission patients and controls. In contrast, the concentration of HETE-12 was the highest in the treatment-naïve UC group.

Mucosal Cytokine Gene Expression in Treatment-Naïve UC Patients, UC Remission Patients, and Controls

Cytokine gene expression in colon biopsies was investigated by the quantification of mRNA using real-time PCR. Comparative analysis of mean differences in the cytokine gene expression levels between treatment-naïve UC patients, UC remission patients, and controls was done by Student *t* test. The results are shown in [Table 2](#). All investigated cytokines

had significantly higher mRNA levels in the inflamed mucosa of treatment-naïve UC patients compared with healthy controls. However, IL-5 did not differ significantly (*P* = 0.057). Furthermore, no significant differences were found in the gene expression of all investigated cytokines between the UC remission group and healthy controls ([Table 2](#)).

Cytokine Gene Expression Correlation With Oxylipins and eCBs

To assess the association between cytokine gene expression and the investigated metabolites in the mucosal biopsies of the study groups, Spearman's rank correlation between cytokines-cytokines and cytokines-metabolites was computed and is presented as an asymmetric heatmap ([Fig. 2](#)), where red represents a positive correlation and blue a negative correlation. All investigated cytokines were positively correlated with each other. Furthermore, the cytokines were found to be negatively correlated with several eCBs, mainly EPEA and DHEA (*r* ≈ -0.4). In contrast, the cytokines were positively correlated with nearly all AA metabolites, specifically PGE₂, 12-HETE, 5-Hydroxy-eicosatetraenoic acid (5-HETE), TXB₂, and LTB₄ (*r* ≈ 0.5). However, there was a negative correlation with lipoxin (LXA₄) and α-Keto prostaglandin F₁ (α-keto PGF₁), as shown in [Figure 2](#). Furthermore, the correlation matrix revealed a negative correlation between cytokines and ω-6 AA-derived vicinal diols (DHETs) and a positive correlation with ω-6 AA-derived epoxides (EpETrEs).

Spearman's rank correlation coefficients were computed for metabolites-metabolites, cytokines-cytokines, and cytokines-metabolites and are represented as a symmetric heatmap ([Supplementary Fig. 1](#)). In addition, the correlation coefficients and the significance *P* values corresponding to all computed correlations are provided in the Supplementary Data.

DISCUSSION

This study provides a unique, quantitative, and comprehensive analysis of a large number of oxylipins and eCBs in the colon mucosa of treatment-naïve newly diagnosed UC patients and deep remission UC patients. Previous studies were restricted to investigating oxylipins related to selected enzymatic pathways (*COX-2* and *5-LOX*) in UC.²⁹⁻³¹ Moreover, in these studies, oxylipins were determined by liquid chromatography-tandem mass spectrometry (LC-MS/MS) untargeted

TABLE 1: Description of Study Group Characteristics

Study Group	No. Subjects	Age, Mean (Range), y	Sex, Female/Male	UCDAI Score, Median (Range)	TNF-α, Mean (Range), Copies/μg of Total RNA
UC patients	15	37 (14-69)	6/9	9 (4-15)	15,207 (4300-44,600)
Healthy controls	10	68 (25-86)	4/6	—	3430 (1100-7900)
UC remission	5	46 (41-70)	0/5	<1	4083 (1400-8500)

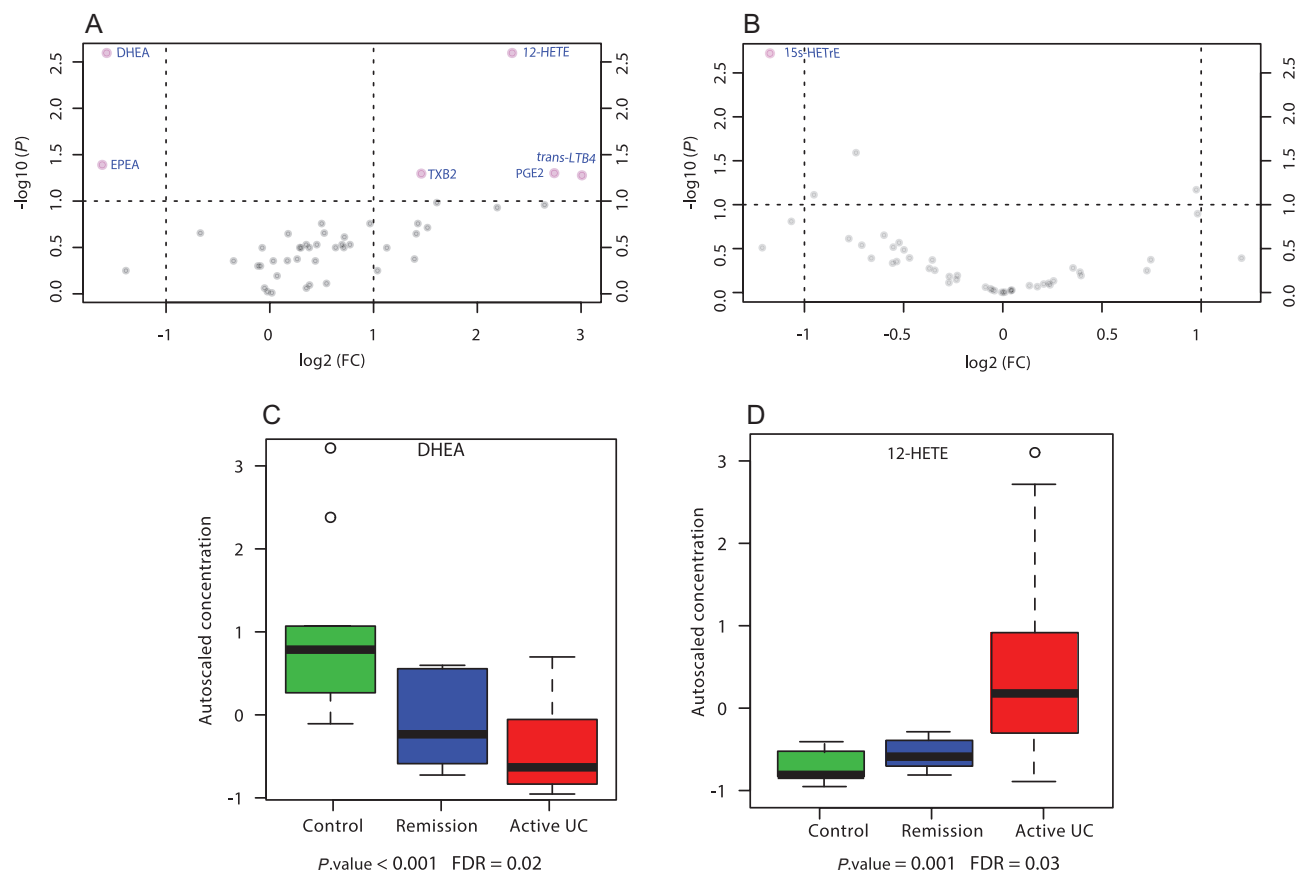


FIGURE 1. Results from univariate analysis of oxylipin and eCB mean mucosal concentrations. A, B, Volcano plots of changes in mean mucosal concentrations of oxylipins and eCBs in treatment-naïve patients vs healthy controls (HCs), and UC deep remission patients vs HC, respectively. The vertical lines correspond to 2.0-fold up- and downregulation, and the horizontal lines represent a *P* value of 0.05 (Mann-Whitney *U* test) at a cutoff FDR value of 0.1. The points in the plots represent metabolite mean concentrations. Metabolites in pink have passed the volcano plot filtering. C, D, Box plots of the autoscaled concentration of DHEA and 12-HETE, respectively. The mean concentrations of these metabolites were found to have significantly changed among the study groups according to Kruskal-Wallis analysis of variance.

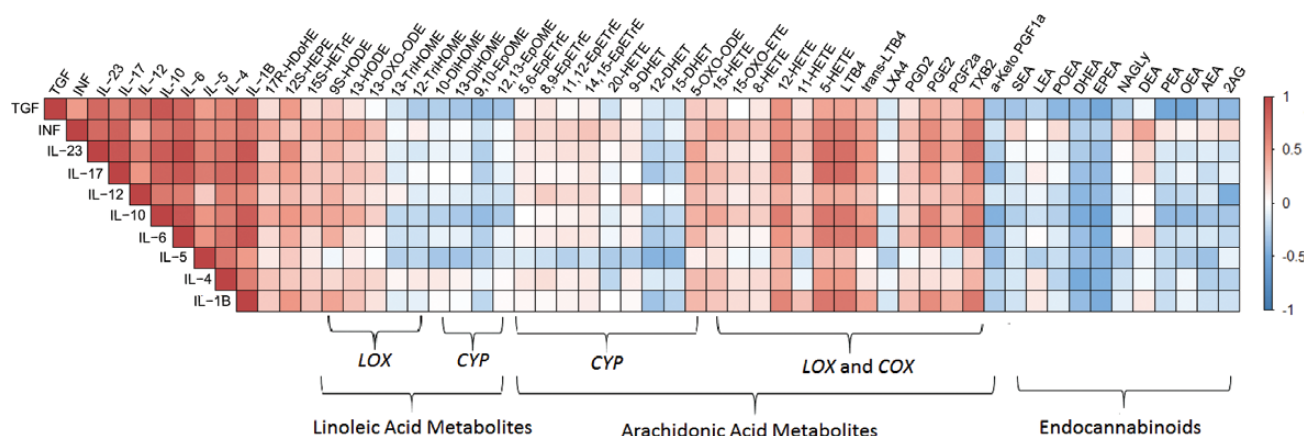


FIGURE 2. Colored heatmap of the pair-wise Spearman's rank correlation coefficients computed for cytokines vs cytokines, cytokines vs eCBs, and cytokines vs oxylipins. The colors refer to the correlation coefficient direction and magnitude, ranging from -1 (blue) to 1 (red). Each box in the heatmap is constructed from the metabolites-cytokines data of the 28 enrolled subjects. The metabolites are ordered according to the corresponding PUFA and the metabolic pathway. The correlation coefficients and the significance *P* values corresponding to all computed correlations are provided in the Supplementary Data.

TABLE 2: Comparison of Cytokine Gene Expressions Between the Study Groups

Cytokine	Treatment-Naïve UC Patients, Cytokine Expression	Deep Remission UC Patients, Cytokine Expression	Treatment-Naïve UC Patients vs Controls ^b	Deep Remission vs Controls ^b
	Fold Change ^a	Fold Change ^a		
IL-1 β	7.88	1.33	<0.001	0.88
IL-6	15.98	1.35	<0.001	0.88
IL-12A	3.35	0.79	0.0404	0.80
IFN	6.53	0.76	0.001	0.80
IL-4	4.58	1.29	0.008	0.95
IL-5	4.18	1.15	0.07	0.98
IL-17A	33.38	0.84	<0.001	0.76
IL-23A	4.26	0.73	0.001	0.35
IL-10	4.13	1.15	<0.001	0.54
TGF- β	1.94	1.17	0.009	0.82

^aMean fold change with respect to controls.

^bAdjusted *P* value from the 2-tailed Student *t* test by Dunnett post hoc.

analysis.³² For a more accurate quantification,³³ we have quantified 35 oxylipin and 11 eCB metabolites using a fully validated targeted high-performance LC-MS/MS method. In addition, previously published studies were performed on a mix of treated and treatment-naïve UC patients,^{29–31} which might be a limitation. Therefore, in this study, only treatment-naïve patients were included in the active UC group (Table 1). Moreover, the deep remission patients were selected based on their endoscopy scores and TNF measurement results.

Our findings suggest that inflammation of the colonic mucosa in UC at debut is associated with a significant elevation in concentrations of ω -6 AA-related oxylipins, specifically, PGE₂, TXB₂, trans-LTB₄, and 12-HETE, in addition to lower concentrations of ω -3 eCBs (DHEA and EPEA) (Fig. 1). The ω -6 AA-related oxylipins are potent immune response regulators. For example, PGE₂, produced via *COX* within the AA cascade, has a pro-inflammatory effect via IL-6 production and dendritic cell activation and an anti-inflammatory effect via local T_{reg}-cell accumulation and lipoxin induction.^{32, 34} Moreover, 12-HETE, produced via 12-*LOX* within the AA cascade, is a potent chemoattractant for neutrophils.³⁵ In addition, LTB₄ and its isomer trans-LTB₄ stimulate the neutrophil chemotaxis in UC.³⁶ Furthermore, TXB₂ is the stable downstream metabolite of thromboxane A₂ (TXA₂), which is known for causing vasoconstriction, platelet aggregation, and T-cell activation.³⁷ Studies on ω -6 and ω -3 PUFAs and their bioactive lipid metabolites in IBD patients have revealed an alteration in their mucosal levels.^{5, 32, 38} To our knowledge, our study is the

first to report alterations in EPEA and DHA levels in colonic mucosa in UC.

Interestingly, our data showed differences in the oxylipin profiles between deep remission patients and healthy controls. The ω -6-related oxylipin 15s-HETrE was significantly higher in the UC deep remission group in comparison with the control group, whereas the other investigated lipid metabolites did not differ significantly. Studies suggest that 15s-HETrE has an anti-inflammatory role via suppressing *COX-2* overexpression³⁹ and inhibiting platelet reactivity and thrombosis.⁴⁰ The UC remission patients enrolled in this study, however, had completely resolved inflammation in the colonic mucosa. Higher levels of 15(s)-HETrE could indicate the importance of this anti-inflammatory oxylipin in maintaining the state of remission. However, due to the low number of patients, this finding was not conclusive, and a further confirmatory study is needed.

We also investigated cytokine gene expression to have an overview of the association between cytokine production at the transcriptomic level and the lipid mediators at the metabolomic level. This allows a deeper interpretation of the variation in the eCB and oxylipin profiles. As our study is purely descriptive, we were more interested in describing the direction and degree of correlation than the statistical significance.

The gene expression of all investigated cytokines was higher in debut patients compared with healthy controls. This finding is in agreement with previous studies.^{24, 41–43} Interestingly, cytokine gene expression was positively correlated with AA-related oxylipins, except for LXA₄ and α -keto PGF₁, where a negative correlation was found (Fig. 2). These 2 oxylipins play an important anti-inflammatory role. For instance, α -keto PGF₁ is a stable metabolite of prostacyclin (PGI₂),⁴⁴ which inhibits platelet activation and reduces the intensity of the inflammatory response.⁴⁵ LXA₄ is a potent inflammation resolution oxylipin that promotes the clearance of apoptotic cells by macrophages and limits the infiltration of pro-inflammatory leukocytes.⁴⁶ In fact, an LXA₄ analog was found to inhibit TNF and IL-2 mucosal expression in induced colitis in mice.⁴⁷ Accordingly, increasing the levels of LXA₄ and PGI₂ may represent promising targets for intervention. Our data also revealed imbalances in the *CYP* pathway (Fig. 2), namely between the anti-inflammatory EpETrEs and the pro-inflammatory DHETs. This has previously been studied in obesity-induced colonic inflammation⁴⁸ but needs to be further explored in IBD.

In contrast to AA-related oxylipins, the correlation matrix revealed a negative correlation between the cytokine profiles and the eCB profile, in particular regarding EPEA and DHEA. Therefore, our findings suggest a potential role of ω -3-derived eCBs in the resolution of inflammation, and we propose novel therapeutic targets. Cannabinoid agonists and endocannabinoid degradation inhibitors in rodent models of IBD have identified a potential therapeutic role for eCBs.^{14, 49} Recently, a potential anti-inflammatory role for EPEA and DHEA was suggested.⁵⁰ This is through the epoxide forms

(EEQ-EA and EDP-EA), which inhibit the production of the pro-inflammatory cytokine IL-6 and promote the anti-inflammatory cytokine IL-10.⁵⁰ However, studies on the effectiveness of ω -3 supplementation in the prevention and treatment of UC have been inconclusive and have failed to establish daily recommended intake.^{51, 52} In contrast, a trial study aiming to restore the lipid signaling balance in the intestinal tract by alkaline sphingomyelinase (Alk-SMase) rectal installation found significantly reduced inflammation and TNF expression.⁹

The small sample size in our study precludes subgroup analysis according to the severity of the disease in the UC treatment-naïve group. In addition, the healthy control group was considerably older than the 2 UC groups, which might affect our results. Furthermore, the small size of the UC remission group, which only consisted of males, is considered a weakness in this study. Due to the imbalanced distribution in the analyzed cohort, the effects of both sex and age were not included in our data analysis. Therefore, our findings are exploratory and need to be validated in a larger cohort, in which, preferably, only sex- and age-matched healthy controls are included. This approach might give normally distributed data, and thus allow for the use of parametric statistical tests, which have more statistical power.

CONCLUSIONS

We demonstrated for the first time that the onset of UC is associated with increased levels of ω -6-related oxylipins and decreased levels of ω -3-related eCBs. Furthermore, we have revealed an association between bioactive lipid mediators and pro- and anti- cytokine production. Our findings highlight the mucosal fingerprints of the metabolism of PUFAs, which may be involved in the progression of inflammation and may be considered as potential targets for intervention that need to be explored in more detail in a larger study.

ACKNOWLEDGMENTS

We thank Renate Meyer for administering the patient samples and Ingrid Christiansen for the technical help performing the TNF levels measurements.

REFERENCES

- Kaplan GG. The global burden of IBD: from 2015 to 2025. *Nat Rev Gastroenterol Hepatol.* 2015;12:720–727.
- Molodecky NA, Kaplan GG. Environmental risk factors for inflammatory bowel disease. *Gastroenterol Hepatol (N Y).* 2010;6:339–346.
- Das UN. Inflammatory bowel disease as a disorder of an imbalance between pro- and anti-inflammatory molecules and deficiency of resolution bioactive lipids. *Lipids Health Dis.* 2016;15:11.
- Sjöqvist U, Hertervig E, Nilsson A, et al. Chronic colitis is associated with a reduction of mucosal alkaline sphingomyelinase activity. *Inflamm Bowel Dis.* 2002;8:258–263.
- Wolfer AM, Gaudin M, Taylor-Robinson SD, et al. Development and validation of a high-throughput ultrahigh-performance liquid chromatography-mass spectrometry approach for screening of oxylipins and their precursors. *Anal Chem.* 2015;87:11721–11731.
- Wallace JL. Prostaglandin biology in inflammatory bowel disease. *Gastroenterol Clin North Am.* 2001;30:971–980.
- Martel-Pelletier J, Lajeunesse D, Reboul P, Pelletier JP. Therapeutic role of dual inhibitors of 5-LOX and COX: selective and non-selective non-steroidal anti-inflammatory drugs. *Ann Rheum Dis.* 2003;62:501–509.
- Serhan CN, Petasis NA. Resolvins and protectins in inflammation resolution. *Chem Rev.* 2011;111:5922–5943.
- Acharya N, Penukonda S, Shcheglova T, et al. Endocannabinoid system acts as a regulator of immune homeostasis in the gut. *Proc Natl Acad Sci U S A.* 2017;114:5005–5010.
- Leinwand KL, Gerich ME, Hoffenberg EJ, Collins CB. Manipulation of the endocannabinoid system in colitis: a comprehensive review. *Inflamm Bowel Dis.* 2017;23:192–199.
- Mackie K. Cannabinoid receptors: where they are and what they do. *J Neuroendocrinol.* 2008;20(Suppl 1):10–14.
- Esposito G, Filippis DD, Cirillo C, et al. Cannabidiol in inflammatory bowel diseases: a brief overview. *Phytother Res.* 2013;27:633–636.
- Marquéz L, Suárez J, Iglesias M, et al. Ulcerative colitis induces changes on the expression of the endocannabinoid system in the human colonic tissue. *PLoS One.* 2009;4:e6893.
- Alhouayek M, Muccioli GG. The endocannabinoid system in inflammatory bowel diseases: from pathophysiology to therapeutic opportunity. *Trends Mol Med.* 2012;18:615–625.
- Di Sabatino A, Battista N, Biancheri P, et al. The endogenous cannabinoid system in the gut of patients with inflammatory bowel disease. *Mucosal Immunol.* 2011;4:574–583.
- D'Argenio G, Valenti M, Scaglione G, et al. Up-regulation of anandamide levels as an endogenous mechanism and a pharmacological strategy to limit colon inflammation. *FASEB J.* 2006;20:568–570.
- Darmani NA, Izzo AA, Degenhardt B, et al. Involvement of the cannabinimetic compound, N-palmitoyl-ethanolamine, in inflammatory and neuropathic conditions: review of the available pre-clinical data, and first human studies. *Neuropharmacology.* 2005;48:1154–1163.
- Stange EF, Travis SP, Vermeire S, et al; European Crohn's and Colitis Organisation (ECCO). European evidence-based consensus on the diagnosis and management of ulcerative colitis: definitions and diagnosis. *J Crohns Colitis.* 2008;2:1–23.
- Sutherland LR, Martin F, Greer S, et al. 5-aminosalicylic acid enema in the treatment of distal ulcerative colitis, proctosigmoiditis, and proctitis. *Gastroenterology.* 1987;92:1894–1898.
- Olsen T, Goll R, Cui G, et al. Tissue levels of tumor necrosis factor- α correlates with grade of inflammation in untreated ulcerative colitis. *Scand J Gastroenterol.* 2007;42:1312–1320.
- Johnsen KM, Goll R, Hansen V, et al. Repeated intensified infliximab induction - results from an 11-year prospective study of ulcerative colitis using a novel treatment algorithm. *Eur J Gastroenterol Hepatol.* 2017;29:98–104.
- Wu J, Gouveia-Figueira S, Domellöf M, et al. Oxylipins, endocannabinoids, and related compounds in human milk: levels and effects of storage conditions. *Prostaglandins Other Lipid Mediat.* 2016;122:28–36.
- Gouveia-Figueira S, Nording ML. Validation of a tandem mass spectrometry method using combined extraction of 37 oxylipins and 14 endocannabinoid-related compounds including prostamides from biological matrices. *Prostaglandins Other Lipid Mediat.* 2015;121:110–121.
- Rismo R, Olsen T, Cui G, et al. Mucosal cytokine gene expression profiles as biomarkers of response to infliximab in ulcerative colitis. *Scand J Gastroenterol.* 2012;47:538–547.
- Schmittgen TD, Livak KJ. Analyzing real-time PCR data by the comparative C(T) method. *Nat Protoc.* 2008;3:1101–1108.
- Xia J, Wishart DS. Using metaboanalyst 3.0 for comprehensive metabolomics data analysis. *Curr Protoc Bioinformatics.* 2016;55:14.10.1–14.10.91.
- van den Berg RA, Hoefsloot HC, Westerhuis JA, et al. Centering, scaling, and transformations: improving the biological information content of metabolomics data. *BMC Genomics.* 2006;7:142.
- Vinaixa M, Samino S, Saez I, et al. A guideline to univariate statistical analysis for LC/MS-based untargeted metabolomics-derived data. *Metabolites.* 2012;2:775–795.
- Boughton-Smith NK, Hawkey CJ, Whittle BJ. Biosynthesis of lipoxygenase and cyclo-oxygenase products from [14C]-arachidonic acid by human colonic mucosa. *Gut.* 1983;24:1176–1182.
- Jupp J, Hillier K, Elliott DH, et al. Colonic expression of leukotriene-pathway enzymes in inflammatory bowel diseases. *Inflamm Bowel Dis.* 2007;13:537–546.
- Carty E, De Brabander M, Feakins RM, Rampton DS. Measurement of in vivo rectal mucosal cytokine and eicosanoid production in ulcerative colitis using filter paper. *Gut.* 2000;46:487–492.
- Masoodi M, Pearl DS, Eiden M, et al. Altered colonic mucosal polyunsaturated fatty acid (PUFA) derived lipid mediators in ulcerative colitis: new insight into relationship with disease activity and pathophysiology. *PLoS One.* 2013;8:e76532.
- Cajka T, Fiehn O. Toward merging untargeted and targeted methods in mass spectrometry-based metabolomics and lipidomics. *Anal Chem.* 2016;88:524–545.
- Kalinski P. Regulation of immune responses by prostaglandin E2. *J Immunol.* 2012;188:21–28.

35. Szczuko M, Zapałowska-Chwyć M, Maciejewska D, et al. Significant improvement selected mediators of inflammation in phenotypes of women with PCOS after reduction and low GI diet. *Mediators Inflamm.* 2017;2017:1–7.
36. Wéra O, Lancellotti P, Oury C. The dual role of neutrophils in inflammatory bowel diseases. *J Clin Med.* 2016;5:1–24.
37. Lone AM, Taskén K. Proinflammatory and immunoregulatory roles of eicosanoids in T cells. *Front Immunol.* 2013;4:1–15.
38. Lee Y, Choo J, Kim SJ, et al. Analysis of endogenous lipids during intestinal wound healing. *PLoS One.* 2017;12:1–23.
39. Pham H, Banerjee T, Ziboh VA. Suppression of cyclooxygenase-2 overexpression by 15S-hydroxyeicosatrienoic acid in androgen-dependent prostatic adenocarcinoma cells. *Int J Cancer.* 2004;111:192–197.
40. Yeung J, Tourdot BE, Adili R, et al. 12(S)-hetre, a 12-lipoxygenase oxylipin of dihomo- γ -linolenic acid, inhibits thrombosis via *gas* signaling in platelets. *Arterioscler Thromb Vasc Biol.* 2016;36:2068–2077.
41. Nemeth ZH, Bogdanovski DA, Barratt-Stopper P, et al. Crohn's disease and ulcerative colitis show unique cytokine profiles. *Cureus.* 2017;9:1–11.
42. Matsuda R, Koide T, Tokoro C, et al. Quantitative cytokine mRNA expression profiles in the colonic mucosa of patients with steroid naïve ulcerative colitis during active and quiescent disease. *Inflamm Bowel Dis.* 2009;15:328–334.
43. Korolkova OY, Myers JN, Pellom ST, et al. Characterization of serum cytokine profile in predominantly colonic inflammatory bowel disease to delineate ulcerative and Crohn's colitides. *Clin Med Insights Gastroenterol.* 2015;8:29–44.
44. Olofsson J, Norjavaara E, Selstam G. Synthesis of prostaglandin F2 alpha, E2 and prostacyclin in isolated corpora lutea of adult pseudopregnant rats throughout the luteal life-span. *Prostaglandins Leukot Essent Fatty Acids.* 1992;46:151–161.
45. Yoshida H, Granger DN. Inflammatory bowel disease: a paradigm for the link between coagulation and inflammation. *Inflamm Bowel Dis.* 2009;15:1245–1255.
46. Biasi F, Leonarduzzi G, Oteiza PI, Poli G. Inflammatory bowel disease: mechanisms, redox considerations, and therapeutic targets. *Antioxid Redox Signal.* 2013;19:1711–1747.
47. Fiorucci S, Wallace JL, Mencarelli A, et al. A beta-oxidation-resistant lipoxin A4 analog treats hapten-induced colitis by attenuating inflammation and immune dysfunction. *Proc Natl Acad Sci U S A.* 2004;101:15736–15741.
48. Wang W, Yang J, Zhang J, et al. Lipidomic profiling reveals soluble epoxide hydrolase as a therapeutic target of obesity-induced colonic inflammation. *Proc Natl Acad Sci U S A.* 2018;115:5283–5288.
49. Lee Y, Jo J, Chung HY, et al. Endocannabinoids in the gastrointestinal tract. *Am J Physiol Gastrointest Liver Physiol.* 2016;311:G655–G666.
50. McDougale DR, Watson JE, Abdeen AA, et al. Anti-inflammatory ω -3 endocannabinoid epoxides. *Proc Natl Acad Sci U S A.* 2017;114:E6034–E6043.
51. Scaioli E, Liverani E, Belluzzi A. The imbalance between n-6/n-3 polyunsaturated fatty acids and inflammatory bowel disease: a comprehensive review and future therapeutic perspectives. *Int J Mol Sci.* 2017;18:1–23.
52. Ungaro F, Rubbino F, Danese S, D'Alessio S. Actors and factors in the resolution of intestinal inflammation: lipid mediators as a new approach to therapy in inflammatory bowel diseases. *Front Immunol.* 2017;8:1–13.

Supplementary Data Content



SUPP. FIGURE 1. Colored heatmap of the pair wise Spearman's rank correlation coefficients computed for the cytokines vs. cytokines, cytokines vs. metabolites, and metabolites vs metabolites. The colors refers to the correlation coefficient direction and magnitude ranging from -1 (blue) to 1 (red). Each box in the heatmap is constructed from the metabolites and cytokines data of the 28 enrolled subjects.

Paper II

Diab, J., Hansen, T., Goll, R., Stenlund, H., Ahnlund, M., Jensen, E., ... Forsdahl, G. (2019). Lipidomics in Ulcerative Colitis Reveal Alteration in Mucosal Lipid Composition Associated With the Disease State. *Inflammatory bowel diseases*, 25(11), 1780-1787.

<https://doi.org/10.1093/ibd/izz098>

Paper III

Diab, J., Hansen, T., Goll, R., Stenlund, H., Jensen, E., Moritz, T., Florholmen, J. & Forsdahl, G. (2019). Mucosal Metabolomic Profiling and Pathway Analysis Reveal the Metabolic Signature of Ulcerative Colitis. *Metabolites*, 9(12), 291.

<https://doi.org/10.3390/metabo9120291>

Article

Mucosal Metabolomic Profiling and Pathway Analysis Reveal the Metabolic Signature of Ulcerative Colitis

Joseph Diab ¹, Terkel Hansen ¹ , Rasmus Goll ^{2,3}, Hans Stenlund ⁴, Einar Jensen ¹, Thomas Moritz ^{4,5} , Jon Florholmen ^{2,3} and Guro Forsdahl ^{1,*} 

- ¹ Natural Products and Medicinal Chemistry Research Group, Department of Pharmacy, Faculty of Health Sciences, University of Tromsø The Arctic University of Norway, 9037 Tromsø, Norway; Joseph.diab@uit.no (J.D.); Terkel.hansen@uit.no (T.H.); Einar.jensen@uit.no (E.J.)
- ² Research Group of Gastroenterology and Nutrition, Department of Clinical Medicine, Faculty of Health Sciences, University of Tromsø The Arctic University of Norway, 9037 Tromsø, Norway; Rasmus.Goll@unn.no (R.G.); Jon.Florholmen@unn.no (J.F.)
- ³ Department of Medical Gastroenterology, University Hospital of North Norway, 9037 Tromsø, Norway
- ⁴ Swedish Metabolomics Center, Department of Molecular Biology, Umeå University, 90736 Umeå, Sweden; hans.stenlund01@umu.se (H.S.); Thomas.Moritz@slu.se (T.M.)
- ⁵ The Novo Nordisk Foundation Center for Basic Metabolic Research, 2200 Copenhagen, Denmark
- * Correspondence: guro.forsdahl@uit.no

Received: 15 October 2019; Accepted: 25 November 2019; Published: 27 November 2019



Abstract: The onset of ulcerative colitis (UC) is characterized by a dysregulated mucosal immune response triggered by several genetic and environmental factors in the context of host–microbe interaction. This complexity makes UC ideal for metabolomic studies to unravel the disease pathobiology and to improve the patient stratification strategies. This study aims to explore the mucosal metabolomic profile in UC patients, and to define the UC metabolic signature. Treatment-naïve UC patients ($n = 18$), UC patients in deep remission ($n = 10$), and healthy volunteers ($n = 14$) were recruited. Mucosa biopsies were collected during colonoscopies. Metabolomic analysis was performed by combined gas chromatography coupled to time-of-flight mass spectrometry (GC-TOF-MS) and ultra-high performance liquid chromatography coupled with mass spectrometry (UHPLC-MS). In total, 177 metabolites from 50 metabolic pathways were identified. The most prominent metabolome changes among the study groups were in lysophosphatidylcholine, acyl carnitine, and amino acid profiles. Several pathways were found perturbed according to the integrated pathway analysis. These pathways ranged from amino acid metabolism (such as tryptophan metabolism) to fatty acid metabolism, namely linoleic and butyrate. These metabolic changes during UC reflect the homeostatic disturbance in the gut, and highlight the importance of system biology approaches to identify key drivers of pathogenesis which prerequisite personalized medicine.

Keywords: inflammatory bowel disease; metabolomics; pathway analysis; ulcerative colitis; tryptophan metabolism; fatty acid metabolism; personalized treatment

1. Introduction

Inflammatory bowel diseases (IBD) are chronic, relapsing inflammatory disorders in the gastrointestinal tract that affect around 0.3% of the population in Europe and North America with increasing worldwide incidence [1]. The two major forms of IBD, ulcerative colitis (UC) and Crohn's disease (CD), are characterized by a dysregulated mucosal immune response triggered by several genetic and environmental factors in the context of host–microbe interaction [2]. The interaction

between these components yield a network effect, defined as ‘IBD interactome’, which results in an overwhelming complexity [3]. This complexity cannot be solved by studying one component in isolation from the others. For instance, only 10% of IBD cases can be explained by genetic variance [4], while it remains unclear whether the alteration in the microbiota is primary or secondary to the chronic inflammation in IBD [5]. Recently, multiomics approaches were suggested as a tool to unravel the IBD interactome, and to improve the patient stratification strategies toward personalized medicine [3,6]. Metabolomics, defined as the comprehensive measurement of all metabolites (low-molecular-weight molecules) in a biological specimen, is perhaps the most closely linked to the phenotype [7]. It describes the pathophysiology of a disease at the molecular level, and provides predictive, prognostic and diagnostic markers of diverse disease states [8]. Previous published metabolomic data from IBD patients have given first hints on metabolic changes during the course of the disease. However, these data are either generated from serum [9–14], stool [12], or urine [15] samples. Moreover, these studies were restricted to pediatric patients [12,14], or treated patients [9,11,13,15].

This study aimed to explore the mucosal metabolomic profile in treatment-naïve UC patients compared to treated UC patients in deep remission and to healthy subjects. The high throughput metabolomic analysis was performed by a combined gas chromatography coupled to time-of-flight mass spectrometry (GC-TOF-MS) and ultra-high performance liquid chromatography coupled with mass spectrometry (UHPLC-MS) on biopsy samples. Our results maps the metabolic changes during IBD, and highlights the metabolic signatures of the IBD interactome network.

2. Results

2.1. Subjects Characteristics

Colon biopsies collected from newly diagnosed treatment-naïve UC patients ($n = 18$), UC patients in state of deep remission ($n = 10$), and healthy controls ($n = 14$) were included in this study. The study group characteristics are shown in Table 1. In addition, clinical data such as tumor necrosis factor (TNF) gene expression, levels of fecal calprotectin and C-reactive protein are provided. Furthermore, data on daily supplementation with omega-3 and previous treatment with antibiotics are included in Table 1.

Table 1. Description of study group characteristics.

Characteristics	Active UC (Debut)	UC Remission	Healthy Controls
Number of Subjects	18	10	14
Age, years (mean, range, P -value *)	40 (20–68) 0.09	48 (31–77) 0.18	55 (26–83)
Gender (Female/Male)	6/12	4/6	4/10
UCDAI Score (Mild, Moderate, Severe)	12/2/4		
Biopsy sampling site (Rectum/sigmoid)	3/15	5/5	4/10
TNF- α , copies/ μ g of total RNA (mean, range, P -value *)	18,122 (4600–31,700) 0.01	4675 (800–7300) 0.11	5478 (1800–11,300)
Fecal calprotectin, μ g/g (mean, range, P -value *)	828 (25–1970) < 0.01	53 (25–150) 0.15	46 (25–180)
C-Reactive protein, mg/L (mean, range, P -value *)	16.5 (5–92) 0.08	5.6 (5–11) 0.31	5.2 (5–11)
Smoking/non-smoking	1/17	1/9	3/11
Omega-3 daily supplementation (Yes/No)	6/12	3/7	7/7
Antibiotic in the last 6 months prior to the biopsy (Yes/No)	3/15	0/10	2/12

* computed P -value from the comparison of two means versus healthy controls group.

2.2. Mucosal Metabolite Profiles in Treatment-Naïve UC Patients, UC Remission Patients and Controls

Mucosal metabolite profiles were compared to identify significant alteration in metabolite composition in treatment-naïve patients and UC deep remission patients compared with controls (Supplementary Table S1). The results are summarized as a Venn diagram in Figure 1. Among the 177 metabolites included in this study, the mucosal levels of 60 metabolites were altered in UC treatment-naïve patients compared with healthy controls. Among these metabolites, the mucosal levels of 38 metabolites were higher, and those of 22 metabolites were lower. Similarly, the mucosal levels of 21 metabolites were changed in UC remission patients compared with healthy controls. Accordingly, the mucosal levels of 10 metabolites were higher and those of 11 metabolites were lower. The most prominent changes among the study groups were in lysophospholipids, acyl carnitine, and amino acid profiles. In addition, 46 metabolites were changed in treatment-naïve UC patients compared to deep remission UC patients.

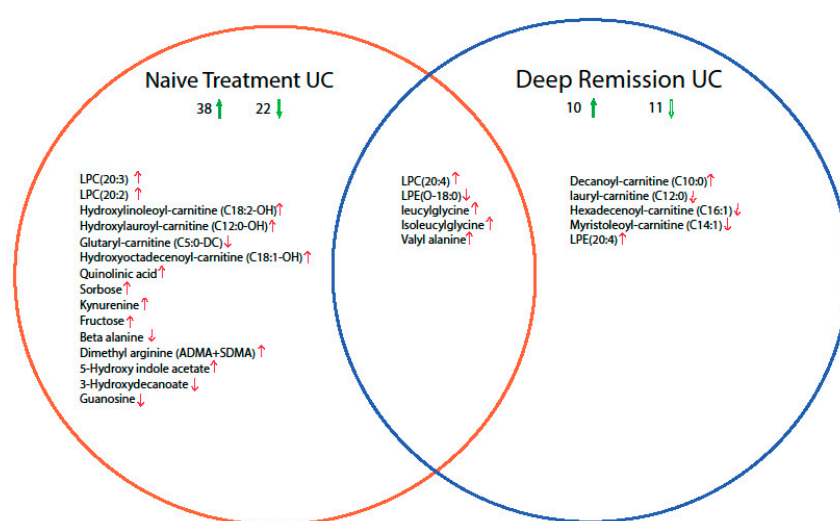


Figure 1. Venn diagram summarizing the comparison between the mucosal levels of metabolites in treatment-naïve ulcerative colitis (UC) patients and UC remission patients with healthy controls. Significantly altered metabolites were determined by Kruskal–Wallis test (False discovery rate (FDR) corrected $P < 0.05$), followed by the Dunn post-hoc test (Bonferroni adjusted $P < 0.017$). In total, the levels of 60 and 21 metabolites were changed in treatment-naïve UC and deep-remission UC, respectively, compared with healthy controls. The number of up/down regulated metabolites is indicated next to up/down green arrows. For simplicity, only the full names of significantly altered metabolites at a cut-off twofold change are presented. The red up/down arrows correspond to the direction of change (up/down regulation).

2.3. Discriminative Models for UC State

Principle component analysis (PCA) was used as an unbiased multivariate analysis to have an overview of the variation within the data, to detect outliers, and to determine subgroups. The two main components explained 29% of the variability in the combined metabolomic data set (42 observations, 177 variables). Accordingly, the PCA t1/t2-scores plot (Figure 2A) revealed a distinct metabolomic profile in inflamed mucosa taken from treatment-naïve UC patients compared to noninflamed mucosa taken from UC remission patients and healthy controls. In addition, it was observed that the UC remission patients differed to a lesser extent from the healthy controls. Conversely, PCA did not show specific clustering patterns of the study subjects according to age, sex or activity score (Supplementary Figure S2).

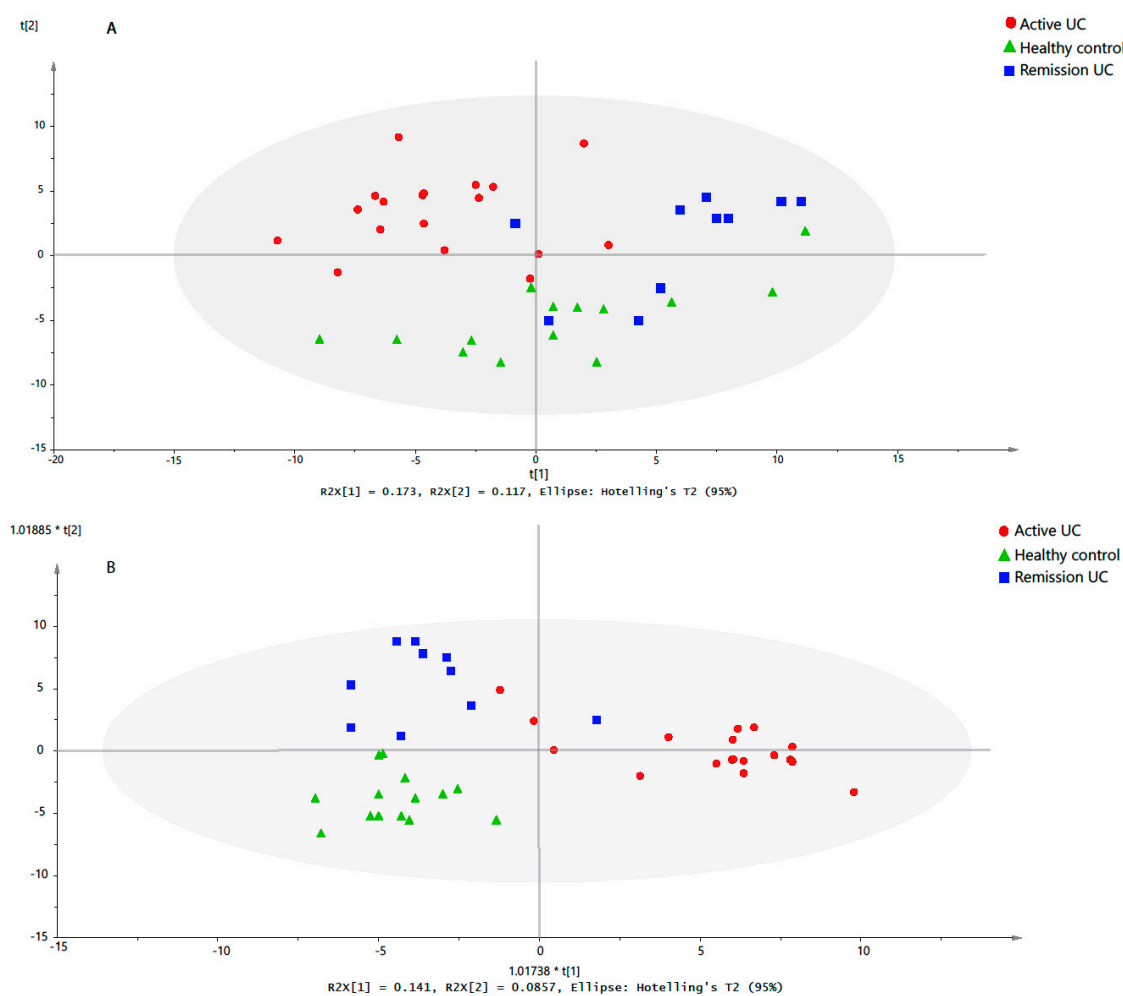


Figure 2. Multivariate analysis of the mucosal metabolomic profiles. Each subject was labeled according to the corresponding study group. **(A)** Principle component analysis (PCA) $t1/t2$ -scores plots. The variation explained by PC1 and PC2 were 17.3% and 11.7%, respectively. $t1$ is the first component, which explains the largest variation, $t2$ is independent of $t1$ and explains second largest variation. **(B)** The $t1/t2$ -score plot of the orthogonal partial least squares projection to latent structures-discriminant analysis (OPLS-DA) model (two predictive components and one orthogonal component) built from the mucosal metabolites profile of UC treatment-naïve patients, UC remission patients and healthy controls. $t1$ and $t2$ show the direction of class separation. The performance parameters R^2X_{cum} , R^2Y_{cum} and Q^2_{cum} were 0.33, 0.77 and 0.53, respectively.

A supervised orthogonal partial least squares projection to latent structures-discriminant analysis (OPLS-DA) model was built to identify the differential metabolites between active UC patients, remission UC patients and healthy controls. A significant OPLS-DA model (P -value from cross-validated analysis of variance (CV-ANOVA) was 6.15×10^{-7}), with maximum separation between the study groups with good predictive ability $Q^2_{cum} > 0.5$ was obtained (Figure 2B). Additionally, a permutation test (Supplementary Figure S2) indicated that the obtained OPLS-DA model was not influenced by overfitting. The metabolites were ranked according to the variables importance in projection (VIP) scores (Supplementary Table S2) to identify the most distinctive metabolites between the study groups at a VIP threshold > 1.5 . Glutamic acid, asparagine, lysophosphatidylethanolamine LPE (O-18:0), hypoxanthine, lysophosphatidylcholine LPC (20:3), hydroxyl carnitine, and LPC (20:4) were identified as the most important metabolites in the model, and the mucosal levels of these metabolites among the study groups are represented in Figure 3.

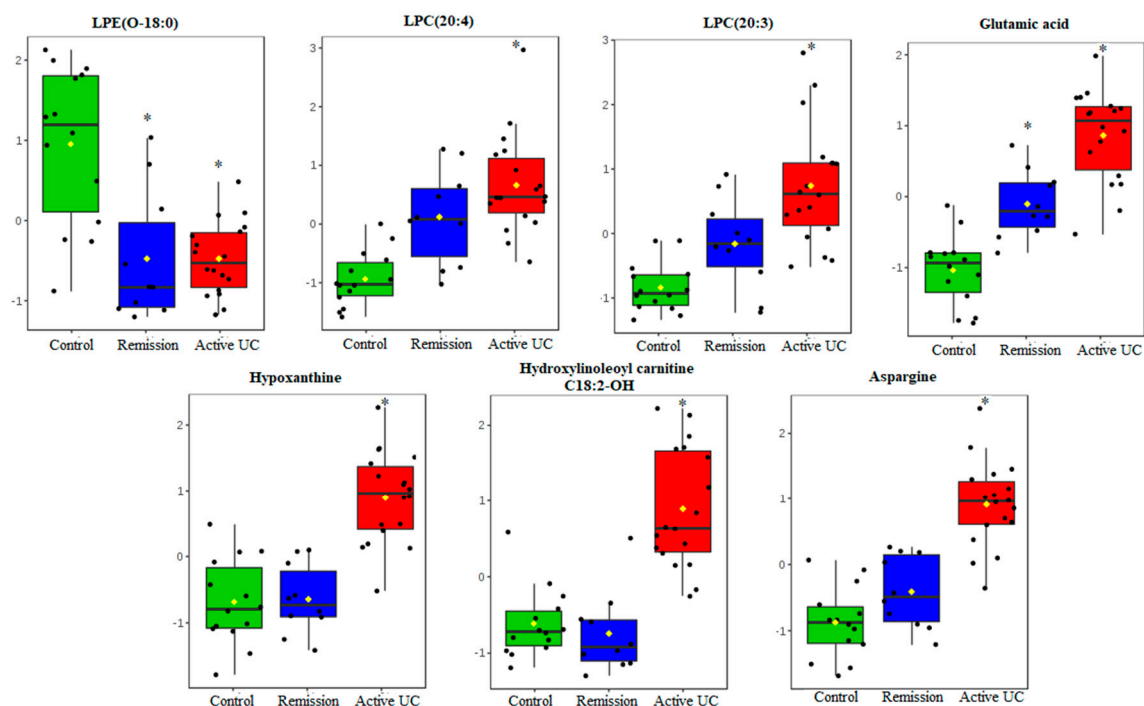


Figure 3. Jitter box plots of the mucosal level of the most discriminant metabolites (Variables importance of projection VIP score > 1.5 in OPLS-DA) between treatment-naïve UC, remission UC, and healthy controls. The levels of the metabolites were autoscaled for visualization. * P -value ≤ 0.017 versus healthy control was obtained by a Dunn post-hoc test.

2.4. Pathway Analysis

Integrated pathway analysis was performed to capture the metabolic pathways disruption during the active UC state, and to ease the biological interpretation. The annotated metabolites were mapped into 50 metabolic pathways (Supplementary Table S3) according to the Kyoto encyclopedia of genes and genomes KEGG database. As Figure 4 shows, several pathways were the most perturbed, ranging from amino acid metabolism (such as tryptophan metabolism, and alanine, aspartate and glutamate metabolism) to antioxidant defense pathway (glutathione pathway). Furthermore, the pathway analysis revealed a disruption in the long- and short-chain fatty acid (LCFA and SCFA) metabolism, namely linoleic metabolism and butyrate metabolism. The impact value of altered metabolic pathways, based on topology analysis, ranged from 0.01–0.66. A summary of significantly altered pathways is provided in Table 2. In addition, the complete result from the pathway analysis containing all 50 metabolic pathways is provided in Supplementary Table S3.

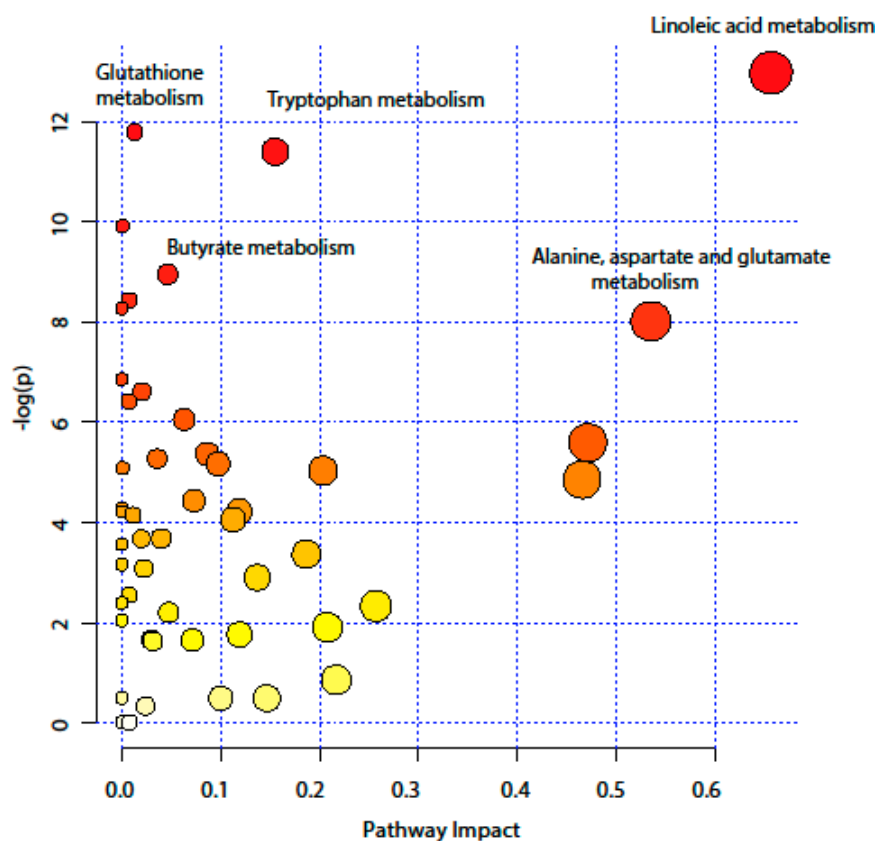


Figure 4. Pathway analysis, combining pathway enrichment and pathway topology analysis, of annotated metabolites in UC treatment-naïve patients and healthy controls. The x-axis marks the pathway impact and the y-axis represents the pathway enrichment. Each node marks a pathway, with larger sizes and darker colours represent higher pathway impact values and higher pathway enrichment.

Table 2. Altered metabolic pathways according to pathway analysis.

KEEG Pathway	Numb. Metabolites	Matched Metabolites from the Metabolomics Data	Adjusted <i>P</i> -value **	Impact ***
Linoleic Acid Metabolism	15	Linoleic acid *	<0.001	0.66
Alanine, Aspartate and Glutamate Metabolism	24	N-Acetyl-L-aspartic acid *; L-Asparagine *; L-Glutamine *; L-Glutamic acid *; Gamma-Aminobutyric acid; Fumaric acid; Succinic acid	0.014	0.53
Tryptophan Metabolism	79	L-Tryptophan *; 5-Hydroxyindoleacetic acid *; L-Kynurenine *; Picolinic acid; Quinolinic acid*	<0.001	0.15
Butyrate Metabolism	40	Gamma-Aminobutyric acid; L-Glutamic acid *; Fumaric acid	0.006	0.05
Glutathione Metabolism	38	L-Glutamic acid *; Cysteinylglycine; Pyroglutamic acid *; Ornithine *	<0.001	0.01

* Altered metabolites (*P*-value ≤ 0.017 versus healthy control obtained by Dunn post-hoc test). ** *P*-values were calculated from the enrichment analysis then adjusted by Holm method. *** Impact is the pathway impact score calculated from pathway topology analysis.

3. Discussion

This study provides a unique and detailed snapshot of the mucosal metabolite profile in clearly stratified UC patients (treatment-naïve, newly diagnosed, and deep remission patients). The reported 177 metabolites revealed a distinctive metabolic fingerprint in active UC patients compared with healthy controls. In addition, the metabolomic profiling coupled with pathway analysis provided a deeper understanding of the metabolome changes among UC patients with ongoing active inflammation. Several metabolic pathways were identified, including pathways related to amino acid metabolism, SCFA and LCFA metabolism, and glutathione metabolism.

To our knowledge, this is the first study of mucosal metabolomic profile in treatment-naïve and deep remission UC patients. In contrast, previous studies were restricted to bio-fluids. It is well established that tissues are under greater homeostatic regulation than plasma¹⁶. Thus, it provides highly consistent measurements among individuals [16], and better understanding of the molecular basis of diseases [17]. Moreover, previous studies included treated and untreated UC patients. In the current work, however, only treatment-naïve UC patients were represented in the active UC group. In addition, the state of remission was defined by strict criteria (endoscopy, histology, and normalized TNF gene expression). Notably, remission patients were excluded from the pathway analysis. This stratification of patients allows capturing key metabolic alterations that are exclusively associated with the UC onset. Furthermore, the combination of two analytical metabolomic platforms allowed analysing metabolites in different polarity and molecular weight ranges, and gaining a wider prospective of the metabolome [18].

According to the pathway analysis, the omega-6 linoleic acid (ω -6 LA 18:2) metabolism had the highest impact score in the pathway analysis. Ω -6 LA, is an essential fatty acid, which is metabolised to dihomo- γ -linolenic acid (ω -6 DGLA 20:3). The latter is converted by fatty acid desaturase 1 (FADS1) to ω -6 arachidonic acid (AA 20:4) [19]. DGLA and AA are esterified with glycerol in the phospholipids, such as LPC, in the cell membrane, and released by phospholipase A2 during inflammation [19]. The released AA and DGLA are metabolised to form bioactive pro- and anti-inflammatory mediators. In the current data, LA was found to be lower in active UC patients. In contrast, the mucosal levels of LPC (20:3) and LPC (20:4) were higher in treatment-naïve UC compared to healthy controls, and were considered among the top discriminant metabolites between the study groups. This finding supports evidence suggesting that the onset of IBD is characterized by an imbalance between pro- and anti-inflammatory mediators [20]. For instance, the mucosal levels of AA related pro-inflammatory metabolites were elevated in treatment-naïve UC patients [21]. In addition, variations in the FADS1 gene were found to be associated with higher susceptibility to IBD [22,23]. Therefore, it seems that the increased metabolism of LA to AA is a crucial step in the IBD pathology.

Another important finding is the alteration in the amino acid metabolism, namely the tryptophan (Trp) metabolism and the alanine, aspartate and glutamate metabolism. Recently, Trp emerged as the hub of host–microbiota crosstalk considering that Trp metabolism pathways leading to serotonin, kynurenine (Kyn), and indole derivatives are under the direct or indirect control of the microbiota [24]. It was shown that supplementation with Trp improves the clinical symptoms and reduces the pro-inflammatory cytokines production in experimental colitis [25]. Furthermore, indole derivatives act as ligands for the aryl hydrocarbon receptor (AHR) inducing local production of interleukin-22 (IL-22), which maintains intestinal homeostasis, promotes immune defense and tissue repair. In the current study, we report a decreased mucosal level of Trp and an increased level of Kyn. This is in alignment with previous studies, which have reported low serum level of Trp in UC patients [10,12]. Notably, a large cohort study consisting of 148 UC patients has concluded that a higher Trp metabolism rate is associated with UC activity [26].

Furthermore, the current data demonstrates several perturbation in amino acid metabolism during UC. For instance, the mucosal levels of glutamic acid and asparagine were low in healed mucosa, and were gradually elevated in UC remission patients and active UC patients. Accordingly, glutamic acid and asparagine were discriminative between treatment-naïve UC patients, UC patients in remission

and healthy controls. Interestingly, in a previous study, high levels of amino acids were detected in stool samples from IBD patients, and were linked with the gut microbiota dysbiosis [27]. In addition, higher urinary level of asparagine and glutamic acid were reported [28]. Notably, previous study of mucosal amino acids profile in IBD patients demonstrated increased levels of several amino acid, such as aspartate, glutamine, and glutamic acid in active UC patients [29]. However, we cannot determine to which degree the reported changes in mucosal amino acid levels are caused by gut microbiota.

Altered butyrate metabolism is another evidence of the bacterial dysbiosis in UC. It is well documented that the alteration in butyrate and other short chain fatty acid (SCFA) production is a hallmark of active UC patients [30]. For instance, it was found that dysbiosis in IBD patients is characterized by a decrease in the number of SCFAs/butyrate-producing bacteria [31]. Another study has reported reduction of butyrate and propionate in stool samples of IBD patients [32]. Although the current data did not show significant changes in butyrate related metabolites in the mucosa, the decreased mucosal level of glutamine in UC patients might indicate that glutamine is being used as energy source instead of butyrate, as previously reported [33]. Interestingly, previous data have shown low abundance of proteins related to this specific utilization of butyrate in UC patients' mucosa [34].

The variation in the acylcarnitine profile, demonstrated in the current data, could also indicate energy impairment. Acylcarnitine is a mediator that transfers catabolism products of fatty acids and amino acids into mitochondria for β -oxidation [35]. This is a key step in the process of energy production. Therefore, the accumulation of medium and long chain fatty acyl carnitine, according to the current data, provides further evidence of the mitochondrial dysfunction. However, it is unclear yet whether the mitochondrial dysfunction in IBD is caused by a dysbiosis or if it is induced by the pro-inflammatory cytokines, such as TNF [36].

Although the inclusion criteria for remission patients was mucosal healing and immunological remission [37], the present work reveals a distinct metabolome in UC deep remission patients with respect to healthy controls and active UC patients. This comes in alignment with previously published data which reports a distinct mucosal lipid composition fingerprint in UC deep remission patients compared with healthy controls and treatment-naïve UC patients [38]. Consequently, from a clinical point of view, these findings supports the emerging importance of 'Omics' analysis in improving the current scoring system, monitoring the disease progression and improving the treatment strategies [39].

The relatively small sample size in the current study preclude subgroup analysis according to the severity of the disease. Hence, the reported results are exploratory and need to be validated by a larger cohort, which include inflamed and non-inflamed mucosa from UC patients. In addition, to further get insight in the mechanistic behind the alteration in the metabolic pathways, gene expression and/or protein data, preferably from the same patients, should be studied. Combining such multi omics data might also underline metabolite changes caused by the gut microbiota. Furthermore, we suggest the absolute quantification and identification of metabolites involved in the pathways of interest, especially tryptophan and butyrate pathways using targeted analysis. This is especially of interest for future evaluation of clinical validity, where absolute quantitative levels is a necessity. Suggestively, future studies also need to explore the relationship between metabolic changes, microbiota dysbiosis, and the activity of IBD. This approach will provide key insight into the disease outcome and response to treatment.

4. Materials and Methods

4.1. Patients and Biopsy Collection

Mucosal biopsies were collected from newly diagnosed treatment-naïve UC patients ($n = 18$) and UC patients in deep remission ($n = 10$). The UC diagnosis was made upon clinical, endoscopic and histological criteria established by the European Crohn and Colitis Organization (ECCO) guidelines [40]. The degree of inflammation was endoscopic evaluated by the scoring system of ulcerative colitis disease activity index (UCDAI); UCDAI score of 3–5 is defined as mild, 6–8 as moderate, and 9–12

as severe UC [41]. TNF- α mRNA expression levels were measured by real-time PCR in mucosal biopsies to evaluate the UC activity [42]. The state of deep remission was achieved after treatment with anti-TNF- α monoclonal antibody biologics. Deep remission was defined as endoscopic healed mucosa by ECCO 2017 consensus (Mayo score = 0) [43] and, additionally, normalized mucosal TNF- α level [44]. Subjects performing endoscopy for colonic cancer screening, with normal findings (no ulcer, no redness) and normal colonic histological examination, served as healthy controls ($n = 14$).

All biopsies were acquired from the rectum or sigmoid colon (Table 1). In active UC patients, biopsies were obtained from the most inflamed mucosa. The dry weight of the biopsies ranged from 2–8 mg. All biopsies were dry-frozen immediately at $-80\text{ }^{\circ}\text{C}$, and kept at this temperature until further analysis. The Regional Committee of Medical Ethics of North Norway and the Norwegian Social Science Data Services approved the study and the storage of biological material under the number (REK NORD 2012/1349).

In addition, all enrolled subjects have signed an informed consent form, and the study was conducted in accordance with the Declaration of Helsinki.

4.2. Chemicals and Reagents

Detailed information of chemicals used for GC-MS and UHPLC-MS analysis is provided in the supplementary data section.

4.3. Sample Preparation

Metabolite extraction was carried out as previously described [45]. Briefly, each biopsy was transferred to an Eppendorf tube and kept on ice. Then, the extraction solution (methanol:water (8:1)) with all internal standards was added to the biopsy in a solid-to-solvent ratio of 1:15 (w/v). The final concentration of UPLC-MS standards and GC-MS standards was 0.625 ng/mL and 5 ng/ μL respectively. Two tungsten beads were added to each tube, and the samples were shaken at 30 Hz for 3 min in a MM301 Vibration Mill (Retsch GmbH & Company KG). The beads were removed, and the samples were further centrifuged at 14,000 rpm and $4\text{ }^{\circ}\text{C}$ for 3 min. Finally, the supernatant was transferred to a micro vials for UHPLC-MS and GC-MS analysis, 200 μL was used for UHPLC-MS analysis and 150 μL for GC-MS analysis. Samples were dried using a vacuum concentrator (MIVac, SP, Warminster, PA, USA). Quality Control (QC) samples were prepared by pooling 10 μL from each extract. Extracts were stored at $-80\text{ }^{\circ}\text{C}$ until analysis.

4.4. UHPLC-MS Analysis

On the day of analysis, samples were reconstituted in 20 μL of methanol:water (1:1) solution. The UHPLC-MS analysis was performed with an Infinity 1290 Agilent (Agilent Technologies, Santa Clara, CA, USA) ultra-high performance liquid chromatograph coupled with tandem mass spectrometry (UHPLC-MS-MS) as previously described [46]. Briefly, 1 μL of each extract was injected into the UHPLC system equipped with an Acquity column (HSS T3, $2.1 \times 50\text{ mm}$, $1.8\text{ }\mu\text{m}$ C18) in combination with a $2.1\text{ mm} \times 5\text{ mm}$, $1.7\text{ }\mu\text{m}$ VanGuard charged-surface hybrid (CSH) precolumn (Waters Corporation, Milford, MA, USA), held at $60\text{ }^{\circ}\text{C}$. Mobile phases used were MilliQ water with 0.1% formic acid (A) and 75:25 acetonitrile: 2-propanol with 0.1% formic acid (B). The following gradient was used: 10% B for 2 min, then B was increased to 99% in 5 min and held at 99% for 2 min. Subsequently, B was decreased to 0.1% in 0.3 min and the flow-rate was increased to 0.8 mL min^{-1} for 0.5 min. These conditions were held for 0.9 min, after which the flow-rate was reduced to 0.5 mL min^{-1} for 0.1 min before the next injection. Samples were randomly injected. The first parallel of extracts was analyzed in positive mode. Then, the instrument was switched to negative mode and the second parallel of extracts was injected. Blank samples with only methanol:water (1:1) solution were run prior and after each samples set. MS parameters were kept identical between the modes, with exception of the capillary voltage. The exact masses of metabolites were detected with an Agilent 6550 Q-TOF mass spectrometer equipped with an iFunnel jet stream electrospray ion source (Agilent Technologies,

Santa Clara, CA, USA). The flow gas temperature was set at 150 °C, the drying gas flow at 16 L min⁻¹ and the nebulizer pressure at 35 psi. The sheath gas temperature was set at 350 °C and the sheath gas flow was 11 L min⁻¹. The capillary voltage was set at 4000 V for the positive mode and 4500 V for the negative mode. The *m/z* range was 70–1700, and data were collected in centroid mode with an acquisition rate of 4 scans/s. The QC-samples were a part of the quality control of the analysis were run in the beginning of the sample set. Auto MS/MS acquisition was used when running QC samples to generate MS/MS data.

4.5. GC-MS Analysis

Prior to injection, derivatization was performed as previously described [47]. Briefly, 30 µL of a methoxyamine solution in pyridine (15 µg µL⁻¹) was added to the dry extract, and then shaken for 15 min on a shaking table. Derivatization was carried out at 70 °C for 1 h followed by room temperature for 16 h. Afterwards, the samples were trimethylsilylated (TMS) with 30 µL methyl-N-(trimethylsilyl) trifluoroacetamide MSTFA at room temperature for 1 h. Finally, 30 µL of heptane (including 15 ng methylstearate µL⁻¹) was added and the vials were vortexed before 1 µL was injected splitless by a CTC Combi Pal autosampler (CTC Analytics AG, Switzerland) into an Agilent 6890 GC equipped with a fused silica capillary column (10 m × 0.18 mm I.D.) with a chemically bonded 0.18 µm DB 5-MS stationary phase (J&W Scientific, Folsom, CA, USA). Samples were randomly injected. Blank samples with only heptane were run prior and after the samples set. The injector temperature was 270 °C and the purge flow-rate was 20 mL min⁻¹. The column temperature was set to 70 °C for 2 min, then increased to 320 °C by a rate of 40 °C min⁻¹, and held there for 2 min using a gas flow rate of 1 mL min⁻¹. The GC was coupled to the ion source of a Pegasus III TOF-MS (Leco Corp., St Joseph, MI, USA). The transfer line and MS instrument settings were as follows: Transfer lines and ion source temperature were set to 300 and 350 respectively. The mass detecting range was set to 50 to 800 *m/z*. An alkane series (C10–C40) was run together with all samples.

4.6. Metabolites Identification and Data Processing

Targeted feature extraction of the acquired UHPLC–MS data was performed using the Profinder™ software package, version B.08.00 (Agilent Technologies Inc., Santa Clara, CA, USA). In-house libraries with exact masses and experimental retention times were used for identification. The libraries contained metabolites from the following chemical classes: acylcarnitines, amino acids, carbohydrates, fatty acids, bile acids, nucleotides, small peptides, and lysophospholipids, namely lysophosphatidylcholine (LPC) and lysophosphatidylethanolamine (LPE). The allowed ion species for metabolites identification were ⁺H, ⁺Na, ⁺K, and ⁺NH₄ in positive ionization mode, and ⁻H, ⁺HCOO in negative ionization mode. The mass tolerance was 10 ppm and the retention time tolerance 0.1 min. Only one charge for each metabolite was allowed. The extracted peaks were aligned and matched between samples, and then each compound was manually checked for mass and retention time agreement with the library. A two-step filtering approach was used for peak quality control: First, peaks with bad characteristics (e.g., overloaded, sample noise, non-Gaussian) were excluded from the analysis. Second, only peaks present in at least 75% of at least one study group were included.

Raw GC–MS data files were exported in NetCDF format to a MATLAB 8.3 (R2014a) (Mathworks, Natick, MA) based in-house script for baseline correction, chromatogram alignment, and peak deconvolution. Metabolite annotation was performed based on the retention index (RI) values and MS spectra from the in-house mass spectra library established by the Swedish Metabolomics Centre (Umeå, Sweden). The total number of annotated metabolites by UHPLC-MS and GC-MS was 128 and 66 respectively. Seventeen metabolites were detected with both methodologies, the signal detected with the UHPLC method was included in the statistical analyses. The UHPLC–MS metabolites were normalized by the total peak areas, whereas GC–MS metabolites were normalized by internal standards as described before [48]. A combined data set containing 177 metabolites was submitted to statistical analysis.

4.7. Statistical Analysis

Statistical analysis was carried out using RStudio: Integrated Development Environment (version 1.0.143). Undetectable Metabolites, which represented 0.6% of the total reported metabolites, were assigned a value corresponding to half of the minimum positive value in the original data. Shapiro–Wilk test of normality was applied, and the data was not found normally distributed. Kruskal–Wallis one way analysis of variance test was performed to compare the mean concentration of metabolites between treatment-naïve UC, remission UC, and control groups. Acquired *p*-values were adjusted using Benjamini and Hochberg FDR method [49]. Dunn’s test [50] was applied as a post-hoc test, and significant *p*-value cut-off was corrected to 0.017 by Bonferroni multiple comparison method [51]. Multivariate analysis was carried out using SIMCA software (version 14.0.0.135559; Sartorius AB, Umea, Sweden). The metabolites were auto-scaled and mean-centered in order to adjust the importance of high and low abundance metabolites to an equal level [52]. Unsupervised PCA was first performed to assess the unicity of the metabolome for each of the study groups. Then, supervised OPLS-DA [53] was employed and metabolites were classified according to corresponding regression coefficients to identify the most important metabolites in discriminating between the study groups. The parameters of the OPLS-DA model were described by R^2X_{cum} , R^2Y_{cum} and Q^2_{cum} , whereas, R^2X_{cum} is the cumulative modeled variation in X, R^2Y_{cum} is the amount of variation in X correlated to Y (response matrix) and Q^2_{cum} is the cumulative predicted ability of the model [54]. The validity and degree of overfitting of the OPLS-DA model was assessed by conducting analysis of variance testing of cross-validated predictive residuals (CV-ANOVA), and permutation analyses.

Pathway analysis was performed using MetaboAnalyst 4.0, a web tool for metabolomics data analysis (<http://www.metaboanalyst.ca/>) [55]. First, all 177 metabolites were annotated according to ‘Human Metabolome Database’ (HMDB) [56] and linked to a metabolic pathway according to KEGG database [57]. Secondly, powerful pathway enrichment analysis coupled with pathway topology analysis was carried out to identify the altered metabolic pathways in active UC compared with healthy state. The enrichment analysis was based on a global test [58] while, the node/metabolite importance was measured by relative betweenness centrality [59]. Obtained *P*-values from the enrichment analysis were adjusted by Holm method [60]. Adjusted *P*-values lower than 0.05 were considered significant.

5. Conclusions

The present report provides an in-depth description of the mucosal metabolome in UC via a high-throughput metabolomic analysis of colon biopsies taken from UC treatment-naïve patients, UC patients in state of deep remission, and healthy subjects. The study of mucosal metabolites revealed the main metabolic signatures in active UC, and reflects the homeostatic disturbance in the gut. The reported metabolites were identified by searching the human-only metabolites database, and only human metabolic pathways were included in the pathway analysis. However, the gut microbiota seems to be heavily involved in altering several metabolic pathways in the colon mucosa. This highlights the importance of integrating IBD-ome compartments by system biology approaches to identify key drivers of pathogenesis that require personalized treatment.

Supplementary Materials: The following are available online at <http://www.mdpi.com/2218-1989/9/12/291/s1>, Figure S1: Multivariate analysis of the mucosal metabolomic profiles according to the subjects’ sex, age, and activity score., Figure S2: Permutation test of the OPLS-DA model, Table S1: Kruskal Wallis analysis comparing the mucosal metabolomic profile among the study groups, Table S2: The variables importance in projection (VIP) scores of the 177 metabolites included in this study according to the OPLS-DA model, Table S3: Pathway analysis of the 177 metabolites included in this study in active UC compared with healthy controls.

Author Contributions: J.D. and G.F. prepared the manuscript. J.D., G.F., E.J., T.M. and J.F. planned the experiments. J.D. performed the lipidomics analysis and data processing. J.D., T.H. and H.S. performed the data analysis. J.F. and R.G. recruited patients, provided colon mucosa biopsies, reported the baseline characteristics, and provided clinical interpretation. All authors revised and approved the final version of the manuscript.

Funding: This work belongs to the Advanced Study of Inflammatory Bowel disease (ASIB) study supported by the Northern Norway Regional Health Authority [SFP-1134-13], and the University of Tromsø, The Arctic University of Norway. The publication fees for this article have been funded by a grant from the publication fund of UiT—The Arctic University of Norway.

Acknowledgments: We thank Renate Meyer for administrating the patient samples. Swedish Metabolomics Centre is acknowledged for help with the metabolomics analysis.

Conflicts of Interest: All authors certify that they have no financial interests or connections, direct or indirect, or other situations that might raise the question of bias in the work reported. This includes pertinent commercial or other sources of funding for the individual author(s) or for the associated department(s) or organization(s), personal relationships, or direct academic competition.

References

1. Ng, S.C.; Shi, H.Y.; Hamidi, N.; Underwood, F.E.; Tang, W.; Benchimol, E.I.; Panaccione, R.; Ghosh, S.; Wu, J.C.Y.; Chan, F.K.L.; et al. Worldwide incidence and prevalence of inflammatory bowel disease in the 21st century: A systematic review of population-based studies. *Lancet* **2017**, *390*, 2769–2778. [[CrossRef](#)]
2. Neurath, M.F. Targeting immune cell circuits and trafficking in inflammatory bowel disease. *Nat. Immunol.* **2019**, *20*, 970–979. [[CrossRef](#)] [[PubMed](#)]
3. DeSouza, H.S.P.; Fiocchi, C.; Iliopoulos, D. The IBD interactome: An integrated view of aetiology, pathogenesis and therapy. *Nat. Rev. Gastroenterol. Hepatol.* **2017**, *14*, 739–749. [[CrossRef](#)] [[PubMed](#)]
4. Liu, J.Z.; van Sommeren, S.; Huang, H.; Ng, S.C.; Alberts, R.; Takahashi, A.; Ripke, S.; Lee, J.C.; Jostins, L.; Shah, T.; et al. Association analyses identify 38 susceptibility loci for inflammatory bowel disease and highlight shared genetic risk across populations. *Nat. Genet.* **2015**, *47*, 979–986. [[CrossRef](#)] [[PubMed](#)]
5. Manichanh, C.; Borruel, N.; Casellas, F.; Guarner, F. The gut microbiota in IBD. *Nat. Rev. Gastroenterol. Amp Hepatol.* **2012**, *9*, 599. [[CrossRef](#)] [[PubMed](#)]
6. Orazio, P.; Tommaso, M.; Stefano, C.; Panza, A.; Latiano, T.; Corritore, G.; Andriulli, A.; Latiano, A. Inflammatory bowel disease meets systems biology: A multi-omics challenge and frontier. *OMICS J. Integr. Biol.* **2016**, *20*, 692–698.
7. Trivedi, D.K.; Hollywood, K.A.; Goodacre, R. Metabolomics for the masses: The future of metabolomics in a personalized world. *New Horiz. Transl. Med.* **2017**, *3*, 294–305. [[CrossRef](#)]
8. Beger, R.D.; Dunn, W.; Schmidt, M.A.; Gross, S.S.; Kirwan, J.A.; Cascante, M.; Brennan, L.; Wishart, D.S.; Oresic, M.; Hankemeier, T.; et al. Metabolomics enables precision medicine: “A White Paper, Community Perspective”. *Metab. Off. J. Metab. Soc.* **2016**, *12*, 149. [[CrossRef](#)]
9. Scoville, E.A.; Allaman, M.M.; Brown, C.T.; Motley, A.K.; Horst, S.N.; Williams, C.S.; Koyama, T.; Zhao, Z.; Adams, D.W.; Beaulieu, D.B.; et al. Alterations in lipid, amino acid, and energy metabolism distinguish crohn’s disease from ulcerative colitis and control subjects by serum metabolomic profiling. *Metabolomics* **2018**, *14*, 17. [[CrossRef](#)]
10. Kohashi, M.; Nishiumi, S.; Ooi, M.; Yoshie, T.; Matsubara, A.; Suzuki, M.; Hoshi, N.; Kamikozuru, K.; Yokoyama, Y.; Fukunaga, K.; et al. A novel gas chromatography mass spectrometry-based serum diagnostic and assessment approach to ulcerative colitis. *J. Crohns Colitis* **2014**, *8*, 1010–1021. [[CrossRef](#)]
11. Lai, Y.; Xue, J.; Liu, C.W.; Gao, B.; Chi, L.; Tu, P.; Lu, K.; Ru, H. Serum metabolomics identifies altered bioenergetics, signaling cascades in parallel with exposome markers in Crohn’s disease. *Molecules* **2019**, *24*, 449. [[CrossRef](#)] [[PubMed](#)]
12. Kolho, K.L.; Pessia, A.; Jaakkola, T.; de Vos, W.M.; Velagapudi, V. Faecal and serum metabolomics in paediatric inflammatory bowel disease. *J. Crohns Colitis* **2017**, *11*, 321–334. [[CrossRef](#)] [[PubMed](#)]
13. Murgia, A.; Hinz, C.; Liggi, S.; Denes, J.; Hall, Z.; West, J.; Santoru, M.L.; Piras, C.; Manis, C.; Usai, P.; et al. Italian cohort of patients affected by inflammatory bowel disease is characterised by variation in glycerophospholipid, free fatty acids and amino acid levels. *Metabolomics* **2018**, *14*, 140. [[CrossRef](#)] [[PubMed](#)]
14. Daniluk, U.; Daniluk, J.; Kucharski, R.; Kowalczyk, T.; Pietrowska, K.; Samczuk, P.; Filimoniuk, A.; Kretowski, A.; Lebensztejn, D.; Ciborowski, M. Untargeted metabolomics and inflammatory markers profiling in children with Crohn’s disease and ulcerative colitis—A preliminary study. *Inflamm. Bowel Dis.* **2019**, *25*, 1120–1128. [[CrossRef](#)]
15. Stephens, N.S.; Siffledeen, J.; Su, X.; Murdoch, T.B.; Fedorak, R.N.; Slupsky, C.M. Urinary NMR metabolomic profiles discriminate inflammatory bowel disease from healthy. *J. Crohns Colitis* **2013**, *7*, e42–e48. [[CrossRef](#)]

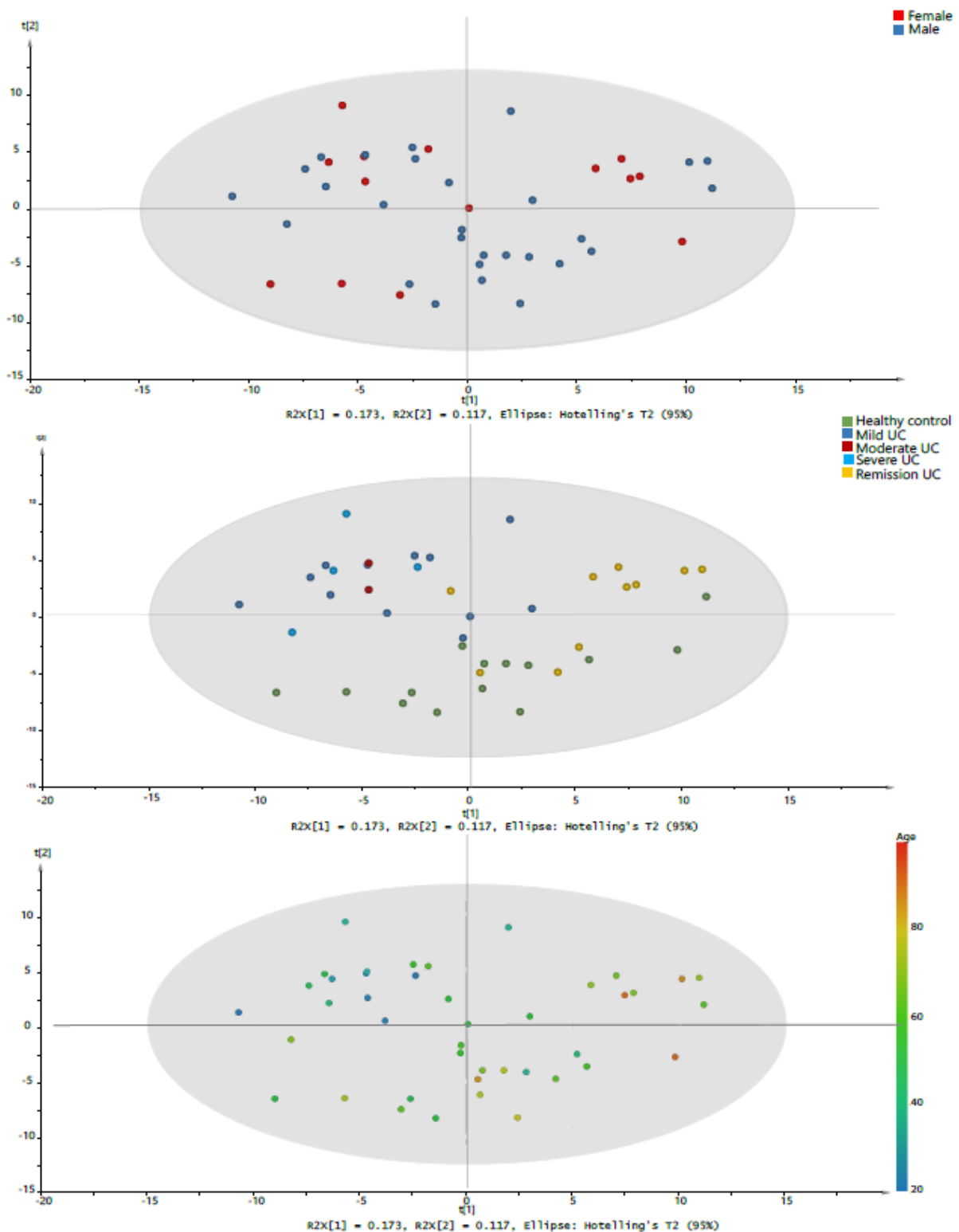
16. Viant, M.R.; Ludwig, C.; Günther, U. 1D and 2D NMR spectroscopy: From metabolic fingerprinting to profiling. *RSC Biomol. Sci.* **2007**, *44*, 44–70. [[CrossRef](#)]
17. Gowda, G.A.N.; Zhang, S.; Gu, H.; Asiago, V.; Shanaiah, N.; Raftery, D. Metabolomics-based methods for early disease diagnostics. *Expert Rev. Mol. Diagn.* **2008**, *8*, 617–633. [[CrossRef](#)]
18. Shulaev, V. Metabolomics technology and bioinformatics. *Brief. Bioinform.* **2006**, *7*, 128–139. [[CrossRef](#)]
19. Hanna, V.S.; Hafez, E.A.A. Synopsi of arachidonic acid metabolism: A review. *J. Adv. Res.* **2018**, *11*, 23–32. [[CrossRef](#)]
20. Das, U.N. Inflammatory bowel disease as a disorder of an imbalance between pro- and anti-inflammatory molecules and deficiency of resolution bioactive lipids. *Lipids Health Dis.* **2016**, *15*, 11–18. [[CrossRef](#)]
21. Diab, J.; Al-Mahdi, R.; Gouveia-Figueira, S.; Hansen, T.; Jensen, E.; Goll, R.; Moritz, T.; Florholmen, J.; Forsdahl, G. A quantitative analysis of colonic mucosal oxylipins and endocannabinoids in treatment-naïve and deep remission ulcerative colitis patients and the potential link with cytokine gene expression. *Inflamm. Bowel Dis.* **2018**, *25*, 490–497. [[CrossRef](#)] [[PubMed](#)]
22. Costea, I.; Mack, D.R.; Lemaitre, R.N.; Israel, D.; Marcil, V.; Ahmad, A.; Amre, D.K. Interactions between the dietary polyunsaturated fatty acid ratio and genetic factors determine susceptibility to pediatric Crohn’s disease. *Gastroenterology* **2014**, *146*, 929–931.e3. [[CrossRef](#)] [[PubMed](#)]
23. Mesbah-Uddin, M.; Elango, R.; Banaganapalli, B.; Shaik, N.A.; Al-Abbasi, F.A. In-silico analysis of inflammatory bowel disease (IBD) GWAS loci to novel connections. *PLoS ONE* **2015**, *10*, e0119420. [[CrossRef](#)] [[PubMed](#)]
24. Agus, A.; Planchais, J.; Sokol, H. Gut microbiota regulation of tryptophan metabolism in health and disease. *Cell Host Microbe* **2018**, *23*, 716–724. [[CrossRef](#)]
25. Kim, C.J.; Kovacs-Nolan, J.A.; Yang, C.; Archbold, T.; Fan, M.Z.; Mine, Y. l-Tryptophan exhibits therapeutic function in a porcine model of dextran sodium sulfate (DSS)-induced colitis. *J. Nutr. Biochem.* **2010**, *21*, 468–475. [[CrossRef](#)]
26. Nikolaus, S.; Schulte, B.; Al-Massad, N.; Thieme, F.; Schulte, D.M.; Bethge, J.; Rehman, A.; Tran, F.; Aden, K.; Häslar, R.; et al. Increased tryptophan metabolism is associated with activity of inflammatory bowel diseases. *Gastroenterology* **2017**, *153*, 1504–1516.e2. [[CrossRef](#)]
27. Ni, J.; Shen, T.-C.D.; Chen, E.Z.; Bittinger, K.; Bailey, A.; Roggiani, M.; Sirota-Madi, A.; Friedman, E.S.; Chau, L.; Lin, A.; et al. A role for bacterial urease in gut dysbiosis and Crohn’s disease. *Sci. Transl. Med.* **2017**, *9*, eaah6888. [[CrossRef](#)]
28. Martin, F.P.; Su, M.M.; Xie, G.X.; Guiraud, S.P.; Kussmann, M.; Godin, J.P.; Jia, W.; Nydegger, A. Urinary metabolic insights into host-gut microbial interactions in healthy and IBD children. *World J. Gastroenterol.* **2017**, *23*, 3643–3654. [[CrossRef](#)]
29. Bjerrum, J.T.; Nielsen, O.H.; Hao, F.; Tang, H.; Nicholson, J.K.; Wang, Y.; Olsen, J. Metabonomics in ulcerative colitis: Diagnostics, biomarker identification, and insight into the pathophysiology. *J. Proteome Res.* **2010**, *9*, 954–962. [[CrossRef](#)]
30. Parada Venegas, D.; De la Fuente, M.K.; Landskron, G.; González, M.J.; Quera, R.; Dijkstra, G.; Harmsen, H.J.M.; Faber, K.N.; Hermoso, M.A. Short Chain Fatty Acids (SCFAs)-mediated gut epithelial and immune regulation and its relevance for inflammatory bowel diseases. *Front. Immunol.* **2019**, *10*, 277. [[CrossRef](#)]
31. Machiels, K.; Joossens, M.; Sabino, J.; De Preter, V.; Arijis, I.; Eeckhaut, V.; Ballet, V.; Claes, K.; Van Immerseel, F.; Verbeke, K.; et al. A decrease of the butyrate-producing species *Roseburia hominis* and *Faecalibacterium prausnitzii* defines dysbiosis in patients with ulcerative colitis. *Gut* **2014**, *63*, 1275–1283. [[CrossRef](#)] [[PubMed](#)]
32. Huda-Faujan, N.; Abdulamir, A.S.; Fatimah, A.B.; Anas, O.M.; Shuhaimi, M.; Yazid, A.M.; Loong, Y.Y. The impact of the level of the intestinal short chain Fatty acids in inflammatory bowel disease patients versus healthy subjects. *Open Biochem. J.* **2010**, *4*, 53–58. [[CrossRef](#)] [[PubMed](#)]
33. Roediger, W.E.W. The colonic epithelium in ulcerative colitis: An energy-deficiency disease? *Lancet* **1980**, *316*, 712–715. [[CrossRef](#)]
34. Schniers, A.; Goll, R.; Pasing, Y.; Sørbye, S.W.; Florholmen, J.; Hansen, T. Ulcerative colitis: Functional analysis of the in-depth proteome. *Clin. Proteom.* **2019**, *16*, 4. [[CrossRef](#)] [[PubMed](#)]
35. Eaton, S.; Bartlett, K.; Pourfarzam, M. Mammalian mitochondrial beta-oxidation. *Biochem. J.* **1996**, *320 Pt 2*, 345–357. [[CrossRef](#)]

36. Jackson, D.N.; Theiss, A.L. Gut bacteria signaling to mitochondria in intestinal inflammation and cancer. *Gut Microbes* **2019**, *1*, 1–20. [[CrossRef](#)]
37. Florholmen, J. Mucosal healing in the era of biologic agents in treatment of inflammatory bowel disease. *Scand. J. Gastroenterol.* **2015**, *50*, 43–52. [[CrossRef](#)]
38. Diab, J.; Hansen, T.; Goll, R.; Stenlund, H.; Ahnlund, M.; Jensen, E.; Moritz, T.; Florholmen, J.; Forsdahl, G. Lipidomics in ulcerative colitis reveal alteration in mucosal lipid composition associated with the disease state. *Inflamm. Bowel Dis.* **2019**, *25*, 1780–1787. [[CrossRef](#)]
39. Polytarchou, C.; Koukos, G.; Iliopoulos, D. Systems biology in inflammatory bowel diseases: Ready for prime time. *Curr. Opin. Gastroenterol.* **2014**, *30*, 339–346. [[CrossRef](#)]
40. Stange, E.F.; Travis, S.P.; Vermeire, S.; Reinisch, W.; Geboes, K.; Barakauskiene, A.; Feakins, R.; Fléjou, J.F.; Herfarth, H.; Hommes, D.W.; et al. European evidence-based Consensus on the diagnosis and management of ulcerative colitis: Definitions and diagnosis. *J. Crohns Colitis* **2008**, *2*, 1–23. [[CrossRef](#)]
41. Marteau, P.; Probert, C.S.; Lindgren, S.; Gassul, M.; Tan, T.G.; Dignass, A.; Befrits, R.; Midhagen, G.; Rademaker, J.; Foldager, M. Combined oral and enema treatment with Pentasa (mesalazine) is superior to oral therapy alone in patients with extensive mild/moderate active ulcerative colitis: A randomised, double blind, placebo controlled study. *Gut* **2005**, *54*, 960–965. [[CrossRef](#)] [[PubMed](#)]
42. Olsen, T.; Goll, R.; Cui, G.; Husebekk, A.; Vonen, B.; Birketvedt, G.S.; Florholmen, J. Tissue levels of tumor necrosis factor-alpha correlates with grade of inflammation in untreated ulcerative colitis. *Scand. J. Gastroenterol.* **2007**, *42*, 1312–1320. [[CrossRef](#)] [[PubMed](#)]
43. Magro, F.; Gionchetti, P.; Eliakim, R.; Ardizzone, S.; Armuzzi, A.; Barreiro-de Acosta, M.; Burisch, J.; Gecse, K.B.; Hart, A.L.; Hindryckx, P.; et al. Third European evidence-based consensus on diagnosis and management of ulcerative colitis. Part 1: Definitions, diagnosis, extra-intestinal manifestations, pregnancy, cancer surveillance, surgery, and ileo-anal pouch disorders. *J. Crohns Colitis* **2017**, *11*, 649–670. [[CrossRef](#)] [[PubMed](#)]
44. Johnsen, K.M.; Goll, R.; Hansen, V.; Olsen, T.; Rismo, R.; Heitmann, R.; Gundersen, M.D.; Kvamme, J.M.; Paulssen, E.J.; Kileng, H.; et al. Repeated intensified infliximab induction—Results from an 11-year prospective study of ulcerative colitis using a novel treatment algorithm. *Eur. J. Gastroenterol. Hepatol.* **2017**, *29*, 98–104. [[CrossRef](#)] [[PubMed](#)]
45. Trygg, J.; Gullberg, J.; Johansson, A.I.; Jonsson, P.; Antti, H.; Marklund, S.L.; Moritz, T. Extraction and GC/MS analysis of the human blood plasma metabolome. *Anal. Chem.* **2005**, *77*, 8086–8094.
46. Lindahl, A.; Forshed, J.; Nordstrom, A. Overlap in serum metabolic profiles between non-related diseases: Implications for LC-MS metabolomics biomarker discovery. *Biochem. Biophys. Res. Commun.* **2016**, *478*, 1472–1477. [[CrossRef](#)]
47. Karimpour, M.; Surowiec, I.; Wu, J.; Gouveia-Figueira, S.; Pinto, R.; Trygg, J.; Zivkovic, A.M.; Nording, M.L. Postprandial metabolomics: A pilot mass spectrometry and NMR study of the human plasma metabolome in response to a challenge meal. *Anal. Chim. Acta* **2016**, *908*, 121–131. [[CrossRef](#)]
48. Redestig, H.; Fukushima, A.; Stenlund, H.; Moritz, T.; Arita, M.; Saito, K.; Kusano, M. Compensation for systematic cross-contribution improves normalization of mass spectrometry based metabolomics data. *Anal. Chem.* **2009**, *81*, 7974–7980. [[CrossRef](#)]
49. Benjamini, Y.; Hochberg, Y. Controlling the false discovery rate: A practical and powerful approach to multiple testing. *J. R. Stat. Soc. Ser. B (Methodol.)* **1995**, *57*, 289–300. [[CrossRef](#)]
50. Dunn, O.J. Multiple comparisons among means. *J. Am. Stat. Assoc.* **1961**, *56*, 52–64. [[CrossRef](#)]
51. Bonferroni, C.E. Teoria statistica delle classi e calcolo delle probabilita. *Pubblicazioni del R Istituto Superiore di Scienze Economiche e Commerciali di Firenze* **1936**, *8*, 3–62.
52. Van den Berg, R.A.; Hoefsloot, H.C.; Westerhuis, J.A.; Smilde, A.K.; van der Werf, M.J. Centering, scaling, and transformations: Improving the biological information content of metabolomics data. *BMC Genom.* **2006**, *7*, 142. [[CrossRef](#)] [[PubMed](#)]
53. Wiklund, S.; Johansson, E.; Sjöström, L.; Mellerowicz, E.J.; Edlund, U.; Shockcor, J.P.; Gottfries, J.; Moritz, T.; Trygg, J. Visualization of GC/TOF-MS-based metabolomics data for identification of biochemically interesting compounds using OPLS class models. *Anal. Chem.* **2008**, *80*, 115–122. [[CrossRef](#)] [[PubMed](#)]
54. Ni, Y.; Su, M.; Lin, J.; Wang, X.; Qiu, Y.; Zhao, A.; Chen, T.; Jia, W. Metabolic profiling reveals disorder of amino acid metabolism in four brain regions from a rat model of chronic unpredictable mild stress. *FEBS Lett.* **2008**, *582*, 2627–2636. [[CrossRef](#)] [[PubMed](#)]

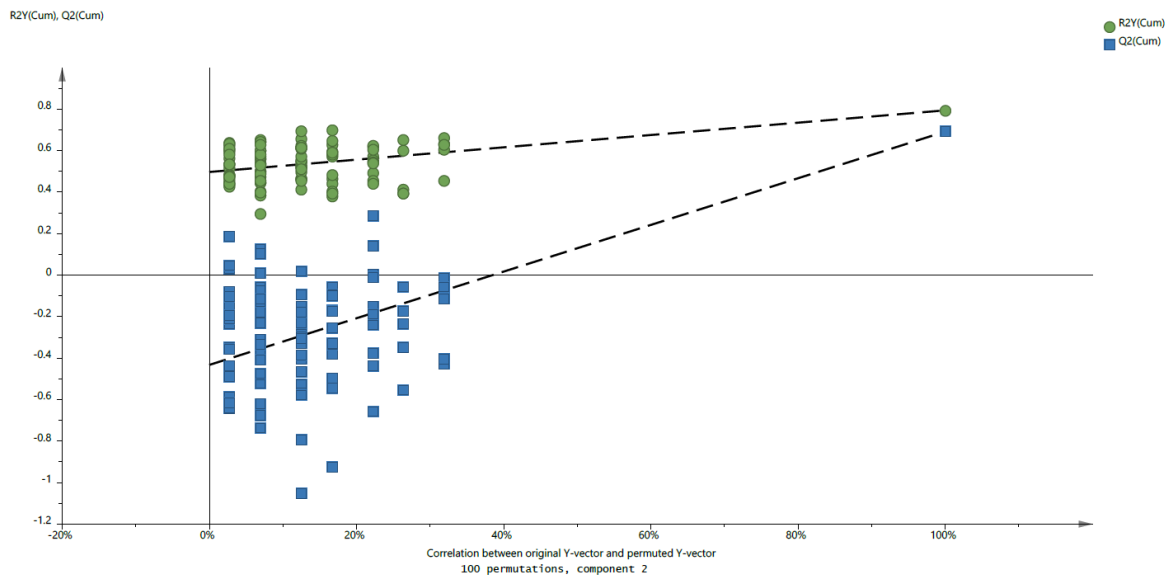
55. Chong, J.; Soufan, O.; Li, C.; Caraus, I.; Li, S.; Bourque, G.; Wishart, D.S.; Xia, J. MetaboAnalyst 4.0: Towards more transparent and integrative metabolomics analysis. *Nucleic Acids Res.* **2018**, *46*, W486–W494. [[CrossRef](#)] [[PubMed](#)]
56. Wishart, D.S.; Feunang, Y.D.; Marcu, A.; Guo, A.C.; Liang, K.; Vázquez-Fresno, R.; Sajed, T.; Johnson, D.; Li, C.; Karu, N.; et al. HMDB 4.0: The human metabolome database for 2018. *Nucleic Acids Res.* **2017**, *46*, D608–D617. [[CrossRef](#)]
57. Kanehisa, M.; Furumichi, M.; Tanabe, M.; Sato, Y.; Morishima, K. KEGG: New perspectives on genomes, pathways, diseases and drugs. *Nucleic Acids Res.* **2017**, *45*, 353–361. [[CrossRef](#)]
58. Goeman, J.J.; van de Geer, S.A.; de Kort, F.; van Houwelingen, H.C. A global test for groups of genes: Testing association with a clinical outcome. *Bioinformatics* **2004**, *20*, 93–99. [[CrossRef](#)]
59. Aittokallio, T.; Schwikowski, B. Graph-based methods for analysing networks in cell biology. *Brief. Bioinform.* **2006**, *7*, 243–255. [[CrossRef](#)]
60. Holm, S. A simple sequentially rejective multiple test procedure. *Scand. J. Stat.* **1979**, *6*, 65–70.



© 2019 by the authors. Licensee MDPI, Basel, Switzerland. This article is an open access article distributed under the terms and conditions of the Creative Commons Attribution (CC BY) license (<http://creativecommons.org/licenses/by/4.0/>).



Supplementary Figure 1. Three PCA t1/t2-scores plots for mucosal metabolite profiles. The variation explained by PC1 and PC2 were 17.3% and 11.7%, respectively. t1 is the first component, which explains the largest variation, t2 is independent of t1 and explains second largest variation which is orthogonal to t1. The study subjects in Supplementary figure 1.A, 1.B, and 1C were colored according to sex, UC disease activity, and age respectively.



Supplementary Figure 2. OPLS-DA permutation plot for the metabolomic data set displaying the correlation coefficients between the original Y variable (naïve treatment UC, remission UC, and healthy controls) and the permuted Y variable on the x-axis versus the cumulative R^2Y and Q^2 on the y-axis, with the regression line between them. The intercept is the measure of the over fit. The Y-axis intercept below 0.5 for R^2Y and below 0.05 for Q^2 .

Kruskal Wallis analysis comparing the mucosal metabolomic profile among the study groups

Metabolites	Kruskal Wallis Test adj. p-value*	Active UC vs Healthy Control		Active UC vs Remission UC		Remission UC vs Healthy Control	
		Fold change	P.value**	Fold change	P.value**	Fold change	P.value**
2-Hydroxyhexanoate	1.000	0.90	0.804	0.82	0.218	0.91	0.166
2-Hydroxyoctanoate	0.297	0.75	0.259	1.18	0.217	1.58	0.032
2-Hydroxypalmitate	0.503	0.92	0.360	1.11	0.247	1.20	0.059
2-Hydroxystearate	0.028	1.15	0.003	1.31	0.622	1.14	0.037
2'-O-methylguanosine	0.153	1.95	0.769	1.31	0.035	0.67	0.024
3-Carboxy-4-methyl-5-propyl-2-furanpropanoate (CMPF)	0.014	0.31	0.529	0.50	0.001	1.60	0.012
3-Hydroxydecanoate	0.021	0.70	0.015	0.43	0.005	0.62	0.562
3-Hydroxylaurate	0.221	0.72	0.216	1.29	0.202	1.80	0.023
3-Hydroxymyristate	0.775	0.82	0.377	1.15	0.355	1.41	0.100
3-Hydroxypalmitate	0.291	0.87	0.296	1.12	0.186	1.28	0.031
3-methylglutaryl carnitine	0.003	0.61	0.001	0.59	0.005	0.97	0.818
3-isomethylglutaryl carnitine	0.003	0.60	0.001	0.59	0.004	0.99	0.897
4-Aminobutyric Acid	1.000	0.82	0.305	1.46	0.703	1.78	0.213
5-hydroxyhexanoate	1.000	0.90	0.765	0.78	0.270	0.86	0.191
5-hydroxyindoleacetate	<0.001	2.44	<0.001	2.81	0.002	1.15	0.520
5-methylthioadenosine	1.000	0.73	0.495	0.80	0.357	1.09	0.772
5-oxoproline	<0.001	1.69	<0.001	1.99	0.002	1.18	0.520
Acetylcarnitine (C2:0)	0.021	0.73	0.151	1.14	0.045	1.55	0.002
acisoga	1.000	0.85	0.833	1.03	0.646	1.22	0.536
Aconitic Acid	1.000	0.50	0.314	0.54	0.453	1.09	0.879

Allothreonine	0.342	1.01	0.061	1.23	0.920	1.22	0.088
Arabinose	1.000	1.08	0.486	0.85	0.783	0.79	0.736
Arachidonate (20:4)	0.033	1.18	0.007	1.21	0.021	1.02	0.915
Arginine	1.000	1.08	0.279	1.02	0.535	0.95	0.734
Aspargene	<0.001	1.48	<0.001	1.78	0.001	1.20	0.215
Aspartylleucine	0.001	2.20	0.007	1.52	<0.001	0.69	0.172
Beta-alanine	<0.001	0.64	<0.001	0.43	0.004	0.68	0.426
Butyrylcarnitine (C4:0)	0.318	1.14	0.136	1.23	0.049	1.08	0.551
Carnitine	0.032	0.57	0.018	0.68	0.008	1.18	0.631
Cellobiose	1.000	1.41	0.397	0.73	0.691	0.52	0.268
Cervonyl-carnitine (C22:6)	0.624	1.35	0.650	0.84	0.163	0.62	0.086
Citric Acid	0.762	0.75	0.098	1.13	0.513	1.50	0.423
Citrulline	<0.001	1.68	<0.001	1.56	0.001	0.93	1.000
Creatine	0.026	0.85	0.010	0.82	0.010	0.97	0.826
Cysteine-glycine	1.000	0.87	0.532	1.11	0.402	1.28	0.182
Cysteine-glutathione disulfide	0.148	0.90	0.053	1.57	0.537	1.74	0.024
Decanoylcarnitine (C10:0)	0.017	0.68	0.026	2.14	0.218	3.17	0.002
Dimethylarginine (ADMA + SDMA)	<0.001	1.85	<0.001	2.09	0.002	1.13	0.696
Docosahexaenoate (DHA; 22:6)	0.437	1.14	0.253	0.91	0.311	0.80	0.051
Docosapentaenoate (DPA; 22:5)	0.142	1.25	0.026	1.28	0.063	1.03	0.882
Docosapentaenoate (n6 DPA; 22:5)	0.002	1.88	0.004	1.54	0.001	0.82	0.475
Dodecanoic Acid	1.000	0.81	0.948	0.58	0.432	0.72	0.489
Eicosadieneoyl-carnitine (C20:2)	0.122	1.68	0.409	1.08	0.012	0.65	0.090
Eicosanoic Acid	1.000	1.05	0.423	0.80	0.563	0.76	0.215
Eicosapentaenoate (EPA; 20:5)	0.018	0.79	0.001	0.52	0.226	0.65	0.110
Eicoseneoyl-carnitine (C20:1)	0.169	1.59	0.506	0.82	0.064	0.51	0.019
Fructose	0.023	0.63	0.002	2.21	0.141	3.52	0.204
Fumaric Acid	0.226	1.09	0.036	1.23	0.101	1.13	0.811

Galactose	0.076	0.49	0.086	0.61	0.009	1.23	0.315
Gamma-glutamylisoleucine	0.001	2.48	0.016	1.50	<0.001	0.60	0.098
Gamma-glutamylmethionine	0.004	2.10	0.007	1.67	0.001	0.80	0.368
Gamma-glutamylphenylalanine	0.001	2.29	0.008	1.54	<0.001	0.67	0.203
Gamma-glutamylvaline	0.001	2.16	0.010	1.50	<0.001	0.69	0.159
Glucose	0.038	0.56	0.069	0.68	0.004	1.21	0.245
Glutamic Acid	<0.001	1.33	<0.001	1.94	0.017	1.46	0.017
Glutaryl carnitine (C5:0-DC)	0.016	0.45	0.006	0.27	0.008	0.60	0.890
Glycerol-3-Phosphate	0.019	0.70	0.002	0.54	0.165	0.76	0.160
Guanidinosuccinate	0.067	0.70	0.228	1.07	0.072	1.53	0.006
Guanosine	<0.001	0.27	0.002	0.36	0.000	1.34	0.141
Heptadecanoic Acid	1.000	1.09	0.505	1.11	0.612	1.02	0.928
Hexadecadienoyl-carnitine (C16:2)	0.263	1.47	0.763	1.02	0.033	0.69	0.077
Hexadecanoic Acid	1.000	0.91	0.250	0.77	0.669	0.84	0.560
Hexadecenoyl-carnitine (C16:1)	0.016	2.06	0.778	1.03	0.002	0.50	0.007
Hexanoyl carnitine (C6:0)	0.313	2.03	0.208	1.47	0.038	0.72	0.374
Homoarginine	0.045	1.20	<0.001	1.16	0.017	0.97	0.860
Hydroxybutyryl carnitine (C4:0-OH)	0.260	0.34	0.623	0.92	0.030	2.70	0.099
Hydroxyisovaleroyl carnitine (C5:0-OH)	1.000	1.40	0.401	1.27	0.149	0.91	0.514
Hydroxylauroyl-carnitine (C12:0-OH)	<0.001	2.46	<0.001	3.17	0.002	1.29	0.527
Hydroxylinoleoyl-carnitine (C18:2-OH)	<0.001	2.90	<0.001	2.52	<0.001	0.87	0.532
Hydroxymyristate	0.264	0.75	0.444	1.11	0.110	1.48	0.029
Hydroxymyristoyl-carnitine (C14:0-OH)	<0.001	2.39	0.003	1.76	<0.001	0.74	0.117
Hydroxyoctadecenoyl-carnitine (C18:1-OH)	<0.001	3.20	0.002	2.08	<0.001	0.65	0.169
Hydroxypalmitoleoyl-carnitine (C16:1-OH)	<0.001	2.20	<0.001	1.83	<0.001	0.83	0.459

Hydroxystearate	0.030	1.17	0.003	1.34	0.607	1.15	0.041
Hypoxanthin	<0.001	1.14	0.001	1.10	<0.001	0.97	0.242
Inosine	1.000	0.76	0.532	1.17	0.402	1.54	0.182
Inositol	0.089	0.82	0.055	0.85	0.015	1.04	0.501
Isobutyrylcarnitine (C4:0)	0.311	1.15	0.140	1.22	0.046	1.07	0.529
Isocitric Acid	0.613	0.71	0.077	1.19	0.610	1.68	0.299
Isoleucylglycine	0.032	0.92	0.007	2.32	0.836	2.51	0.012
Isovalerylcarnitine (C5:0)	0.160	2.02	0.270	1.26	0.016	0.63	0.176
Kynurenine	<0.001	2.46	<0.001	2.97	0.003	1.20	0.453
L-glutamine	0.002	0.64	0.371	1.10	0.002	1.73	<0.001
L-isoleucine	0.035	1.08	0.176	0.96	0.057	0.88	0.003
L-valine	<0.001	1.48	<0.001	1.68	0.001	1.13	0.786
Laminaribiose	0.977	1.30	0.219	0.65	0.764	0.50	0.179
Laurate (12:0)	0.091	0.61	0.770	1.06	0.022	1.72	0.015
Laurylcarnitine (C12:0)	0.006	7.51	0.333	1.51	<0.001	0.20	0.012
leucine	0.039	1.08	0.181	0.96	0.059	0.88	0.003
leucylglycine	0.032	0.84	0.014	2.30	0.523	2.75	0.006
Linoleate (18:2)	0.001	0.77	<0.001	0.60	0.063	0.78	0.080
Linolenate (18:3)	0.442	0.75	0.225	0.79	0.059	1.05	0.449
Linolenoyl-carnitine (C18:3)	0.230	1.61	0.321	1.17	0.024	0.73	0.193
Linoleoylcarnitine (C18:2)	0.171	1.63	0.590	0.89	0.018	0.54	0.075
LPC(14:0)	0.043	0.89	0.028	1.28	0.370	1.43	0.006
LPC(15:0)	0.190	0.85	0.645	1.06	0.053	1.24	0.025
LPC(16:0)	0.005	0.91	0.211	0.96	<0.001	1.05	0.020
LPC(16:1)	0.157	1.19	0.025	1.18	0.080	0.99	0.798
LPC(17:0)	0.002	0.83	<0.001	0.71	0.090	0.85	0.085
LPC(18:0)	0.409	0.93	0.229	1.06	0.322	1.13	0.048
LPC(18:1)	0.015	1.30	0.615	0.94	0.006	0.73	0.002

LPC(18:3n3)	1.000	0.90	0.566	1.01	0.442	1.12	0.811
LPC(19:0)	0.044	0.79	0.160	1.21	0.076	1.54	0.004
LPC(20:0)	0.183	0.64	0.250	0.71	0.019	1.10	0.211
LPC(20:1n9)	0.007	1.27	0.009	1.24	0.002	0.98	0.451
LPC(20:2)	<0.001	2.10	<0.001	2.03	<0.001	0.97	0.917
LPC(20:3)	<0.001	1.42	<0.001	2.10	0.031	1.47	0.040
LPC(20:4)	<0.001	1.26	<0.001	2.51	0.237	2.00	0.003
LPC(20:5n3)	1.000	0.80	0.684	0.90	0.304	1.13	0.529
LPC(22:5n6)	0.001	1.57	<0.001	1.76	0.020	1.12	0.258
LPC(22:6)	0.674	1.11	0.086	1.00	0.385	0.91	0.516
LPE(16:0)	0.006	0.98	0.001	0.83	0.968	0.84	0.005
LPE(18:0)	0.343	1.27	0.802	1.01	0.046	0.80	0.092
LPE(18:2)	0.360	0.81	0.143	0.84	0.056	1.04	0.578
LPE(20:3)	0.004	1.04	<0.001	1.82	0.602	1.76	0.011
LPE(20:4)	0.001	0.90	0.001	1.95	0.575	2.17	<0.001
LPE(20:5n3)	1.000	0.66	0.632	0.74	0.202	1.13	0.423
LPE(O-16:0)	0.006	1.03	0.001	0.76	0.945	0.74	0.006
LPE(O-18:0)	0.001	1.00	<0.001	0.50	0.705	0.50	0.001
Lysine	0.903	0.97	0.164	1.00	0.941	1.03	0.205
Lyxose	1.000	1.16	0.200	1.04	0.651	0.89	0.501
Malic Acid	0.652	1.04	0.081	1.20	0.525	1.15	0.370
Maltose	1.000	1.41	0.339	0.73	0.806	0.52	0.290
Mead Acid (20:3)	0.002	1.34	0.001	1.22	0.003	0.91	0.985
Methionine	1.000	1.03	0.916	0.98	0.818	0.95	0.757
Methylmalonyl carnitine	0.007	0.43	0.027	0.56	0.001	1.28	0.211
Myristic Acid	1.000	0.84	0.297	0.80	0.368	0.95	0.969
Myristoleoylcarnitine (C14:1)	0.028	2.36	0.726	1.07	0.003	0.45	0.013
Myristoylcarnitine (C14:0)	0.034	2.04	0.452	1.11	0.003	0.54	0.030

N-Acetyl-Glucosamine	0.132	0.83	0.083	0.86	0.019	1.04	0.461
N- Acetyl -L-Aapartic Acid	0.007	1.34	0.001	1.68	0.081	1.26	0.189
N6-succinyladenosine	0.944	0.81	0.403	0.78	0.134	0.96	0.480
Nicotinamide	0.001	1.64	<0.001	1.84	0.007	1.12	0.449
Nonanoic Acid	1.000	1.00	0.949	0.36	0.254	0.36	0.254
Octadecadienoic Acid	0.009	1.09	0.017	0.83	0.200	0.76	0.001
Octadecanedioate (C18)	0.133	0.67	0.777	0.86	0.017	1.28	0.042
Octadecenoic Acid	1.000	1.10	0.375	0.45	0.586	0.41	0.200
Octanoyl-carnitine (C8:0)	0.097	2.26	0.019	2.39	0.047	1.06	0.895
Octenoyl-carnitine (C8:1)	0.011	0.54	0.212	0.83	0.001	1.53	0.035
Oleate (18:1)	0.017	0.82	0.002	0.73	0.055	0.89	0.383
Oleoylcarnitine (C18:1)	0.069	1.66	0.938	0.95	0.011	0.57	0.018
Ophthalmic Acid	0.004	0.53	0.005	0.60	0.001	1.14	0.503
Ornithine	0.019	1.47	0.003	1.63	0.033	1.10	0.583
Palmitate (16:0)	1.000	0.87	0.529	0.95	0.142	1.09	0.391
Palmitoleate (16:1)	0.781	0.72	0.818	1.18	0.161	1.63	0.125
Palmitoylcarnitine (C16:0)	0.051	1.31	0.101	0.80	0.135	0.61	0.005
LPC(14:0)	0.075	0.88	0.059	1.19	0.297	1.36	0.009
Pentadecanoic Acid	1.000	0.76	0.872	0.92	0.181	1.21	0.256
Phenylacetylglutamine	1.000	1.11	0.490	1.38	0.626	1.25	0.290
Phenylalanine	0.308	1.17	0.091	1.14	0.063	0.97	0.751
Phenylalanylglutamate	0.001	2.28	0.008	1.53	<0.001	0.67	0.167
Phenylalanylleucine	0.933	0.76	0.181	0.80	0.881	1.05	0.196
Phenylalanylphenylalanine	0.697	0.83	0.139	1.14	0.839	1.38	0.143
Picolinic Acid	1.000	1.00	0.711	1.18	0.858	1.18	0.625
Proline	0.763	1.00	0.131	1.14	0.978	1.14	0.185
Propionylcarnitine (C3:0)	0.102	1.43	0.988	0.90	0.017	0.63	0.023
Pyroglutamic Acid	0.003	1.07	<0.001	1.36	0.169	1.27	0.055

Quinolinic Acid	0.059	2.84	0.007	5.00	0.069	1.76	0.566
Ribose	0.005	1.43	0.001	1.53	0.013	1.07	0.581
S-adenosylhomocysteine (SAH)	0.003	0.78	0.007	1.50	0.175	1.91	<0.001
Sakebiose	1.000	1.41	0.413	0.73	0.683	0.52	0.274
Sorbose	0.005	0.52	<0.001	2.46	0.137	4.77	0.100
Squalene	1.000	0.76	0.439	1.02	0.689	1.35	0.295
Stearoylcarnitine (C18)	0.574	1.17	0.240	0.75	0.418	0.64	0.075
Suberate (octanedioate)	0.393	0.71	0.856	0.97	0.076	1.37	0.065
Succinic Acid	0.196	0.89	0.019	0.71	0.342	0.80	0.269
Sucrose	1.000	0.57	0.248	1.25	0.762	2.19	0.200
Tetradecadienyl-carnitine (C14:2)	0.437	1.74	0.819	1.14	0.060	0.66	0.111
Threonine	0.324	1.02	0.048	1.24	0.918	1.22	0.109
Tiglyl carnitine (C5:1)	0.079	1.84	0.235	1.21	0.007	0.66	0.123
Tryptophan	0.002	0.67	0.001	0.68	0.003	1.01	0.975
Tryptophan betaine	0.767	0.74	0.478	1.66	0.276	2.23	0.099
Tyrosine	0.220	1.25	0.027	1.33	0.164	1.06	0.560
Uracil	<0.001	0.48	0.002	0.55	<0.001	1.14	0.285
Valerylcarnitine (C5:0)	0.311	2.32	0.538	1.47	0.034	0.63	0.138
valylalanine	0.022	0.84	0.009	2.32	0.578	2.75	0.005
Xylose	1.000	1.13	0.163	0.95	0.582	0.84	0.500

* Kruskal Wallis p values adjusted by Benjamini-Hocheberg method

** Dunn post hoc test p values